The Role of Non-Myogenic Mesenchymal Stem Cells in Skeletal Muscle of Dystrophin/Utrophin Double Knockout Mice

by

Jihee Sohn

Bachelor of Science, the George Washington University, 2008

Master of Science, Georgetown University, 2010

Submitted to the Graduate Faculty of

The School of Medicine in partial fulfillment

Of the requirements for the degree of

Doctor of Philosophy

University of Pittsburgh

2015

UNIVERSITY OF PITTSBURGH

SCHOOL OF MEDICINE

This dissertation was presented

by

Jihee Sohn

It was defended on

May 21, 2015

and approved by

Wendy Michelle Mars, PhD, Associate Professor, Department of Pathology

Rocky Sung Chi Tuan, PhD, Professor, Department of Orthopaedic Surgery

Kacey Gribbin Marra, PhD, Associate Professor, Department of Plastic Surgery

Bing Wang, MD, PhD, Associate Professor, Department of Orthopaedic Surgery

Simon C. Watkins, PhD, Professor, Department of Cell Biology

Dissertation Advisor: Johnny Huard, PhD, Professor, Department of Orthopaedic Surgery

The Role of Non-myogenic Mesenchymal Stem Cells in Skeletal Muscle of Dystrophin/Utrophin Double Knockout Mice

Jihee Sohn, PhD

University of Pittsburgh, 2015

Adult skeletal muscle possesses a remarkable regenerative ability, which largely depends on satellite cells; however, in severe muscular dystrophies, such as Duchenne muscular dystrophy (DMD), skeletal muscle integrity is compromised and the muscle is often replaced by a mixture of fibrous tissue and white adipocytes in a process termed fibro-adipogenic degeneration. The precise cellular origin and the environmental cues responsible for accumulation of fat/fibrotic tissues during the course of the disease remain unknown. Using a previously published preplate technique, two distinct populations of muscle derived cells from skeletal muscle were isolated: 1) a rapidly adhering cell population (RACs), which is non-myogenic, $Pax7^-$ and expresses the mesenchymal stem cell (MSC) marker PDGFRα, hence termed non-myogenic MSCs (nmMSCs); and 2) a slowly adhering cell population (SACs) which is $Pax7^+$ and highly myogenic, termed myogenic progenitor cells (MPCs). In this dissertation, the role of nmMSCs in the histopathogenesis of dystrophin/utrophin double knock out (dKO) mice, an animal model of DMD, was investigated. The nmMSCs become activated during the disease progression in dKO mice, displaying increased proliferation and adipogenic, osteogenic, and fibrogenic potentials compared to age-matched WT counterparts. The activated dKO-nmMSCs also significantly reduced the myogenic potential of the dKO-MPCs, an effect, at least partially, mediated by the secreted frizzled-related protein 1 (sFRP1) released by the dKO-nmMSCs. These results suggest that nmMSCs are likely the cell source involved in the deposition of non-

muscle tissues in dKO muscles and activation of nmMSCs likely exacerbates muscle wasting and degeneration during the disease progression by limiting the myogenic potential of MPCs. Interestingly, the nmMSCs also appear to play an important role in muscle regeneration after acute injury in normal WT muscle. The nmMSCs isolated from cardiotoxin injured WT muscle significantly enhanced the myogenic potential of MPCs after co-cultivation, suggesting that the nmMSCs may facilitate muscle repair in normal WT muscle. These results suggest that the muscle micro-environment plays a major role in the fate of nMMSCs. Overall, data from this dissertation proposes that a therapeutic strategy targeting nmMSCs could represent a novel treatment for DMD.

TABLE OF CONTENTS

LIST OF TABLES

LIST OF FIGURES

ACKNOWLEDGMENTS

There are so many people I would like to acknowledge for helping me complete this dissertation. The contributions of many different people, in their different ways, have made this possible. I would like to extend my appreciation especially to the following.

Thank God for the wisdom and perseverance that He has been bestowed upon me during this research, and indeed, throughout my life. Only due to His blessings could I have finished this work: "I can do everything through him who give me strength." (Philippians 4: 13). Thanks to my fellow brothers and sisters in Christ, for their continual support and encouragement throughout this year.

I would like to express my deepest gratitude to my advisor and mentor, Dr. Johnny Huard, for the continuous support of my Ph.D. study and research, for his patience, motivation, enthusiasm, and immense knowledge. His guidance helped me during the time of research and writing of this thesis. I could not have imagined having a better advisor and mentor for my Ph.D. study. Besides my advisor, I would like to thank the members of my thesis committee: Dr. Wendy Mars, Dr. Rocky Tuan, Dr. Kacey Marra, Dr. Bing Wang, and Dr. Simon Watkins, for their encouragement, insightful comments, and hard questions.

I thank my co-workers in the Stem Cell Research Center: Dr. Lu, Dr. Gao, Dr. Li, Dr. Mu, Dr. Wang, Dr. Chen, Ying, Jessica, and Jim for the stimulating discussions, for the sleepless nights we were working together before deadlines, and for all the fun we have had in the last four

years. I especially thank you, Dr. Aiping Lu for helping me to pick up a project and for helping me all the way through the completion of the thesis and publication. Dr. Lu was the one who taught me all the techniques and helped me to push the project forward. I am also grateful to Ying. I wouldn't have finished this work without her hard work and support. Thank Dr. William Chen, for always listening to my problems inside and outside the laboratory and providing me with new ideas and solutions. I cannot forget about Dr. Sarah Beckman, Dr. Jonathan Proto, and Minakshi Podder. Sarah and Jonathan were former graduate students in the laboratory and helped me as I was finishing my required course work and comprehensive exam. They always have been there for me to provide support and encouragement. Also I thank Tim Hannigan and Anthony Ascoli, my awesome and hardworking undergraduate students. They were a tremendous help. Lastly, I would like to thank Abby Stahl, who joined our lab most recently. I cannot fail to thank my friends outside the laboratory, my dearest friends in South Korea and in USA for always praying for me and encouraging me.

Last but not least, I would like to thank my family, my parents and my younger brother, Andy Sohn, for their unconditional support, both financially and emotionally throughout my graduate studies.

1.0 INTRODUCTION

1.1 DUCHENNE MUSCULAR DYSTROPHY

Muscular dystrophy (MD) describes a heterogeneous group of approximately 40 inherited disorders characterized by progressive muscle weakness, degeneration, and wasting. Duchenne muscular dystrophy (DMD) is one of the most common childhood muscular dystrophies, with an incidence rate of approximately one in every 3,500 live male births (1). It is an X-linked, genetic disease caused by frameshift mutations in the dystrophin gene, which results in complete absence of functional dystrophin protein, a relatively large, 472 kilo-Dalton (kD) cytoskeletal protein in both skeletal and cardiac muscle tissues (2-4). Dystrophin, along with other dystrophin-associated proteins (DAPs), stabilize the muscle cell membrane, both physically and physiologically. The major role of dystrophin is to link cytoskeletal F-actin to the dystrophin associated glycoprotein (DAG), which binds to laminin-2 in the overlying basal lamina of the extracellular matrix (5, 6). In dystrophic muscle, this linkage is disrupted and muscle fibers are damaged during muscle contraction. This process results in an efflux of soluble muscle-specific enzymes, such as creatine kinase (CK), an influx of calcium ions, and the recruitment of T cells, macrophages, and mast cells to the damaged muscle, causing progressive myofiber necrosis (7, 8). The damaged fibers degenerate and the muscle progenitor cells are recruited to regenerate new muscle fibers, but this regeneration is inefficient due to repeated cycles of necrosis over

time, which eventually leads to an exhaustion/depletion of the satellite cell population (9). Continuous weakness and degeneration of striated muscle eventually result in kyphosis and scoliosis of the spine (90%-95% of patients), a loss of independent ambulation by the middle of the patient's second decade, and a fatal outcome due to cardiac or respiratory failure by the third decade (6, 10, 11). Interestingly, although the typical histological pattern of degeneration/regeneration of muscle fibers in most skeletal muscle groups and elevated CK concentration in serum are present in affected boys long before the clinical onset of the disease, DMD patients usually exhibit no obvious clinical manifestation until the age of 3 to 5 years (11).

Still no effective treatments are available for DMD patients, and currently corticosteroids, including glucocorticoids, prednisone, and deflazacort, are used to delay the disease progression; however, the mechanism of action of corticosteroids in DMD is not completely understood (6, 12, 13). One possible explanation is that glucocorticoids bind directly to inflammatory cell receptors, enhancing the transcription of anti-inflammatory genes or inhibiting pro-inflammatory factors, such as NF-κB (14). A few studies have shown that prednisolone may increase dystrophin-related protein expression in muscle cell cultures of *mdx* mouse, an animal model of DMD (14, 15). Although there are beneficial effects of medical management of patients with corticosteroids, including increased muscle strength, prolonged walking, delayed decline of pulmonary function, and delayed wheelchair use by up to 4-5 years, there are some major side effects (6, 16, 17). The most frequent side effects of corticosteroids include weight gain, growth retardation, personality changes, and reduced bone density with potential osteoporosis (6, 18). Moreover, as of January 2015, only prednisone is available in the US.

Current research studies on treatment regimens for DMD have centered on the restoration of dystrophin; however, these technologies alone have faced limitations. Over the last decade,

many different gene therapy strategies for DMD, including plasmid transfer, exon skipping, and viral- or non-viral-mediated therapy has been focusing on delivering a dystrophin gene to the dysfunctional muscle tissue and has entered clinical trials. However, the extensive size of the dystrophin gene and the long-term expression of gene construct into skeletal muscle have limited clinical applicability (19). Besides, Adeno-associated virus injection to deliver sarcoglycans reported to cause an immune reaction against the viral proteins in dystrophic dogs (20).

In addition, one of the most striking pathological conditions in advanced cases of DMD is an accumulation of intramuscular fibro-fatty tissues or calcium deposits, with the muscle being almost entirely replaced by non-muscle tissues (6, 21, 22). At an early age, only mild pathology is observed due to sufficient regeneration and repair medicated by muscle stem cells; however, when the stem cell pool is eventually depleted, the functional skeletal muscle is replaced by a mix of fibrous tissue and white adipocytes in a process termed pseudohypertrophy and fatty degeneration **(Fig. 1)**.

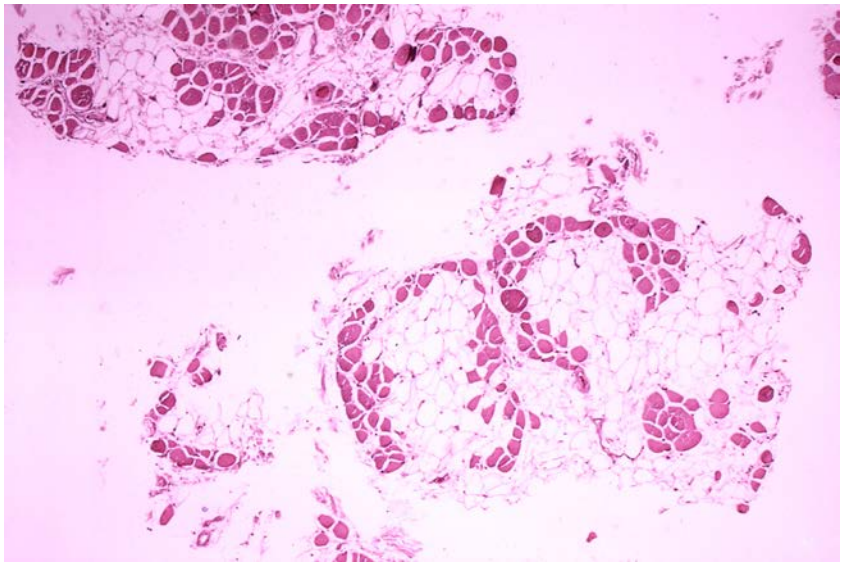

Figure 1. Histopathology of gastrocnemius muscle (GAS) from a patient who died of pseudohypertrophic muscular dystrophy, Duchenne type.

Hematoxylin-eosin staining of muscle from a patient with DMD. Cross section of this patient's muscle shows extensive replacement of muscle fibers by adipose cells. In addition, variation in muscle fiber size, central nuclei, and areas of fibrosis are observed. (Image adapted from http://phil.cdc.gov/phil/home.asp, Edwin P. Ewing Jr., 1972).

In DMD, the accumulation of intramuscular fat and/or fibrotic tissue represents the hallmarks of advanced stage disease and the presence of these non-muscle tissues significantly affects muscle structure, function, and recovery (6). First of all, severe intramuscular adipose tissue development may induce deregulation of muscle homeostasis, which associates with potential insulin resistance (23, 24). Secondly, adipocytes/fatty infiltration/adipose tissue exacerbate the muscle wasting process in DMD patients, compromise muscle function, and alter the tissue environment, severely limiting the success of muscle regeneration (6, 20, 23). Therefore, the use of dystrophin replacement alone to treat the primary defect in DMD patients may not be successful for rescuing muscle from progressive degeneration and wasting, especially

at the later stages of the disease (20, 25). Current therapies have not found a solution to block or replace formation of ectopic non-muscle tissues in the DMD skeletal muscle, and unfortunately, the precise origin of ectopic adipocytes or fibrotic tissue in dystrophic muscle is not clearly understood. More studies on mechanisms regulating the calcification and fibro-fatty degeneration in skeletal muscle of DMD must be performed to improve currently available treatment methods.

1.2 FAT TISSUE DEPOSITION IN SKELETAL MUSCLE

Although adult skeletal muscle has great regenerative potential, some experimental and pathological conditions lead to impaired regeneration with adipose tissue deposition. Ectopic adipocyte deposition in the skeletal muscle characterizes various disorders, including muscular dystrophy (26, 27), inflammatory myopathies (28), scarcopenia due to disuse or aging (29-31), obesity and type-2 diabetes (32). The muscle fat includes both acellular lipid droplets within the fibers, and interstitial adipocytes (33, 34). These intramuscular fat tissue in skeletal muscle is usually white, although brown adipocytes have also been identified, and are characterized by drops of triglycerides and cholesterol ester, which can be identified by Oil-Red O staining and the expressions of peroxisome proliferator-activated receptor γ2 (PPARγ2), perilipin, leptin, adiponection and fatty acid-binding protein 4 (FAP4) (34, 35).

In DMD, intramuscular fat can reach as much as 46% of muscle mass in young boys and older boys can show even higher muscle fatty infiltration, as measured by magnetic resonance imaging (MRI) (36, 37). The gluteus maximus had the most frequent and greatest degree of fatty

infiltration (36), but adipose tissue deposition was also observed in semi-membranous muscles, biceps, and rectus femoris, with the least amount found in gracilis and sartorius muscles (36-39). Interestingly, it has been shown that muscles showing clear signs of inflammation and edema were not necessarily correlated to fatty infiltration. In fact, some muscles were infiltrated by fat tissue without apparent inflammatory reactions (39, 40).

To investigate accumulation of fat tissue in the skeletal muscle, the glycerol-induced fatty degenerating murine model can be used (24); however, ectopic fat deposition has been detected after cardiotoxin induced or freeze injuries as well as rotator cuff injuries (41, 42). The cell population responsible for the development of the adipose tissues in those animal models is still unclear. It has been shown that satellite cells, non-myogenic PDGFRα^+ cells, pericytes or muscle fibroblasts are all capable of forming intramuscular fat in skeletal muscle under a variety of pathological conditions (43-46). Fatty infiltration is irreversible and progressive if left untreated. Given the negative impact of ectopic adipocytes and these conflicting reports about the original cell source responsible for the phenotype, more studies are needed to understand the cellular and molecular players of fat deposition and accumulation in skeletal muscle.

1.3 IN VIVO MODELS FOR DMD

Several animal models are available for use in DMD research, including canine and murine models. These mammalian models for DMD are important to understand the underlying cellular and molecular mechanisms of DMD as well as to test therapeutic approaches to alleviate the muscle weakness in DMD (47).

1.3.1 Canine Model

The canine model of DMD (cxmd), including the dystrophic Golden Retriever (GRMD) and the Beagle (CXMDj) dogs, displays spontaneous mutations of the dystrophin gene, resulting in X-linked muscular dystrophy. They result from a point mutation at the 3' consensus splice site of intron 6 of the dystrophin gene, which leads to skipping of exon 7, a disruption in the open reading frame, and premature termination of translation (47). Of those, GRMD dogs show the most similar pathogenesis to that of human patients with DMD, suffering from a rapidly progressing and fatal muscle wasting and degeneration, fat accumulation, fibrosis, and a shortened life span (47-49). In GRMD, the incomplete muscle repair starts at age of 6-9 weeks, and further results in progressive weakness and gait abnormalities by 6 months. The GRMD dogs become less active at about 9 months of age and the severely affected dogs show difficulties rising and walking only a few steps. They also develop kyphosis by the age of 6 months (47). The canine model has been mostly used for research focusing on myoblast transfer, gene transfer, and oligonucleotide therapy. Although the GRMD model is highly relevant for DMD research, dogs are not considered as an ideal laboratory animal. One important drawback of cxmd is the high degree of variability in the severity of disease between breeds and among littermates as well as the high cost associated with maintaining a dystrophic dog colony (48, 50).

1.3.2 Murine Model

Research on DMD has benefited from the availability of *mdx* mice, in which a point mutation on exon 23 of the mouse dystrophin gene introduces a premature stop codon, eliminating expression of full length dystrophin protein (11, 48, 50). During the first 6 weeks of life, *mdx* mice show

histological signs of muscular dystrophy; however, the subsequent course of their disease is markedly milder compared to that seen in DMD (5, 47, 51). The *mdx* mice show milder weakness, pseudohypertrophy, kyphosis, and have nearly normal life span. Also, the *mdx* mice do not develop the severe myofibrosis, fatty infiltration, and cardiomyopathy characteristic of end-stage DMD (5, 52) until they become around 24 months old **(Fig. 2)**. These differences have limited the value of *mdx* mice as a model for investigating the accurate pathogenesis of DMD and testing potential interventions. It is also important to understand why the dystrophin deficiency is less deleterious to mice than to humans as the information could help in finding therapies for DMD or other muscle diseases. One possible explanation for the difference between *mdx* mice and DMD patients is that utrophin, a homologous protein of dystrophin, compensates for the lack of dystrophin more effectively in *mdx* mice than in DMD patients (51).

The fact that the occurrence of later stage manifestations, including ectopic adipose and fibrotic tissue accumulation and calcium deposits in skeletal muscle, are rare in *mdx* mice have lead researchers to use the glycerol-induced fatty degenerating mice model to investigate histopathogenesis of various skeletal muscle diseases. A routine protocol of 25µl of 50% glycerol intramuscular injection in mouse TA muscles is shown to induce myofiber damage by plasma membrane disruption, followed by some areas of muscle regeneration accompanied by apparent fat deposition between muscle fibers (24). However, these animals still possess pitfalls. It is difficult to fully investigate the degenerative-regenerative events occurring during the progression of disease when using the intramuscular glycerol injection model in a normal, wild type (WT) or *mdx* mouse. The skeletal muscle repair and regeneration processes involve the cascade of many different cells types, cytoskeletal elements, chemoattractant molecules, and immune cells (10, 53). Therefore, one time injection of glycerol to induce fatty degeneration

cannot fully recapitulate the cellular and molecular events that occur in the progressive pseudohypertroph in DMD. Moreover, the degree of adipose tissue formation in chemically induced skeletal muscles is dependent on the genetic background of mice (42, 54) .

In order to overcome challenges with *mdx* mice, Grady et al. developed the dystrophin/utrophin double-knock out (dystrophin$^{-/-}$, utrophin$^{-/-}$, dKO) mice (5). The dKO mouse shows numerous clinically-relevant manifestations, including muscle wasting, crippling, kyphosis, heart failure, degenerative musculoskeletal abnormalities and other life-threatening phenotypes (51, 55). The normal life span of dKO mice is usually 8-10 weeks, and by that stage, dKO mice develop advanced sarcopenia and pseudohypertrophy (51, 55, 56) and the dystrophic phenotype demonstrated by dKO mice closely mimics DMD pathophysiology. Therefore, the dKO mouse is regarded as a better model for therapeutic trials to determine the effectiveness of various treatment modalities. As shown in Figure 2, skeletal muscles of 6-8 week old dKO mice exhibit severe muscle histopathology and muscular dystrophy compared to that of an age-matched *mdx* mouse **(Fig. 2)**. Immunohistochemistry staining of 6-8 week old dKO gastrocnemius muscle (GAS) tissue section shows rigorous muscle damage, necrotic muscle fibers, and accumulation of calcium deposits, fibrotic tissue and lipids. However, the cellular origin and the environmental cues responsible for these changes in the skeletal muscles of DMD or dKO mice remain unknown. For these reasons, studies done in this dissertation will be focusing on utilizing dKO mice to investigate the major cell source responsible for formation of non-muscle tissues in dystrophic skeletal muscle during the disease progression.

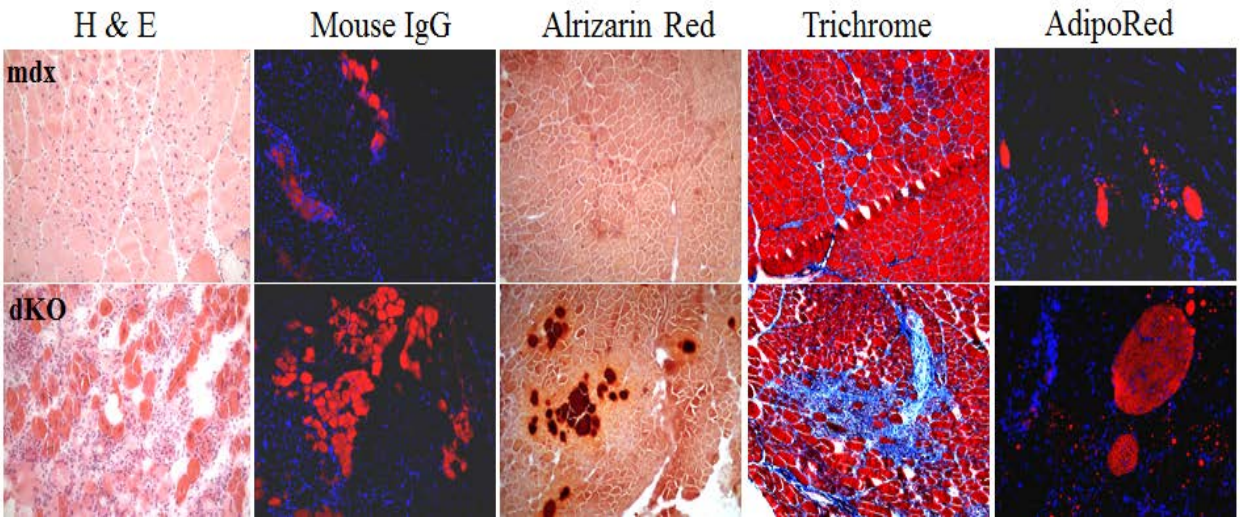

Figure 2. Comparison of *mdx* and dKO skeletal muscle histopathology.

Gastrocnemius muscles (GAS) from 6-8 week old *mdx* and dKO mice was compared. Muscle histopathology and muscular dystrophy were more severe in the dKO mice compared to the age-matched *mdx* mice. H&E staining shows severe muscle damage in the GAS of dKO mice. Larger necrotic areas in the GAS of dKO mice were identified with mouse IgG staining. Alizarin Red staining visualized calcium deposits in 8 week old dKO-GAS. Trichrome staining identified larger fibrotic regions in dKO-GAS. AdipoRed staining identified more lipids accumulation in dKO-GAS. Image adapted from (A. Lu et al. 2014).

1.4 SKELETAL MUSCLE STEM/PROGENITOR CELLS: MDSCS AND RACS

From the time of their initial description in 1961, satellite cells (SCs), located underneath the basal lamina of the muscle fiber, are responsible for the maintenance and regeneration of the adult skeletal muscle (57). SCs are considered to be mitotically quiescent; however, upon activation, they will migrate, rapidly undergo extensive proliferation, differentiate into myoblasts, and finally fuse with existing muscle fibers to form new multinucleated myofibers. Cell surface markers associated with SCs include M-cadherin, Sca-1, CD34, and Pax3 and Pax7 transcription

factors, which are known to play essential roles in the early specification, migration, and myogenic differentiation (58-60) **(Fig. 3)**. During population expansion, quiescent SCs undergo asymmetric division to produce myoblast, while a portion retains "stemness" in order to repopulate the stem cell niche (57, 61). Therefore, SCs are often referred to as muscle stem cells which can regenerate skeletal muscle and display self-renewal properties; however, they are mainly committed to myogenic lineage (62). Myoblasts, so-called activated SCs, loose expression of Pax7 and begin to express myogenic regulatory factors (MRFs) including Myf5, MyoD, and myogenin **(Fig. 3)** (63, 64). They have been extensively studied as candidates for cell therapy for treating muscular dystrophies and other skeletal muscle disorders (65-68).

Other cell populations with myogenic or without myogenic potential, including PICs ($PW1^+$ interstitial cells), pericytes, side population cells, muscle derived stem cells, myogenic endothelial cells, Fibro/adipogenic Progenitors (FAPs), and $PDGFR\alpha^+$ cells, have been isolated from skeletal muscle utilizing a variety of methods, including cell culture selection techniques, flow cytometry-based sorting, and Hoechst dye exclusion **(Table 1)** (44, 69-73). Our research group has reported the isolation of muscle resident stem/progenitor cells using the modified preplate technique (74). As shown in Figure 3, the preplating process consists of serial plating of muscle derived cells to separate them according to their adhesion properties to type I Collagen (74-76). The most rapidly adhering cell (RAC) fractions consist of cells that adhere during the early stages of the preplate technique, within minutes to two hours of seeding. RACs are known to be comprised of a mixture of fibroblast-like and mesenchymal progenitor cells that are highly positive for Sca-1, which is expressed by progenitor populations of multiple tissues, and CD34, which is expressed by muscle stem cells (73, 77). Although RACs are partially able to regenerate muscle *in vivo*, higher regeneration potential is exhibited mostly by the slowly adhering cell

(SAC) fractions, which consist of cells obtained by successive re-plating of non-adherent cells for 6 days (78). Previously in our lab, we have characterized murine SACs as "muscle derived stem cells" (MDSCs) since they exhibit the stem cell characteristics of self-renewal and multi-lineage differentiation (75, 79). SACs also express both stem (Sca-1, CD34), myogenic (desmin, MyoD), and endothelial (CD31, CD144) cell surface markers, distinguishing them from SCs (74, 77).

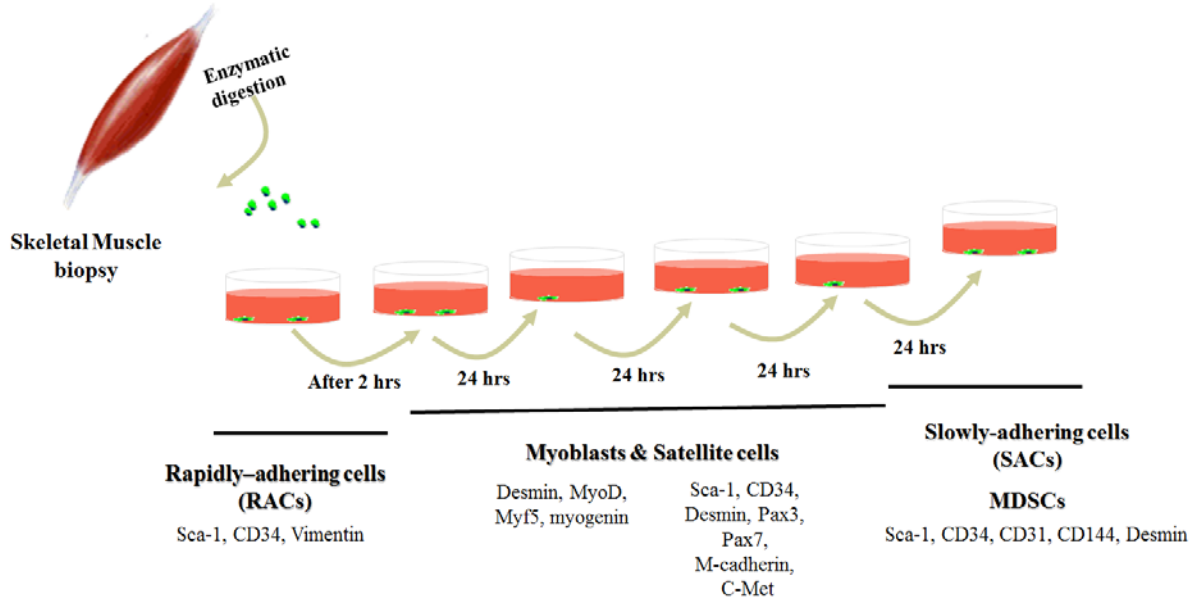

Figure 3. Schematic isolation of mouse muscle derived cell populations via modified preplate technique.

The mouse skeletal muscle biopsy was first enzymatically digested, and then, cells were preplated on collagen I coated flasks. After separation of cells by adherence rates, two main populations were acquired, rapidly-adhering cells, RACs, and slowly-adhering cells, SACs. RACs express Sca-1 and CD34, and SACs express Sca-1, CD34, CD31, CD144, and desmin (Gharaibeh et al. 2008 and Jankowski et al. 2001). SACs were found to contain a population of stem and progenitor cells and were named as muscle derived stem cells, MDSCs.

1.4.1 Muscle derived stem cells (MDSCs) and muscle regeneration

The MDSCs are characterized by slow cycling, long term self-renewing cells, as they can divide for more than 30 passages in proliferation medium with an average division time of 15.1 hours (74). It was previously reported that when compared to committed muscle precursor cells (myoblast), the MDSCs demonstrated a higher intramuscular engraftment capability in both skeletal and cardiac muscles (75, 80). In addition to healing skeletal muscle damage, MDSCs are also shown to aid in the repair of bone and cartilage defects, and improve heart function in murine models of acute myocardial infarction (81-83). The exact mechanism involved in the improved regenerative potential of the MDSCs remains unclear; however, current evidence from animal studies suggests that their high survival property due to elevated resistance to stress is critical (84-86) as well as their release of soluble factors such as vascular endothelial growth factor (VEGF) (83, 87). Our previous studies suggest that improved regenerative capacity of MDSCs is linked to their increased level of antioxidants, including glutathione and superoxide dismutase (84, 85) and elevated aldehyde dehydrogenase level, which endowed MDSCs with enhanced stress resistance capability post cell transplantation (86). In addition, soluble factors, such as VEGF have been found to promote MDSCs mediated tissue repair (83, 87).

In addition to murine MDSCs, systemic delivery of allogeneic wild type canine SACs to immunosuppressed dystrophic dogs has been reported to significantly improve dystrophic phenotype. Donor SACs have been shown to contribute to myofiber regeneration, SCs replenishment, and long-term dystrophin expression, which consequently improve muscle weakness in the dystrophic dog (88). Furthermore, evidence already exists that SACs isolated from humans also have the potential for skeletal and cardiac muscle regeneration (78, 89). SACs are currently undergoing clinical trials for the treatment of urinary incontinence and ischemic

heart failure (90). Therefore, MDSCs could provide an attractive therapeutic avenue for muscle diseases.

1.4.2 Rapidly adhering cells (RACs) and muscle regeneration

Rapidly adhering cells (RACs) have been shown by our group to be comprised of mostly fibroblastic-like cells that are highly positive for Sca-1 and CD34, but are negative for muscle progenitor cell markers, including Pax7, desmin and MyoD (74, 77). Another study on human RACs further indicated that they are also highly positive for CD44, CD73, CD90, and CD105 (78), cell surface markers known to be expressed by mesenchymal stem cells (MSCs) (91). However, few studies have been done to characterize RACs or investigate their role in muscle regeneration/degeneration under muscle injury or pathological conditions (74, 77, 78).

Recently, several investigations suggest that muscle resident Sca-1^+/$CD34^+$ cells, isolated using fluorescence activated cell sorting (FACS), play an important role in maintaining muscle homeostasis by interacting with SCs (44, 73, 92, 93). These Sca-1^+/$CD34^+$ cells are referred as Fibro/Adipogenic Progenitors (FAPs) since they have the dual potential to differentiate into both adipocytes and fibroblasts *in vitro* and *in vivo*. Although FAPs do not arise from the myogenic lineage, nor directly participate in forming myotubes/myofibers, they have been shown to facilitate muscle regeneration after injury (92). Muscle damage results in rapid recruitment of eosinophils, which secrete IL-4/IL-13 immune signals. The activation of IL-4/IL-13 signaling further promotes proliferation of FAPs to support myogenesis while inhibiting their differentiation into adipocytes (92). Another *in vitro* co-culture experiment shows that signals originating from FAPs generate a transient pro-myogenic differentiation niche for myoblast or SCs (73). A recent study suggests that follistatin secreted by FAPs might contribute to FAPs

ability to promote SC myogenic activity (93). Moreover, it has been reported that FAPs can also mediate the ability of histone deacetylase (HDAC) inhibitors to promote satellite cell-based regeneration in *mdx* mice (93).

Interestingly, FAPs are also known to be highly positive for platelet derived growth factor receptor α (PDGFRα), a well-known marker for muscle resident mesenchymal stem cells (44). It has been reported that, of the muscle-derived cell populations, only FAPs or PDGFRα^+ mesenchymal progenitor cells display efficient *in vitro* and *in vivo* adipogenic/fibrogenic differentiation potentials and can participate in ectopic adipocyte formation when transplanted into glycerol induced fatty degenerating muscle or *mdx* mouse (44, 73, 94). However, others report inconsistent results and show that SCs, muscle fibroblasts, or pericytes are also all capable of forming intramuscular fat and fibrotic tissue in a variety of pathological conditions (45, 46, 95, 96). Furthermore, the cellular origin responsible for the formation of non-muscle tissues in severe dystrophic mouse model, such as dKO mouse remains unexplored. It appears to be that the RACs are also expressing high levels of Sca-1 and CD34, two cell surface markers expressed by FAPs, and therefore, it will be important to examine whether RACs can contribute to dystrophic muscle histopathology or influence myogenic activity of muscle progenitor cells (MPCs) of dKO mice.

Population	Cell markers	Location	Differentiation In vitro	Differentiation In vivo	Reference
Satellite cells	Pax7, CD34, Myf5, VCAM-1	Between the basal lamina and sarcolemma	Myogenic, adipogenic, osteogenic, fibrogenic?	myogenic	(51, 95, 97)
MDSCs	Sca-1, CD34, CD31, CD144, PW1?	Muscle interstitium	Myogenic, Adipogenic, Osteogenic, Chondrogenic, haematopoietic	Myogenic, osteogenic, chondrogenic, fibrogenic	(98-102)
PICs	PW1, Sca-1 CD34,	Muscle interstitium	Myogenic	myogenic	(70, 103)
IAP	PW1, Sca-1, PDGFRα	Muscle interstitium	Adipogenic	Adipogenic	(103)
Pericytes	AP, PDGFRβ, NG2	endothelium	Myogenic, adipogenic, osteogenic, fibrogenic	Myogenic, adipogenic	(45, 69, 96, 104, 105)
RACs	Sca-1, CD34,	Muscle interstitium	Adipogenic? osteogenic? chondrogenic? fibrogenic?	Adipogenic? osteogenic? fibrogenic?	(74, 77)
FAPs	Sca-1, CD34	Muscle interstitium	Adipogenic, fibrogenic	Adipogenic, fibrogenic	(73)
PDGFRα+ cells	PDGFRα, Tie2	Muscle interstitium	Adipogenic, osteogenic, chondrogenic, fibrogenic	Adipogenic, fibrogenic	(44, 94, 106)
Fibroblasts	Tcf4, Vimentin	Muscle interstitium	Adipogenic, fibrogenic	Adipogenic, fibrogenic	(107, 108)
Side population cells	Hoechst-negative	Muscle interstitium	Myogenic, adipogenic, fibrogenic, osteogenic, haematopoietic	Myogenic	(67, 109, 110)

Table 1. Summary of a different population of skeletal muscle-resident progenitors.

MDSCs, muscle derived stem cells; PICs, PW1+/Pax7- interstitial cells; IAP, interstitial adipogenic progenitors; RACs, rapidly adhering cells; FAPs, fibro/adipogenic progenitors; PDGFRα/β, platelet derived growth factor receptor α/β; Tcf4, transcription factor 7-like 2.

1.5 EFFECT OF MUSCLE MICROENVIRONMENT ON STEM CELL FUNCTION

Stem cells exhibit two key characteristics, which are the ability to both self-renew and differentiate into specialized, mature cell types (111). These two properties endow stem cells with great promise for cell replacement therapy in regenerative medicine. Therefore, understanding the mechanisms underlying stem cell maintenance and differentiation are central to increase the efficacy of stem cell use in therapeutic applications.

The phenotypic characterization and function of stem cells are controlled by both intrinsic and extrinsic mechanisms (112). During past years, studies have tried to identify intrinsic regulatory mechanisms shared by all self-renewing cells by examining tissue-specific stem cells; however, gene expression profiling from these studies showed inconclusive results and have not been yet able to define a common set of genes responsible for stem cell behavior (113-115). This finding has led to a shift in research focus from investigating intrinsic regulatory mechanisms to studying the extrinsic micro environmental factors. The extrinsic regulation of stem cells is largely dependent on the local multi-cellular microenvironment, also known as the "stem cell niche", which includes growth factors, cytokines, matrix-mediated signals, and cell-cell interactions (112, 116, 117). For example, in tumor-bearing hosts, stem cells might be affected within their niches by the tumor microenvironment (TME), which consists of many different cell types, including cancer cells, immune cells, fibroblasts, and myofibroblasts, as well as the surrounding extracellular matrix. Several studies have shown that the TME can disrupt localization, stability, self-renewal, and differentiation potentials of normal adult stem cells, including bone-marrow derived MSCs and hematopoietic stem cells (HSCs), by altering signaling pathways and gene-expression profiles in these cell types (118-120).

The process of aging also contributes to stem cell niche dysfunction. Aging is evident in most tissues and organ system, and studies done on cellular and molecular changes in aged muscle have suggested that the aged niche can also disrupt proliferation and function of muscle stem cells, including SCs and $Pax7^{+}$ MPCs (121, 122). For example, Brack and colleagues reported that aged-muscle microenvironment induces Wnt signaling, alters SC fate from myogenic to fibrogenic fate and increases fibrosis in skeletal muscle (121). The authors further demonstrated that such myogenic-to-fibrogenic transition is influenced by the systemic environment, suggesting that stem cell functionality conversion is reversible, at least to some extent. When they exposed the old tissue to a youthful systemic environment, by establishing parabiotic pairings of old animals to young animals (heterochronic pairings), they were able to reduce the collagen deposition in regenerating areas of muscles of aged mice compared to isochronic pairings (parabiotic parings of old animals to old animals) (121). More recent investigation further suggests that aged-muscle niche also increases fibroblast growth factor (FGF) signaling, which leads to an initial loss of quiescence followed by a depletion of the muscle stem cell pool (122). These changes in aged-muscle, can explain at least in part, the declined regenerative potential of skeletal muscle with age.

Other studies also report that the muscle microenvironment dictates stem cell survival and differentiation potentials. For example, Jackson et al. reported that mesenchymal progenitor cells isolated from traumatized human skeletal muscle exhibited stronger adipogenic differentiation potentials compared to osteogenic or chondrogenic potentials, suggesting that muscle injury may cause alteration in these cells activity (123). Additionally, another study showed that survival and differentiation of FAPs were modulated by the environment of the recipient tissue as FAPs engrafted and formed adipocytes only when they were transplanted into

muscles injected with glycerol to induce fatty degeneration. In healthy, normal muscles, FAPs do not survive or engraft post transplantation (73). Our previous studies also demonstrated that the release of local environmental stimuli after skeletal muscle injury alters the differentiation potential of MPCs, including MDSCs, into fibrotic cells (102). All of these studies illustrate the importance of signals from the local microenvironment within the skeletal muscle on determining the function and fate of stem cells.

The effects of the muscle microenvironment on stem cell function have also been examined in the context of chronic muscle disease, such as DMD. It is now well established that many of the pathological phenotypes of DMD are not only caused by the lack of dystrophin, but are also due to the complex interactions of muscle resident stem/progenitor cells with the surrounding microenvironment (56, 95, 124). For example, adipocytes accumulated in DMD skeletal muscle may influence the skeletal muscle microenvironment by secreting various cytokines and by modifying the basal lamina (24). These changes in muscle milieu will impact stem cell function to delay repair and regeneration, but enhance inflammation, which exacerbates the disease condition. Recently, Biressi and colleagues observed that SCs isolated from *mdx* muscles have compromised myogenic potentials. These SCs were less myogenic and more fibrogenic and showed elevated expression of fibrogenic genes rather than myogenic genes.

Another study done by Saccone and colleagues also demonstrated that the dystrophic muscle environment causes changes in FAPs plasticity only in a young *mdx* mouse, which is a mild dystrophic animal model. The study shows that FAPs isolated from HDAC inhibitor (TSA) treated young *mdx* mice behave differently from their wild type (WT) controls and could form myosin heavy chain–positive myotubes (125). The authors suggest that HDAC inhibition induces two core components of the myogenic transcriptional machinery, MyoD and BAF60C, which

ultimately directs pro-myogenic differentiation at the expense of fibro/adipogenic differentiation. Under normal conditions, such as WT mice that were not exposed to TSA, FAPs are known to lack myogenic potential and thus do not directly contribute to regenerating myofibers. Importantly, the beneficial effect of HDAC inhibitors on myogenic potential of FAPs was completely lost in old *mdx* mice, which exhibit significantly more severe dystrophic features, including fat accumulation and fibrosis, compared to young *mdx* mice. Thus, FAPs isolated from TSA treated old *mdx* mice were unable to adopt a myogenic gene expression program at all (125).

As normal tissue stem/progenitor cells are ultimately responsible for tissue regeneration and repair following targeted cell- or gene-based therapies in most tissue types, including skeletal muscle, understanding how normal muscle stem/progenitor cells are influenced by dystrophic microenvironments is of great importance. Our recent studies also revealed the complexities of the dKO muscle microenvironment, including chronic inflammation, fibrosis, heterotrophic ossification, fatty infiltration as well as elevated FGF expressions compared to age-matched WT controls or *mdx* mice (24, 56), which lead us to postulate that these changes in local milieu may have significant impacts on determining fate of stem/progenitor cells in dKO muscles. Therefore, in this dissertation, we will investigate how changes in muscle micro-milieu regulate proliferation and differentiation as well as the activity of stem/progenitor cells in dKO mice.

1.6 WNT SIGNALING IN SKELETAL MUSCLE

The formation of skeletal muscle is tightly regulated process that is modulated by several different signaling pathways including wingless-type mouse mammary tumor virus integration site family (Wnt) signaling (126). Wnt is a secreted protein that is essential during embryonic muscle development and in the maintenance of skeletal muscle homeostasis in the adult (127-129). Skeletal muscles, except for some craniofacial and esophageal muscles, are derived from somites, segmented structures that form pair-wise along the anterior and posterior axis of the developing embryo, during embryonic development (130, 131). In embryonic stage, Wnt signaling is necessary to specify early somites into myogenic lineage and initiate the myogenesis. Within the embryonic MPCs, Wnt regulates expressions of Pax3, Pax7, MyoD, and Myf5, also known as myogenic regulatory factors (MRFs), key transcription factors for myogenic lineage progression (126, 132, 133). In adult skeletal muscle, both canonical and non-canonical Wnt signals are required for regulating SC differentiation and mediate the self-renewal of SCs and the growth of muscle fibers (127, 129).

1.6.1 Wnt Signaling during adult muscle regeneration

Skeletal muscle is regenerated by muscle progenitor cells. After muscle injury, satellite cells actively proliferate and differentiate into myoblasts. Afterward, they fuse together or with regenerating myofibers to repair skeletal muscle (57). The molecular events determining each step are still unclear; however, numerous investigations suggest that Wnt signaling molecules are involved in governing self-renewal and differentiation of SCs (126, 127, 134).

The canonical Wnt signals **(Fig. 4)** are mediated by Frizzled (Fzd) receptors and their low-density lipoprotein receptor-related protein (LRP) co-receptors. In the absence of Wnt molecules, constitutively synthesized cytosolic β-catenin induces the formation of degradation complex with two tumor suppressor proteins; adenomatous polyposis coli (APC) and Axin, which acts as scaffolds to capture newly synthesized β-catenin. This complex mediates phosphorylation of β-catenin by glycogen synthase kinase 3 (GSK3) and active kinase casein kinase-1 (Ck1) molecules. In the presence of Wnt ligand, Dishevelled (Dsh) is activated to recruit Axin-APC complex to LRP and this will disassemble the β-catenin degradation complex. As a result, β-catenin (lacking phosphorylation) is accumulated in the cytosol and is imported into the nucleus. In the nucleus β-catenin binds to T-cell transcription factor/lymphoid enhance factor (Tcf/Lef) upon replacement of the transcriptional Groucho repressors to activate Wnt target genes (126, 135). Several secreted antagonists control Wnt signaling activity. The non-canonical Wnt signals do not require the transcriptional activity of β-catenin and are mostly transduced through Fzd receptors without involvement of LRPs. Stimulation of Wnt could be through Fzd, other small G proteins, or JNK. By contrast to canonical Wnt, non-canonical Wnt signaling pathways are not well characterized and understood (126). Secreted Frizzled-related proteins (sFRP1, 2, 4, and 5), Frzb and Wnt inhibitory factor (Wif) can bind Wnt directly and prevent it from activating their receptors (135). Additionally, there are other Wnt antagonists that bind to the LRP co-receptors include Dickkopf 1 (Dkk1) (136) and Wise (137).

In skeletal muscle, Wnt5a, Wnt5b, Wnt7a, and Wnt4 are expressed. Early stages of muscle regeneration are linked to upregulation of Wnt5a, Wnt5b, and Wnt7a and downregulation of Wnt4 expressions whereas later stages after injury are characterized with increased Wnt7b and Wnt3a expressions (129). Several studies indicated that non-canonical Wnt signaling stimulated

by Wnt7a and Fzd7, is essential for self-renewal of SCs (127, 129). It has been reported that Wnt7a-deficient mice exhibit significantly reduced numbers of SCs following regeneration, supporting the idea that non-canonical Wnt is involved with SC proliferation (138). On the other hand, the differentiation of SCs and myoblasts are controlled mostly through canonical Wnt signaling. Several *in vitro* studies involving inhibitors of GSK3β or pharmacological activators of canonical Wnt signaling strongly supports a role for canonical Wnt signaling in facilitating the differentiation of SCs and myoblasts (127, 139). Moreover, exogenous induction of canonical Wnt signaling with Wnt3a during the early stage of muscle regeneration resulted in premature differentiation of SCs and eventually led to depletion of the stem cell pool (126). All of the above supports that Wnt molecules play critical roles in different aspects of muscle development and regeneration.

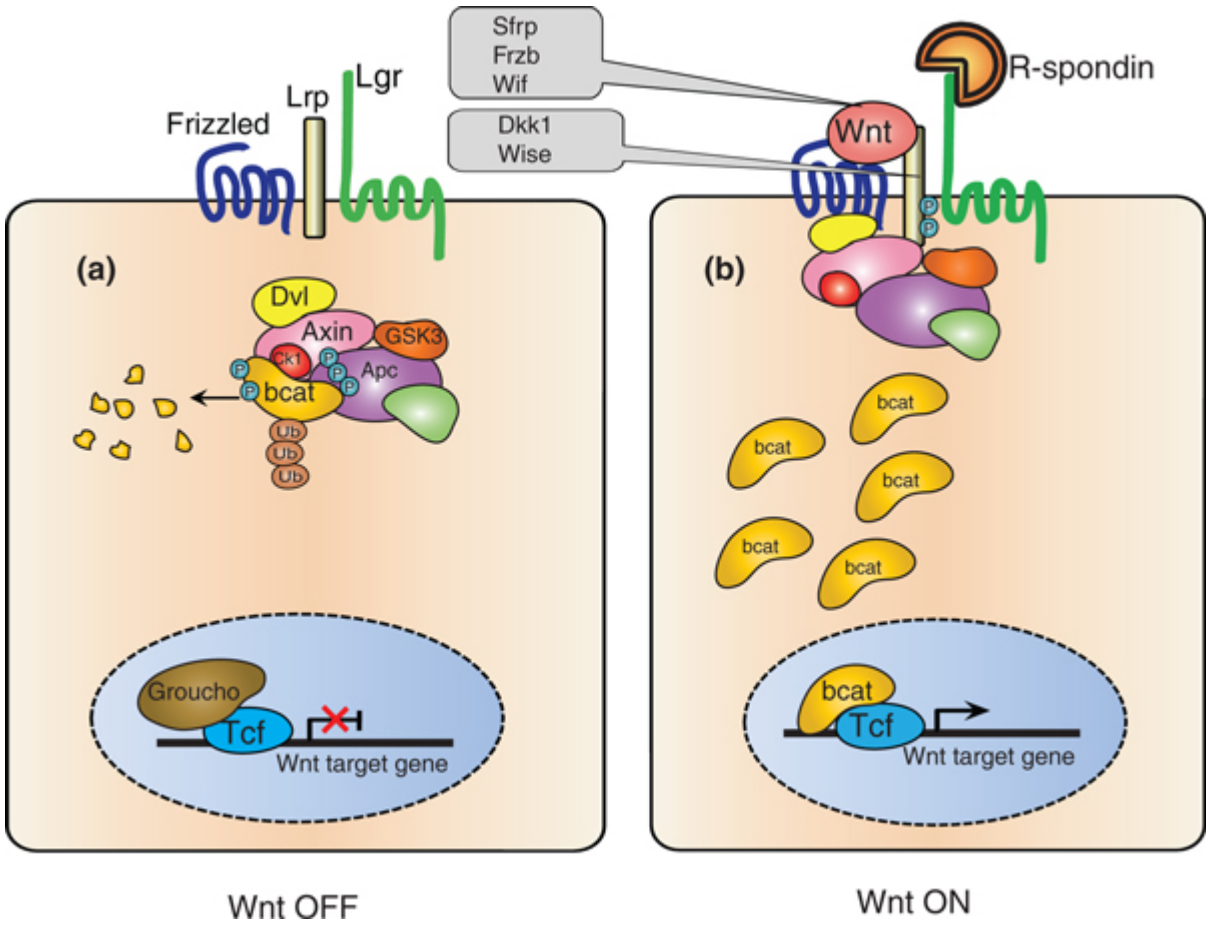

Figure 4. Overview of the canonical Wnt signaling cascades.

In canonical Wnt signaling pathway, Wnt binds to Frizzled (Fzds) receptors and their low-density lipoprotein receptor related protein 5 or 6 (LRP5/6). This will further activate dishelleved, (Dsh) to recruit β-catenin degradation complex, which consists of adenomatous polyposis coli (APC), Axin, case in kinase I (CK1) and glycogen synthase kinase-3 (GSK-3). These events free the β-catenin from degradation complex and leads to an accumulation of stabilized β-catenin (lacking phosphorylation) in the cytosol, resulting in nuclear translocation. In the nucleus, β-catenin complexes with TCF/LEF (T-cell factor/lymphoid enhancer factor) transcription factors and acts as a transcriptional co-activator to induce context-dependent Wnt/β-catenin target genes. In the absence of Wnt molecules, constitutively synthesized cyotosolic β-catenin forms degradation complex with APC, CK1, Axin, and GSK-3. This complex mediates phosphorylation of β-catenin by CK1, which further primes β-catenin and GSK-3 for proteasome-mediated degradation. (Image adapted from de Lau et al. 2012)

1.6.2 Wnt signaling during aging and disease

Wnts are well-known signaling molecules that are active in muscle tissue during development and regeneration; however, they are also involved in the build-up of connective tissue in the muscles of aged mice (121). The regenerative potential of skeletal muscle declines with age and is usually associated with increased fibrous connective tissue and adipose tissue. Interestingly, Brack and colleagues linked enhanced canonical Wnt signaling by circulating Wnt molecules or Wnt-like factors, to decreased myogenic potential of SCs with age (121). Moreover, numerous studies suggest that dysregulation of Wnt co-receptors or Wnt inhibitors occurs in multiple diseases, including cancer, osteoporosis, obesity, and cardiovascular diseases (140-142). For example, secreted frizzled related protein 1 (sFRP1), an endogenous modulator of Wnt/β-catenin signaling, participates in the paracrine regulation of human adipogenesis. It has been reported that constitutive ectopic expression of sFRP1 results in extensive adipose tissue expansion during the early stages of high fat diet (HFD) – induced obesity (140). Additionally, dysregulation of Wnt inhibitory factor 1 (Wif1) in bone marrow niche has reported to be associated with exhaustion of Hematopoietic stem cells (HSCs) (141).

It has been shown that Wnt signaling is elevated in dystrophic *mdx* muscle (95); however, the mechanism behind this Wnt signaling elevation is still unknown. Also unknown is whether Wnt is upregulated in dKO mice, a more severe dystrophic mouse model than a *mdx* mouse. Further studies are necessary to investigate if Wnt is also elevated in dKO mice and whether increased Wnt may induce any changes in function of stem/progenitor cells, including not only MPCs but also non-myogenic stem/progenitor cells in dKO mice.

1.6.3 Wnt signaling in adipogenesis

Wnt protein has an important function, not only in myogenesis, but also in adipogenesis. In general, Wnt signaling negatively regulates adipogenesis and favors myogenesis (143) and its effect on directing myogenic vs adipogenic potentials in myoblasts had been well investigated (144-146). Although myoblasts are highly committed cells for skeletal muscle regeneration, these cells are reported to exhibit plasticity in developmental potential and can be differentiated into myogenic, adipogenic, or osteogenic lineages (144). Numerous investigations demonstrated that the canonical Wnt-β-catenin pathway, likely mediated by Wnt10, has an important role in the control of intramuscular adipose tissue expansion as well as adipogenic potential of different cell types, including myoblasts (144-146). For instance, myoblasts from Wnt10b deficient mice were transdifferentiated into C/EBPα and PPAR-γ2 expressing adipocytes, suggesting that disruption in Wnt signaling may contribute to impaired myoblast regenerative capacity and to increased fat deposition in skeletal muscle (144). Additionally, these studies showed that deficiency or inhibition of Wnt10 is involved in adipose tissue deposition in skeletal muscle after cardiotoxin injury and rotator cuff tear (144, 146). These results indicated that Wnt is one of the important molecular regulators in fatty infiltration in skeletal muscle. Therefore, examining Wnt signaling in dKO mice will help the understanding of the mechanism behind the accumulation of adipose tissue in dystrophic muscles.

2.0 ISOLATION AND CHARACTERIZATION OF MULTIPOTENT, NON-MYOGENIC MESENCHYNMAL STEM CELLS RESIDING IN SKELETAL MUSCLE

2.1 INTRODUCTION

Figures 5, 6&8 of Chapter 2 are adapted from a published article in *Human Molecular Genetics:*

Jihee Sohn[1], Aiping Lu[1], Ying Tang[1], Bing Wang[1], and Johnny Huard[1,2*]. (2015) Activation of non-myogenic mesenchymal stem cells during the disease progression in dystrophic dystrophin/utrophin knockout mice. *Hum Mol Gen* In press.

[1]Stem Cell Research Center, Department of Orthopaedic Surgery, University of Pittsburgh, School of Medicine

[2]Department of Microbiology and Molecular Genetics, University of Pittsburgh School of Medicine

Mesenchymal stem cell (MSC) therapy offers the possibility of a renewable source of replacement cells and tissues to treat various types of diseases (147, 148). MSCs are especially considered a strong candidate for clinical use in injury healing because they are believed to be responsible for tissue growth, wound healing, and replacing cells during normal tissue homeostasis (149-153). Since their first identification in 1974 by Friedenstein and colleagues, MSCs, also called mesenchymal stromal cells, are characterized as a subset of fibroblast-like,

non-hematopoietic adult stem cells that originate from the mesoderm (154-156). MSCs are readily grown in culture and maintain pluripotency after prolonged culture and under appropriate stimulus, they can differentiate into cells of the mesodermal lineages, including bone, fat, and cartilage cells both *in vitro* and *in vivo* (91, 155). Interestingly, recently reported studies suggest that MSCs are able to differentiate into non-mesenchymal cell lineages as well, such as tenocytes, skeletal myocytes, and neurons (157, 158). Moreover, numerous preclinical studies suggested that MSCs are effective in treating both mesenchymal and non-mesenchymal lineage derived tissues, myocardial infarction, cornea damage, brain, spinal cord, lung injuries and in immune disorders, including systemic lupus erythematosus (SLE), amyotrophic lateral sclerosis, and Crohn's disease (147, 149, 151, 152, 159, 160). Greater research interest has developed in MSCs because they are free of both ethical concerns, can be use autologously, easy to collect, express trophic factors, and have immunomodulatory effects (161, 162).

MSCs are present in many different tissues of young and adult individuals, including adipose tissue, bone marrow, umbilical cord, lung, amniotic fluid, and even peripheral blood (147). Recently, PDGFRα^+ mesenchymal progenitors, Tie2$^+$ progenitors and Sca-1$^+$/CD34$^+$ fibro/adipogenic progenitors (FAPs) have been identified as skeletal muscle resident mesenchymal lineage cells, utilizing fluorescence activated cell sorting (FACS) (44, 73, 106, 163). Platelet derived growth factor receptor α (PDGFR α) with stem cell antigen 1 (Sca-1) are known to be expressed by a population of cells isolated from mouse bone marrow, that are highly enriched for MSCs (164, 165). Interestingly, PDGFRα^+ cells and FAPs seem to show discrepancy in their phenotypic features since PDGFRα^+ cells can undergo adipogenic, osteogenic, and chondrogenic differentiation whereas FAPs fail to give rise to mineralized bone, or cartilage under *in vitro* induction (44, 73).

Our research group has isolated various populations of muscle derived cells from skeletal muscle of mice based on their adhesion properties to type I collagen-coated flasks through utilizing a preplate technique, a marker profile-independent method (74). The most rapidly adhering cell fraction, (RAC) or preplate 1-2 (PP1-2) can be collected within 2-24 hours of isolation. The PP3-5 cells adhere within 5 days of plating and are composed of satellite cells and myoblasts. They have been shown to be mainly committed to the myogenic lineage and readily fuse to form myotubes (56). Finally, slowly adhering cell fraction (SACs) or PP6 can be collected 6 days after isolation. SACs have been characterized as muscle derived stem cells (MDSCs), which are capable of undergoing multilineage differentiation with a strong myogenic potential and self-renewing ability (98-100). MDSCs are superior when compared to myoblasts for muscle regeneration and repair (75). RACs, have been shown to be comprised of mostly fibroblastic-like cells with no myogenic potential; however, they have never been thoroughly characterized (74).

In this study, we isolated the PP1, or RACs that are attached to the flask within two hours of preplating and characterized them as non-myogenic mesenchymal stem cells (nmMSCs) with adipogenic, osteogenic, and chondrogenic differentiation potentials. The nmMSCs express PDGFRα and Sca-1 proteins, but lack desmin or Pax7 expressions and has no myogenic potential. Further immunostaining of muscle cryosections indicated that the nmMSCs were located at the muscle interstitium, which separates them physically from satellite cells (SCs), which are located underneath the basal lamina. Results shown here indicated that preplate technique successfully enabled us to isolate a population of multipotent, non-myogenic MSCs from skeletal muscle independent of cell surface marker profiles.

2.2 MATERIALS AND METHODS

Animals: C57BL/10J (wild type; WT) mice were purchased from the Jackson Laboratory (Bar Harbor, ME). Mice ranged in age from 3 to 8 weeks. Specific ages for each experiment are described below. All animal protocols used for these experiments were approved by the University of Pittsburgh's Institutional Animal Care and Use Committee.

Cell isolation and culture: Primary non-myogenic mesenchymal stem cells (nmMSCs) and muscle derived stem cells (MDSCs) were isolated from 3 - 8 week old WT mice using a modified preplate method previously described (56, 74, 166). Briefly, following enzymatic digestion of skeletal muscle tissue, muscle derived cells were re-plated on collagen type I (C9791, Sigma-Aldrich) coated flasks over a period of days. Two hours after isolation, a rapidly adhering cell population was collected and characterized as nmMSCs. Six days after preplating, a slowly adhering cell population was obtained, which has been described to contain the MDSC fraction of cells (75). The nmMSCs and MDSCs were cultured in proliferation medium (PM) containing 10% fetal bovine serum, 10% horse serum, 0.5% chick embryo extract and 1% Penicillin-Streptomycin in Dulbecco's modified Eagle's medium (DMEM, 11995-073, Invitrogen).

Immunophenotyping: Flow cytometry was performed on nmMSCs and MDSCs. One-hundred thousand WT-nmMSCs and WT-MDSCs were collected, washed with PBS containing 2% FBS, centrifuged, and then placed on ice. The cells were then re-suspended in a 1:10 dilution of mouse serum (M5905, Sigma-Aldrich) in PBS and incubated for 10 minutes. PE-conjugated rat anti-PDGFRα (12140181, eBioscience) and FITC-conjugated rat anti-CD34 (553733, BD) were added to each tube (1µl/100,000 cells) and incubated for 30 minutes on ice. Only one antibody was used in each tube. The cells were then rinsed in 300µl of cold washing buffer (2%

FBS in PBS, 4 degrees). A single color antibody was used to optimize fluorescence compensation settings for multicolor analyses.

mRNA analysis was performed via reverse transcriptase polymerase chain reaction (RT-PCR): Total RNA was obtained from nmMSCs and MDSCs isolated from 6-8 week old WT animals using Trizol reagent (Invitrogen) and a RNeasy Mini Kit (Qiagen, Valencia, CA) according to the manufacturer's instructions. Reverse transcription was performed using a Maxima first strand cDNA synthesis kit (Fermentas) according to the manufacturer's protocol. PCR reactions were performed using an iCycler Thermal Cycler (Bio-Rad) as previously described (24) and PCR products were separated by electrophoresis with 1% agarose gels. The primers used for PCR are listed in Table 1. Each set of oligonucleotides were designed to span two different exons to avoid background amplification of genomic DNA. The data was quantified by densitometry using Adobe Photoshop 7.0.

Gene	Forward primer	Reverse primer	Location
desmin	AACCTGATAGACGACCTGCAG	GCTTGGACATGTCCATCTCCA	615-873
Pax7	GTGCCCTCAGTGAGTTCGAT	CCACATCTGAGCCCTCATCC	499-667
Sca-1	CCTACTGTGTGCAGAAAGAGC	CAGGAAGTCTTCACGTTGACC	89-331
PDGFRα	GACGAGTGTCCTTCGCCAAAGTG	CAAAATCCGACCAAGCACGAGG	1658-1976
β-actin	CCACACCCGCCACCAGTTCG	TACAGCCCGGGGAGCATCGT	234-772

Table 2. Primer sequences used in Chapter 2.

Immunofluorescence staining: Muscle cryosections or cells were fixed with 4% paraformaldehyde for 10 minutes and blocked with 10% donkey serum plus 0.1% Triton X-100 for 1 hour at room temperature. Slides or cells were then incubated with goat anti PDGFRα (1:100, R&D) or chicken anti-mouse laminin (1:500, Abcam) in 5% donkey serum. Next,

sections were incubated with secondary antibodies including Alexa488-conjugated anti-goat IgG (1:300, Invitrogen) or Alexa594-conjugated anti-chicken IgG (1:300, Invitrogen) in PBS for 45 minutes. WT-nmMSCs and WT-MDSCs were fixed and permeabilized with 10% formalin plus 0.1% Triton X-100 for 10 minutes at room temperature and rinsed 2 times with PBS. Cells were stained for Pax7 or desmin using a mouse monoclonal anti-Pax7 antibody (1:150, DSHB, Iowa city, Iowa) and mouse monoclonal anti-desmin antibody (1:100, Sigma) with a mouse-on-mouse (M.O.M) staining kit (Vector Labs, Burlingame, CA), according to manufacturer's directions.

Differentiation Assays

Adipogenic differentiation assay: A total of 35,000 nmMSCs were cultured in 24-well collagen type I-coated plates for 21 days in adipogenic differentiation medium (PT-3004, Lonza). When the cells reached 100% confluence, three cycles of induction/maintenance medium were applied to the cells to induce optimal adipogenic differentiation. Each cycle consisted of incubating the nmMSCs with supplemented adipogenic induction medium and cultured for 2-3 days, followed by 2-3 days of culture in supplemented adipogenic maintenance medium. At the end of the third cycle, the cells were incubated in adipogenic maintenance medium for an additional 5-7 days. Adipogenesis was assessed using Oil Red O (O0625, Sigma-Aldrich) to stain for intracellular lipid accumulation. For adipocyte differentiation quantification, cells were stained with AdipoRed (NC9049267, 30µl/ml, Fisher) and DAPI, and fluorescence intensities were analyzed with a spectrophotometer. The AdipoRed fluorescence emission readings were normalized to the total number of cells in each well.

Osteogenic differentiation assays: A total of 35,000 nmMSCs were cultured in osteogenic medium which contained DMEM, 10% FBS, supplemented with dexamethasone (D2915, 0.1µM, Sigma-Aldrich), ascorbic-acid-2-phosphate (A8960, 50µg/ml, Sigma-Aldrich), 10mM β-

glycerophosphate (G6251, Sigma-Aldrich), and BMP2 (M11306AAB, 100ng/ml, Medtronic). Osteogenesis was assessed using a Fast Blue Alkaline Phosphatase (ALP) kit (041M4338, Sigma) and by staining mineralized matrix with alizarin red. ALP activity was quantified with an ELISA-based assay according to the manufacturer's protocol (123).

Chondrogenic differentiation assays: A micromass culture technique was used as described by Kishimoto and colleagues (167). One-hundred thousand cells were incubated for a week in chondrogenic induction medium (PT3003, Lonza) supplemented with 100ng/ml BMP2 and 20ng/ml TGFβ3 (PHG9305, Invitrogen). Micromass cultured cells were fixed with 10% formalin and stained with 1% alcian blue (pH 1.0) for 30 min. For quantification, 250,000 cells were cultured in pellets for 4 weeks in chondrogenic induction media. Sulphated glycosaminoglycans (GAGs) production was quantified using a Blyscan assay kit (Biocolor, Carrickfergus) according to the manufacturer's protocol.

Myogenic differentiation: 30,000 cells were plated on 24-well plates in DMEM supplemented with 2% FBS (Fusion medium, FM) to stimulate myotube formation. Three days after differentiation, the cells were fixed with 10% formalin for 8 min and bright field images were taken.

Statistical analysis: Data from ≥ 4 samples from each subject were pooled for statistical analysis. Results are given as means ± SD. Statistical significance of any difference was calculated using Student's *t* test. Values of $p < 0.05$ were considered statistically significant.

2.3 RESULTS

Isolation of rapidly adhering cells (RACs) utilizing preplate technique.

Utilizing the preplate technique, rapidly adhering cells (RACs) were obtained within 2 hours of isolation, which is similar to the isolation method utilized to collect bone marrow derived mesenchymal stem cells (BM-MSCs) (168), and muscle derived stem cells (MDSCs) were obtained 6 days after isolation **(Fig. 5)**. RACs were isolated from skeletal muscles of 3-6 week old wild type (WT) mice and characterized by examining their cell surface markers and stem cell behaviors. After 3-4 passages, the RAC population **(Fig. 5B)** had a very similar morphology to that of BM-MSCs **(Fig. 5A)**, which is substantially different from the MDSCs that are small, spherical and refractive under phase contrast microscopy **(Fig. 5C)**.

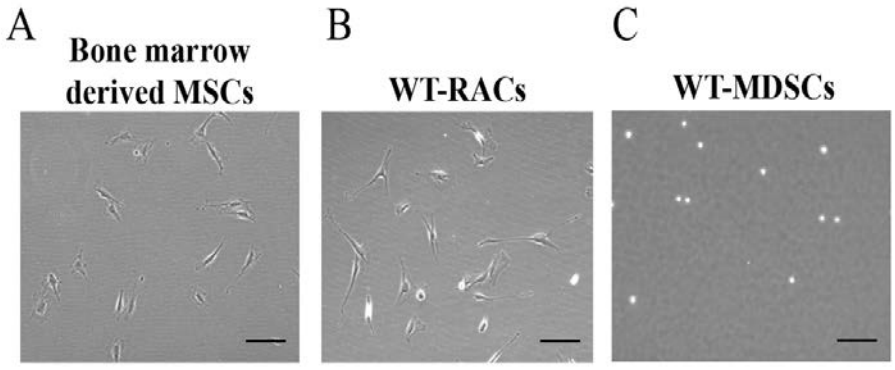

Figure 5. Morphology of rapidly adhering cells (RACs) isolated from skeletal muscle.

Phase contrast microscopy images of (A) bone marrow derived mesenchymal stem cells (MSCs), (B) RACs, and (C) muscle derived stem cells (MDSCs) isolated from 3-6 week old WT mice. Scale bar = 50μm.

RACs and MDSCs are expressing different markers.

Next, we performed RT-PCR, flow cytometry of PDGFRα and CD34, and immunostaining for muscle progenitor cell markers (MPCs), Pax7 and desmin, to identify progenitor lineages from dissociated skeletal muscle. RT-PCR analysis **(Fig. 6A)** and quantification **(Fig. 6B)** of the relative gene expression levels in the MDSCs and RACs showed that the MDSCs expressed significantly higher levels of Pax7 and desmin, while the RACs expressed significantly higher levels of Sca-1, which is expressed by progenitor populations of multiple tissues (73), and PDGFRα, a well-known marker of mesenchymal stem cells (MSC) (44). Further flow cytometry analysis of PDGFRα indicated that more than 99% of the MDSCs were PDGFRα negative **(Fig. 6C)** while nearly 99% of the RACs were PDGFRα positive. We next examined the expression of desmin and PDGFRα protein by immunostaining and observed that the RACs expressed PDGFRα while the MDSCs expressed desmin **(Fig. 6D&F)**. Lastly, immunostaining for Pax7 showed that nuclear-localized Pax7 expression was only observed in MDSCs and not in the RACs **(Fig. 6E&F)**. Therefore, upon myogenic induction, only MDSCs were able to differentiate into myotubes **(Fig. 6E)**. These results suggested that preplate technique enabled us to prospectively isolate myogenic progenitors (MDSCs) and non-myogenic progenitor cells (RACs) from skeletal muscle.

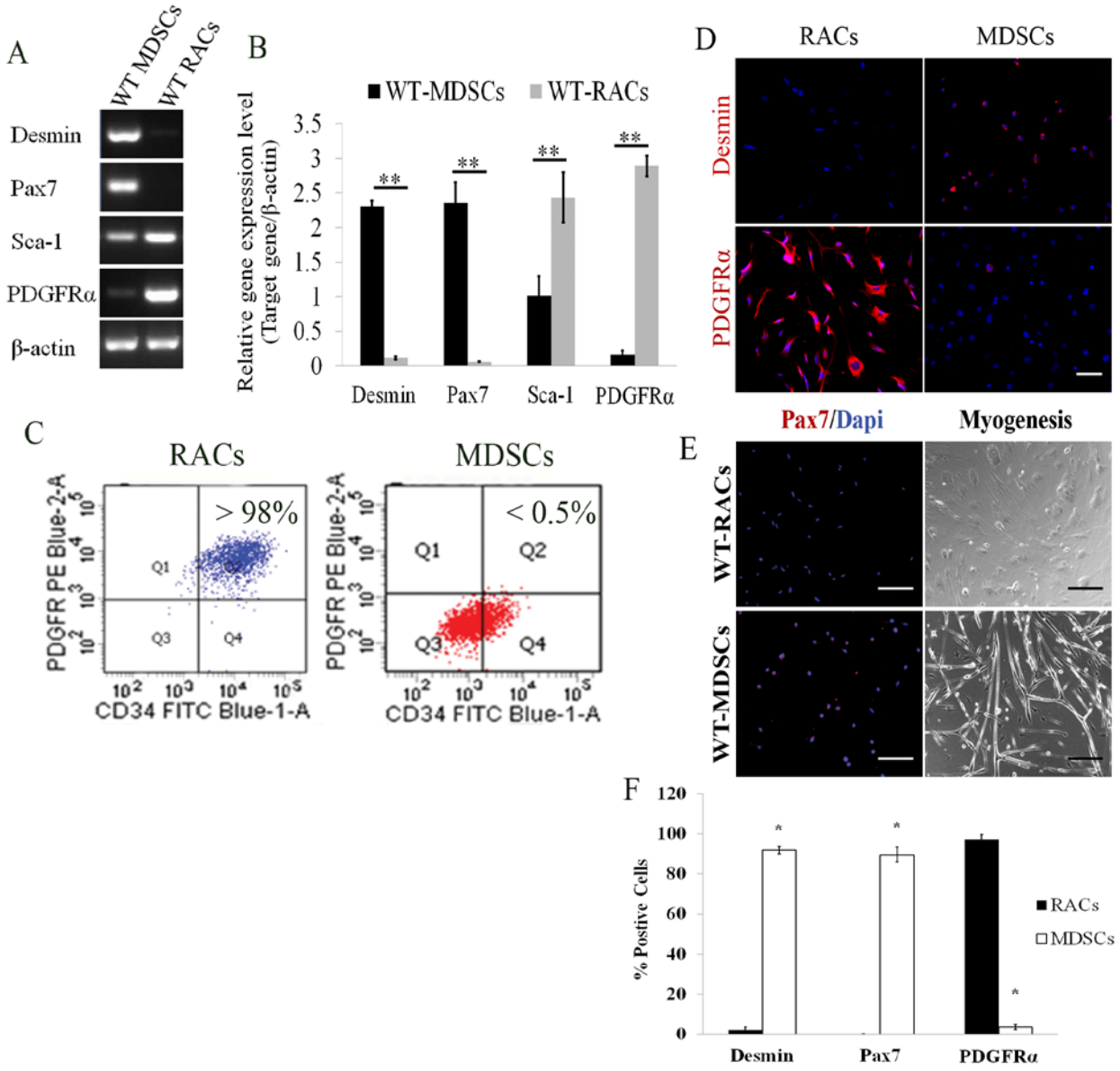

Figure 6. Phenotypic characterization of the WT- RACs and the WT-MDSCs.

(A) RT-PCR analysis of lineage markers desmin, Pax7, Sca-1, and PDGFRα of freshly isolated WT-MDSCs and WT-RACs. (B) Quantification of desmin, Pax7, Sca-1, and PDGFRα expression levels by the WT-RACs and the WT-MDSCs. (C) Fluorescence activated cell sorting (FACS) plots show that the RACs are CD34 and PDGFRα positive cells while the MDSCs are PDGFRα negative cells. (D) Immunostaining for desmin and PDGFRα were performed. scale bar = 25μm (E) Immunostaining for Pax7 indicated that the WT-RACs are Pax7 negative and are unable to differentiate into myotubes, while WT-MDSCs are Pax7 positive and are highly myogenic, scale bar = 50μm. (F) Quantification of immunostaining of desmin, PDGFRα, and Pax7. (n=3). Error bars indicate 'mean ± SD'. * p <0.05.

Anatomic localization of RACs in skeletal muscle.

Next, we examined the anatomical localization of the RACs in the skeletal muscle. We performed immunostaining for PDGFRα, Pax7, and laminin in gastrocnemius muscle (GAS) cryosections from 4 week old WT mice **(Fig. 7)**. PDGFRα^{+} RACs were localized at the interstitial space of muscle tissue, **(Fig. 7C-E)** whereas Pax7^{+} cells, most likely satellite cells, were located beneath the basement membrane as indicated by laminin staining **(Fig 7A, B, and E)**. These localizations suggest that PDGFRα^{+} cells and Pax7^{+} muscle progenitor cells represent discrete cell populations.

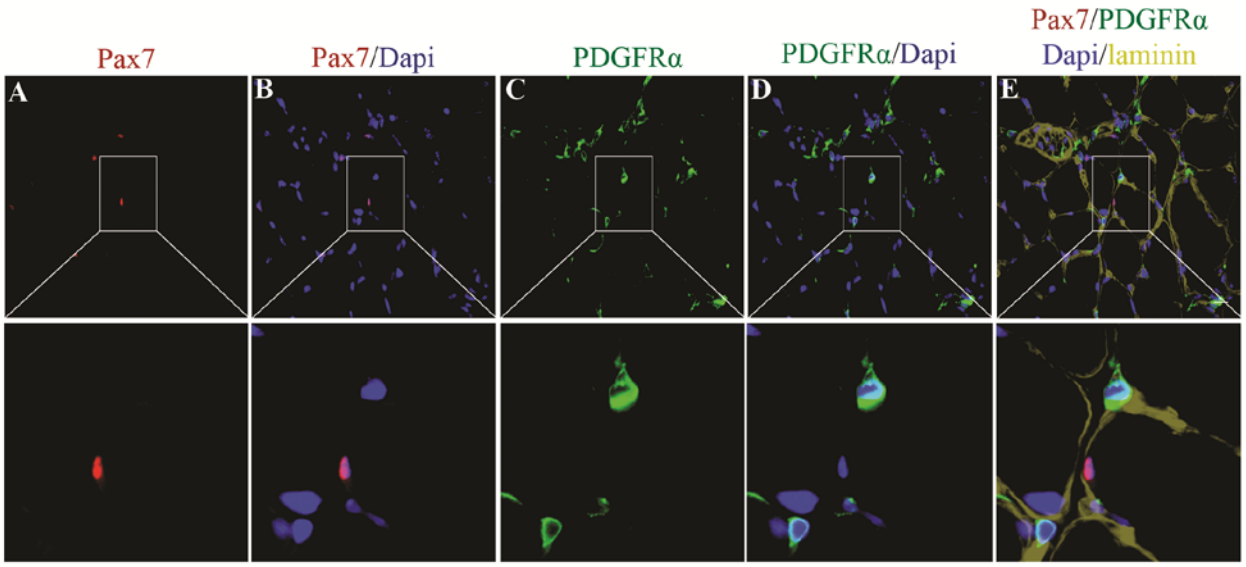

Figure 7. Localization of PDGFRα^{+} cells in adult skeletal muscle.

(A-E) Gastrocnemius muscle sections were stained with antibodies against Pax7, PDGFRα, and laminin (A); Pax7 (B); Pax7 and Dapi (C); PDGFRα (D); PDGFRα and Dapi (E); Pax7, PDGFRα, Dapi, and laminin. PDGFRα^{+} cells were located at the interstitial space of muscle tissue while Pax7^{+} cells were localized under the basal lamina. Scale bar = 25μm

Multilineage differentiation potentials of WT-RACs.

The biological property that most uniquely identifies MSCs is their capacity for trilineage mesenchymal differentiation (91). We confirmed that under appropriate induction conditions, the WT-RACs exhibited evidence of osteogenic, adipogenic, and chondrogenic differentiation potentials **(Fig. 3)**. The WT-RACs upregulated their surface expression of alkaline phosphatase (ALP) and began to generate a mineralized deposits, which was visualized with Alizarin Red staining, under osteogenic conditions **(Fig. 3A)**. Under adipogenic conditions, WT-RACs also accumulated intracellular lipid, which was visualized with AdipoRed staining **(Fig. 3B)**. Furthermore, WT-RACs began to express sulphated glycosaminoglycans (GAGs), which were visualized with alcian blue staining, under chondrogenic conditions **(Fig. 3C)**. Based on the RAC's marker expression and their trilineage differentiation capacities **(Fig. 2&3)**, we referred to the RACs as non-myogenic mesenchymal stem cells (nmMSCs).

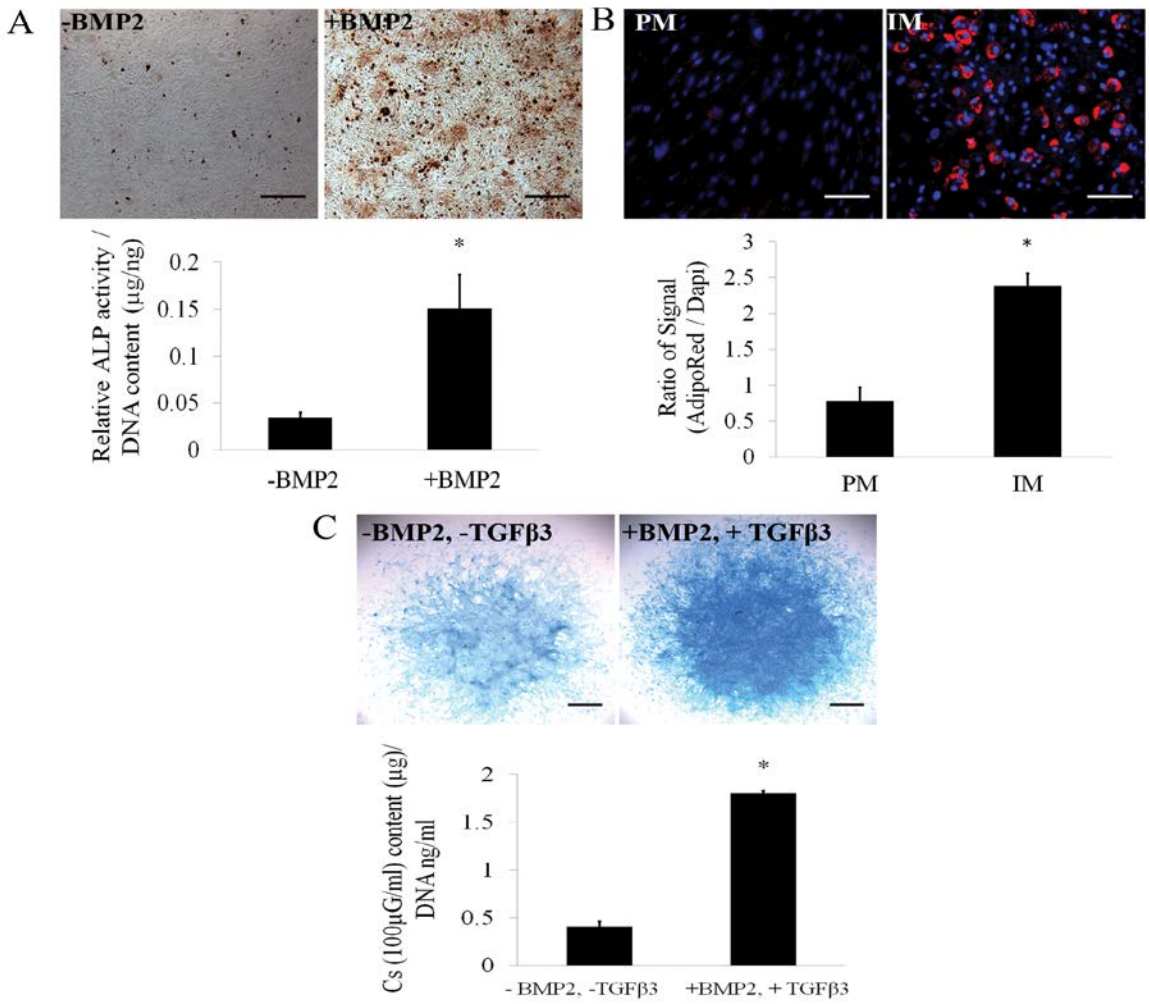

Figure 8. Trilineage differentiation potentials of the WT-RACs.

The WT-RACs were able to undergo (A) osteogenic (Alizarin Red staining for mineralization) (B) adipogenic (AdipoRed staining for lipid accumulated in the cells) and (C) chondrogenic differentiation (Alcian blue staining for glycosaminoglycans and chondroitin sulfate (Cs)) (n>4). Error bars indicate 'mean ± SD'. * p <0.05. Scale bar = 50µm.

2.4 DISCUSSION

Mesenchymal stem cells (MSCs) are adult stem cells traditionally found in the bone marrow, but they can be harvested from a variety of adult tissues. Here we isolated the non-myogenic MSCs from mouse skeletal muscle and examined their marker profiles and differentiation potentials. Cells were obtained after two hours of isolation using previously published modified preplate technique and further analyzed for their cell surface marker expressions. Although RACs were previously considered as fibroblast-like cells, our data from this study suggest that RACs are strongly positive for the expressions of Sca-1 and PDGFRα, mesenchymal stem cell surface markers. Further differentiation assays confirmed that RACs can undergo adipogenesis, osteogenesis, and chondrogenesis, but fail to undergo myogenesis as they lack Pax7 and desmin expression. Based on their marker expression and trilineage differentiation potentials, we termed RACs as non-myogenic mesenchymal stem cells (nmMSCs).

Other groups also have reported MSCs isolated from skeletal muscle using FACS, a method used to isolate and purify cells on the basis of cell surface markers. Sca-1, PDGFRα, and/or CD34 are reported to be highly expressed by muscle resident MSCs (44, 73, 163, 169); however, isolating stem cells based on the cell surface marker has some limitations. First, the degree of marker expressions may change during cell expansion and under different cell culture conditions. For example, it has been reported that positive or negative CD34 expression on MSCs is controversial and likely a consequence of cell culturing (170-172). The CD34 antigen, a transmembrane cell surface glycoprotein, has been reported as a hematopoietic stem cell (HSC) marker (173), and only recently, has a population of $CD34^+$ cells been found in mouse skeletal muscle (77, 169). In the past, The Mesenchymal and Tissue Stem Cell Committee of the International Society for Cellular Therapy stated the minimal criteria for identifying MSCs is

lack of CD34 expression (91); however, more recently, it has been suggested that lack of CD34 expression is not reliable since the expression of CD34 is a potential culture-inducing phenomena (170). In fact, some studies have reported persistent CD34 expression in cultured murine MSCs, although they were initially sorted as $CD34^-$ population (174, 175). In contrast, other studies indicated that CD34 protein is either gradually downregulated or modified to a form that is nonreactive to CD34 antibodies during cell culture (176-178).

Another possible problem with FACS isolated stem cell is that defined cell markers for MSCs may not be exclusive to MSCs but are shared with other populations. For instance, Sca-1 is known to be expressed by stem/progenitor cells of many different tissues and is expressed by SCs as well as MDSCs (77). Furthermore, CD70, CD90, and CD105 antigens have been used to identify MSCs; however, these three markers are co-expressed in a wide variety of cells, including fibroblasts, chondrocytes, and hematopoietic progenitor cells, neurons, and endothelial cells (171, 179). Therefore, even when used in combination, they are certainly incapable of identifying MSCs.

Characterization of the nmMSCs indicated that we have isolated two heterogeneous, but highly purified, functionally different cell populations, nmMSCs and MDSCs, residing in the skeletal muscle. It has been reported that MDSCs are $Pax7^+$ multipotent, muscle progenitor cells (MPCs) with high myogenic regeneration potentials both *in vitro* and *in vivo* (74, 75, 80). We confirmed that the nmMSCs are 100% $Pax7^-$ cells that are unable to fuse, and therefore, the nmMSCs are unlikely to contain MDSCs. Moreover, since the MDSCs are Pax7 positive and highly myogenic in nature (myotube formation) and are PDGFRα negative (>99%), it is unlikely that MDSCs contain nmMSCs.

As we already mentioned, other studies also have reported the presence of non-myogenic cell populations in skeletal muscles of mouse and human that exhibit mesenchymal lineage differentiation or regeneration potentials. These cell populations include PDGFRα^+ mesenchymal progenitors (44, 163), fibro/adipogenic progenitors (FAPs), and mesenchymal progenitor cells (123). These cells possess abilities to become adipocytes, osteoblasts, and chondrocytes, but fail to form myotubes. Our results indicate that the cell surface marker expression, multipotency, and the anatomical location of the nmMSCs are very similar to that of these cells reported by others. Although Joe and colleagues initially reported that FAPs do not differentiate into osteogenic cells *in vitro* (73), studies done by Goldhamer and colleagues demonstrated that FAPs also possess osteo-/chondrogenic potentials *in vivo* (106). Osteogenic potential of FAPs were probably underestimated since osteogenesis performed by Joe and colleagues was only assessed *in vitro* without bone morphogenic protein (BMP) in induction medium. Taken together, our data suggest that preplate technique is highly efficient in isolating stem/progenitor cells from skeletal muscle.

More interestingly, mesenchymal progenitor cells isolated from traumatized human muscle tissue were reported to be multipotent, although somewhat limited compared to bone marrow derived MSCs (BM-MSCs), and exhibit trophic properties of stem cells, including immunoregulatory and pro-angiogenic effects (123). These studies, including ours, suggest that previously recognized muscle fibroblasts may represent multipotent MSCs, which can be used as a substitute for BM-MSCs for regenerative medicine therapies. One important area that remains unclear is whether these nmMSCs maintain their multi-lineage potentials *in vivo.* Therefore, future studies focusing on examining the *in vivo* characteristics and behavior of nmMSCs will be necessary.

In conclusion, the preplate technique was utilized to isolate rapidly adhering cells that are strongly positive for PDGFRα and Sca-1 and exhibit multipotency *in vitro*. These cells have no ability to undergo myogenic differentiation and therefore are named non-myogenic mesenchymal stem cells (nmMSCs). Lacking myogenic potential restricts nmMSCs' utility for muscle regeneration and repair; however, their capacity for adipocyte, osteocyte, and chondrocyte differentiation suggest that they might be a useful cell source for tissue repair especially bone and articular cartilage regeneration and repair.

3.0 ACTIVATION OF NON-MYOGENIC MESENCHYMAL STEM CELLS DURING THE DISEASE PROGRESSION IN DYSTROPHIC DYSTROPHIN/UTROPHIN KNOCKOUT MICE

3.1 INTRODUCTION

Chapter 3 is adapted from a published article in *Human Molecular Genetics:*

Jihee Sohn[1], Aiping Lu[1], Ying Tang[1], Bing Wang[1], and Johnny Huard[1,2*]. (2015) Activation of non-myogenic mesenchymal stem cells during the disease progression in dystrophic dystrophin/utrophin knockout mice. *Hum Mol Gen* In press.

[1]Stem Cell Research Center, Department of Orthopaedic Surgery, University of Pittsburgh, School of Medicine

[2]Department of Microbiology and Molecular Genetics, University of Pittsburgh School of Medicine

Adult skeletal muscle possesses a remarkable regenerative ability dependent on muscle progenitor cells such as satellite cells which reside beneath the basal lamina, closely juxtaposed to the muscle fibers (57, 180, 181). Despite the presence of these muscle regenerative cell populations, skeletal muscle integrity can be debilitated by the deposition of adipose and fibrotic

tissues in a variety of pathological conditions including Duchenne muscular dystrophy (DMD) (21, 22).

DMD is one of the most common childhood muscular dystrophy, with an incidence of approximately one in every 3,500 live male births (182). It is an X-linked, inherited disease caused by a lack of functional dystrophin, an essential transmembrane muscle protein within the dystrophin-glycoprotein complex in both skeletal and cardiac muscle cells (2, 3). In dystrophic muscle, the damaged fibers degenerate, undergo necrosis, and lose their ability to regenerate during the progression of the disease. Satellite cells are recruited to regenerate new myofibers, but this regeneration is often inefficient due to repeated cycles of degeneration and regeneration, which eventually leads to an exhaustion/depletion of the satellite cell population (9). Progressive muscle weakness and degeneration usually leads to the loss of independent ambulation by the middle of the patient's second decade and a fatal outcome due to cardiac or respiratory failure by their third decade of life (10, 11).

Recent evidence has emerged implicating adult stem cell dysfunction in the progression of histopathology in DMD. These studies have reported that the rapid progression of muscle weakness in DMD might correlate with the decline in the number of functional muscle progenitor cells (MPCs) (56, 124, 183). Of note, despite the lack of dystrophin from birth, the onset of the muscle weakness typically does not occur until patients reach 4-8 years of age, which happens to coincide with the exhaustion/depletion of the MPC pool due to the repeated cycles of degeneration and regeneration that the muscle fibers undergo (9, 183).

One of the most striking pathological conditions in advanced cases of DMD is the accumulation of adipocytes, calcium deposits, and fibrosis. Importantly, even with the occurrence of MPC depletion, we observed the formation of more adipose and fibrotic tissue in

the skeletal muscle, heart, and diaphragm of 6-8 week old dKO mice compared to age-matched *mdx* mice (24, 56). However, it remains unclear what cell population is responsible for the formation of these non-skeletal muscle tissues. Of note, although the *mdx* mouse is commonly used as an animal model of DMD, 6-8 week old *mdx* mice exhibit only a mild dystrophic phenotype (muscle fiber degeneration and necrosis) and do not develop the severe histopathologies exhibited by age matched dKO mice, such as the accumulation of calcium deposits and fibrosis (56). Therefore, we focused this study on examining a population of cell potentially responsible for the formation of the above dystrophic histopathology.

Our research group has isolated two distinct populations of muscle derived cells from the skeletal muscle of dKO mice utilizing a previously published preplate technique (74); 1) a rapidly adhering cell (RAC) fraction, and 2) a slowly adhering cell (SAC) fraction. In previous publications, we characterized the SACs as a heterogeneous population of $Pax7^{+}$ cells called muscle-derived stem cells (MDSCs), which are muscle progenitor cells (MPCs) with high myogenic potentials, both *in vitro* and *in vivo* (74, 75, 79). We recently reported that MPCs isolated from 6-8 week old dKO mice display a significant reduction in their proliferation capacity, resistance to oxidative stress, and multilineage differentiation potentials, when compared to MPCs isolated from age-matched *mdx* and WT mice. These results suggest that in contrast to *mdx* and WT mice, rapid stem cell depletion occurs in the dKO mice (56). We therefore postulated that the decline in MPCs may be responsible for the progressive reduction in muscle regeneration and the rapid occurrence of the histopathology observed in the dKO mice (56). Since MPCs become impaired during the progression of the disease, it is unlikely that these cells are involved in the formation of ectopic non-muscle tissues. In the previous chapter, we characterized RACs as non-myogenic mesenchymal stem cells (nmMSCs) that are highly

positive for PDGFRα, Sca-1 and CD34 (77), cell surface markers that are also expressed by fibro/adipogenic progenitors (FAPs) (73); however, their role in skeletal muscle has not been thoroughly investigated. Therefore, we hypothesized that the RACs might be responsible for the deposition of fibrotic tissue, ectopic bone and fat observed in dystrophic mice.

In this study, we show that the rapid accumulation of lipids, calcium deposits, and fibrosis correlate with the progression of the disease in dKO mice. We determined that the proliferation and adipogenic/osteogenic potentials of nmMSCs isolated from 1, 4, and 6-8 week old dKO mice were progressively activated as the disease progresses, suggesting that the activation of nmMSCs is closely associated with the deposition of non-muscle tissues in the dKO mice. In addition, 6-8 week old dKO-nmMSCs displayed significantly enhanced proliferation potentials, *in vitro* and *in vivo,* as was their adipogenic, osteogenic, and fibrogenic differentiation capacities, in comparison to age-matched WT-nmMSCs. Our co-cultivation study further suggests that the activated dKO-nmMSCs exert a negative effect on dKO-MDSCs by inhibiting their myogenic potential (reduced ability to form myotubes). Results shown here indicate that activation of nmMSCs is not only closely associated with the rapid occurrence of fibrosis, ectopic calcification and fat accumulation, but may also contribute to continuous muscle degeneration and weakness in the dystrophic dKO mice.

3.2 MATERIALS AND METHODS

Animals: C57BL/10J (wild type; WT) mice were purchased from the Jackson Laboratory (Bar Harbor, ME). Dystrophin/utrophin knockout (dKO) mice, originally characterized by Deconinck and colleagues (51), were generated by crossing heterozygous dystrophin-/-; utrophin+/- mice

(55, 184). Genotyping was performed by polymerase chain reaction (PCR) analysis of tail samples. Mice ranged in age from 5 days to 8 weeks. Specific ages for each experiment are described below. All animal protocols used for these experiments were approved by the University of Pittsburgh's Institutional Animal Care and Use Committee.

Cell isolation and culture: Primary WT and dKO non-myogenic mesenchymal stem cells (nmMSCs) and muscle derived stem cells (MDSCs) were isolated from 1 - 8 week old WT and dKO mice using a modified preplate method previously described (56, 74, 166). Briefly, after enzymatic digestion of skeletal muscle tissue, muscle derived cells were re-plated on collagen type I (C9791, Sigma-Aldrich) coated flasks over a period of days. Two hours after isolation, a rapidly adhering cell population was collected and characterized as nmMSCs. Seven days after preplating, a slowly adhering cell population was obtained, which has been described to contain the MDSC fraction of cells (75). nmMSCs and MDSCs were cultured in proliferation medium (PM) containing 10% fetal bovine serum, 10% horse serum, 0.5% chick embryo extract and 1% Penicillin-Streptomycin in Dulbecco's modified Eagle's medium (DMEM, 11995-073, Invitrogen)

Immunophenotyping: Flow cytometry was performed on WT- and dKO-nmMSCs at the end of their third expansion passage. One-hundred thousand WT and dKO nmMSCs were collected, washed with PBS containing 2% FBS, centrifuged, and then placed on ice. The cells were then re-suspended in a 1:10 dilution of mouse serum (M5905, Sigma-Aldrich) in PBS and incubated for 10 minutes. PE-conjugated rat anti-PDGFRα (12140181, eBioscience), PE-conjugated rat anti-Sca-1 (553108, BD), FITC-conjugated rat anti-CD34 (553733, BD), APC-conjugated rat anti-CD90 (553007, BD), PE-conjugated rat anti-CD105 (562759, BD), and FITC-conjugated rat anti-CD45 (553080, BD) were added to each tube (1µl/100,000 cells) and

incubated for 30 minutes on ice. Only one antibody was used in each tube. The cells were then rinsed in 300µl of cold washing buffer (2% FBS in PBS, 4 degrees). A single color antibody was used to optimize fluorescence compensation settings for multicolor analyses.

Immunofluorescence and histology: Muscle cryosections were fixed with 5% formalin for 8 minutes and blocked with 10% donkey serum for 1 hour. Slides were then incubated with goat anti PDGFRα (1:100, R&D) and rabbit anti-mouse Ki67 (1:200, Abcam) or chicken anti-mouse laminin (1:500, Abcam) in 5% donkey serum. Next, sections were incubated with secondary antibodies including Alexa594-conjugated anti-rabbit IgG (1:300, Invitrogen), Alexa594-conjugated anti-chicken IgG (1:300, Invitrogen), or Alexa488-conjugated anti-goat IgG (1:300, Invitrogen) in PBS for 45 minutes.

Differentiation Assays

Adipogenic and osteogenic differentiation assays: Adipogenic and osteogenic differentiation was performed as described in Chapter 2. After differentiation, adipogenic cells were stained with rabbit anti-PPARγ (1:200, Cell Signaling) or goat anti-C/EBPα (1:50, Santa Cruz Biotechonology) in 5% donkey serum in PBS.

Myogenic differentiation: 30,000 cells were plated on 24-well plates in DMEM supplemented with 2% FBS (Fusion medium, FM) to stimulate myotube formation. Three days after differentiation, the cells were fixed with 10% formalin for 8 min, and stained for fast myosin heavy chain (fMyHC) using a mouse anti-MyCHf antibody (1:250, M4276, Sigma-Aldrich). The primary antibody was detected using a mouse-on-mouse (M.O.M) staining kit (Vector Labs, Burlingame, CA), according to manufacturer's directions.

Fibrogenic differentiation: 10,000 cells were plated on 24-well plates in PM supplemented with TGFβ1 (5ng/mL, R&D) for 3-5 days. After differentiation, fibrotic cells were

stained with mouse anti-collagen I (1:400, Abcam) using a M.O.M kit or rabbit anti-collagen III (1:500, Abcam) in 5% donkey serum.

mRNA analysis was performed via reverse transcriptase polymerase chain reaction (RT-PCR): Total RNA was obtained from nmMSCs, MDSCs and gastrocnemius muscle tissues isolated from 6-8 week old WT animals using Trizol reagent (Invitrogen) and a RNeasy Mini Kit (Qiagen, Valencia, CA) according to the manufacturer's instructions. Reverse transcription was performed using a Maxima first strand cDNA synthesis kit (Fermentas) according to the manufacturer's protocol. PCR reactions were performed using an iCycler Thermal Cycler (Bio-Rad) as previously described (24). Realtime RT-PCR was carried out using a Maxima Syber Green Assay kit (Thermo Scientific) in an iQ5 thermocycler (Bio Rad). Primers used in the study can be found in Table 2.

Cell proliferation: To compare the proliferative potentials of the WT and dKO-nmMSCs, a Live Cell Imaging system (LCI) (Kairos Instruments LLC) was used as previously described (185). In triplicate, 5000 nmMSCs per well were plated in a 24 well plate and incubated in a biobox incubator that sits atop a Nikon Eclipse TE 2000 U microscope stage equipped with a CCD camera. 10x bright field images were taken at fifteen minute intervals over a 72 hour period. Three locations were randomly chosen per well for imaging, capturing 9 fields of view per population, per experiment. To measure the proliferation rates the LCI was used to capture images of different fields in each of the cultures over a 72 hour period. The number of cells per field of view at 12 hours intervals was determined using ImageJ software (National Institutes of Health, Bethesda, MD, USA).

Gene	Forward primer	Reverse primer	Size
β-actin	CCACACCCGCCACCAGTTCG	TACAGCCCGGGGAGCATCGT	111
Pax7	GTGCCCTCAGTGAGTTCGAT	CCACATCTGAGCCCTCATCC	203
Pax3	ACCCAAGCAGGTGACAACG	CTAGATCCGCCTCCTCCTCT	168
Myf5	GTCAACCAAGCTTTCGAGACG	CGGAGCTTTTATCTGCAGCAC	306
MyoD	TACCCAAGGTGGAGATCCTG	CATCATGCCATCAGAGCAGT	200
Myogenin	AGATTGTGGGCGTCTGTAGG	CTACAGGCCTTGCTCAGCTC	199
MyHC	AGGACGACTGCAGACCGAAT	CCCTCTGCAGTTCAGCCTTTACTTCC	157
eMyHC	GGAGGCTGATGAACAAGCCA	GCTAGAGGTGAAGTCACGGG	141
PPARγ	TTGCTGAACGTAAGCCCATCGAGG	GTCCTTGTAGATCTCCTGGAGCAG	228
C/EBPα	GCCGAGATAAAGCCAAACAAC	GACCCGAAACCATCCTCTG	248
OPN	AGCAAGAAACTCTTCCAAGCAA	GTGAGATTCGTCAGATTCATCCG	111
OCN	CTGACCTCACAGATCCCAAGC	TGGTCTGATAGCTCGTCACAAG	165
RUNX2	GACTGTGGTTACCGTCATGGC	ACTTGGTTTTTCATAACAGCGGA	83
Col1a	TCATCGTGGCTTCTCTGGTC	GACCGTTGAGTCCGTCTTTG	142
Col3a	ACGTAAGCACTGGTGGACAGA	ACGTAAGCACTGGTGGACAGA	20

Table 3. Primer sequences used in Chapter 3.

Myogenic co-culture experiments: dKO-MDSCs were plated in the lower compartment of Transwell Permeable Supports (Costar) in PM media at a density of 30,000 cells per well. WT- and dKO-nmMSCs were seeded onto 6.5mm transwell membrane inserts at the same density in PM media and placed above the dKO-MDSCs. As a control, each plate contained wells of dKO-MDSCs without transwell membrane inserts. To measure differentiation, the PM

media was switched to FM. After 3 days, myogenic differentiation of the dKO-MDSCs was analyzed via immunostaining for fMyHC, as described above.

Statistical analysis: Data from ≥ 4 samples from each subject were pooled for statistical analysis. Results are given as means ± SD. Statistical significance of any difference was calculated using Student's *t* test. Values of $p < 0.05$ were considered statistically significant.

3.3 RESULTS

Rapid accumulation of lipids, calcium deposits, and fibrosis during the disease progression in the skeletal muscles of dKO mice.

Previously, we reported that the onset of muscular dystrophy in the dKO mice occurred as early as 5 days of age and dystrophic histopathology became progressively worse by 6-8 weeks of age. At this age, we also observed that the accumulation of connective tissue, ectopic calcium and fat deposits in the gastrocnemius muscles (GAS) of the dKO mice were substantially increased compared to that of age-matched WT-GAS (24, 56). To determine the age of onset of these events, the GAS from 1, 4 and 6-8 week old dKO mice were examined. Oil Red O, Alizarin Red, and Trichrome staining indicated that the accumulation of fat, calcium deposits and fibrosis started to occur in the GAS by 4 weeks of age and the severity of the histopathology increased substantially by 6-8 weeks of age in the dKO mice. There was a higher level of lipid accumulation observed in the 4 week old dKO-GAS compared to that of the 1 week old dKO-GAS, but lipid droplets were significantly increased in the GAS of 6 week old dKO mice compared to that of the 1 and 4week old dKO mice **(Fig. 9A)**. Alizarin Red staining

showed more extensive calcium deposition in the GAS of 4 and 6-8 week old dKO mice compared to that of the 1 week old GAS **(Fig. 9B)**. We observed larger areas of fibrosis between the muscle fibers of 6-8 week old dKO-GAS compared to 1 week old dKO muscle **(Fig. 9C)**. Very small amounts of lipid, calcium and fibrosis accumulation was observed in the 1 week old dKO GAS **(Fig. 9A-C)**. GAS of 1, 4, and 6-8 week old dKO mice were collected and analyzed for mRNA expression of adipogenic (peroxisome proliferator-activated receptor gamma (PPARγ) and CCAAT/enhancer binding protein alpha (C/EBPα)), osteogenic (osteopontin (OPN), osteocalcin (OCN), and runt-related transcription factor 2 (RUNX2)) and fibrogenic (collagen type 1 alpha (Col 1a) and collagen type 3 alpha (Col 3a)) markers by real time RT-PCR **(Fig. 9D)**. The expression levels of the markers in the 4 week old dKO-GAS were significantly higher than those in the 1 week old dKO-GAS, except OCN. Adipogenic, osteogenic, and fibrogenic markers in the 6-8 week old dKO-GAS were significantly up-regulated compared to those in the 1 and 4 week old dKO-GAS. There were no significant differences in osteogenic (OPN and RUNX2) and fibrogenic (Col 1a) gene expressions between the 4 and 6 week old dKO-GAS. Taken together, our results demonstrated that the dKO mice rapidly developed skeletal muscle abnormalities that worsened with age which was similar to DMD patients (21, 22) .

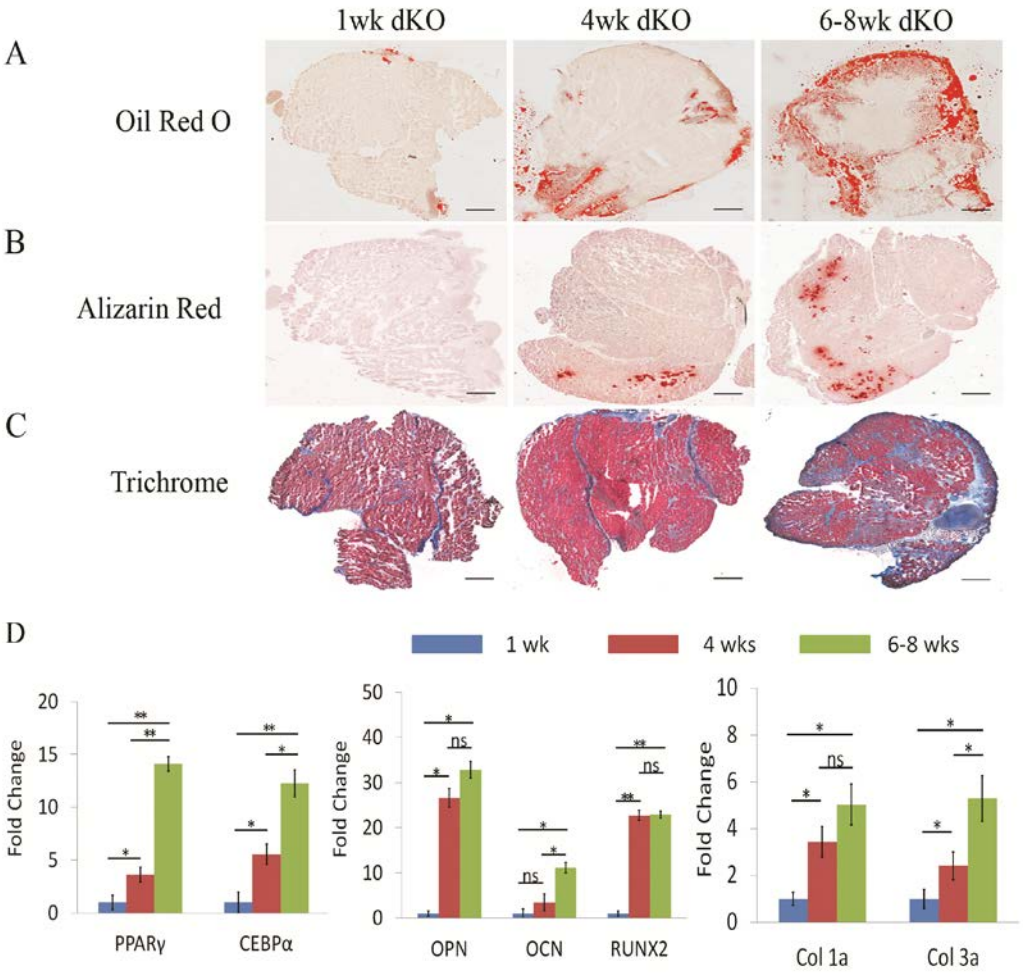

Figure 9. Severe skeletal muscle pathologies including lipid accumulation, ectopic calcification, and development of fibrosis were observed in old dKO mice.

(A) Oil Red O staining revealed the presence of lipid droplets in the gastrocnemius muscles of 1, 4, and 6-8 week old dKO mice. Severe lipid accumulation was observed in 6-8 week old dKO muscle (n>4). Scale bar = 100µm. (B) Alizarin Red staining showed calcium deposits in the dKO muscle sections. More extensive calcium deposits were detected in old dKO muscle (n>4). Scale bar = 100µm. (C) Trichrome staining was performed to identify fibrotic regions of the gastrocnemius of dKO mice. Increased fibrotic areas were observed in old dKO muscle (n>4). Scale bar = 100µm. (D) RNA was extracted from freshly collected muscle tissues of 1, 4, and 6-8 week old dKO mice and real time RT-PCR was performed (n>4) for PPARγ, C/EBPα, OPN, OCN, RUNX2, COL1a and COL3a mRNA expression. Error bars indicate 'mean ± SD'. * p <0.05, ** p <0.001.

The phenotypic characterization of non-myogenic mesenchymal stem cells (nmMSCs) from dKO and WT mice.

Next, we sought to determine what cell populations in the skeletal muscle were associated with the accumulation of lipid, calcium deposits and fibrosis in the dKO mice. Previously, we found that muscle progenitor cells (MPCs), including muscle derived stem cells (MDSCs) isolated from 6-8 week old dKO mice were defective in their proliferation capacities and adipogenic and osteogenic differentiation potentials (56); therefore, we searched for another population of skeletal muscle cells that were non-myogenic. Utilizing the preplate technique, rapidly adhering cells (RACs) were obtained, which we previously characterized as non-myogenic mesenchymal stem cells (nmMSCs). Since adipocytes are thought to be derived from multipotent MSCs, we isolated nmMSCs from dKO mice and examined their behavior in dystrophic muscle.

First, the immunophenotypes of the WT- and dKO-nmMSCs were compared using fluorescence-activated cell sorting (FACS) analysis using multiple MSC markers. The FACS results indicated that both the WT- and dKO-nmMSCs were positive for PDGFRα, CD90 and CD105 (markers reported to be expressed by mesenchymal cells) (91), and Sca-1. More than 90% of the RACs from both WT and dKO mice were positive for CD34 (an endothelial cell marker) and less than 1% of the nmMSCs expressed CD45, a hematopoietic cell marker **(Fig. 10 A&B)**. Quantification of the FACS analysis indicated that there was no significant difference in the percentage of positive cells between the WT- and dKO-RACs for each of the markers tested **(Fig. 10C)**.

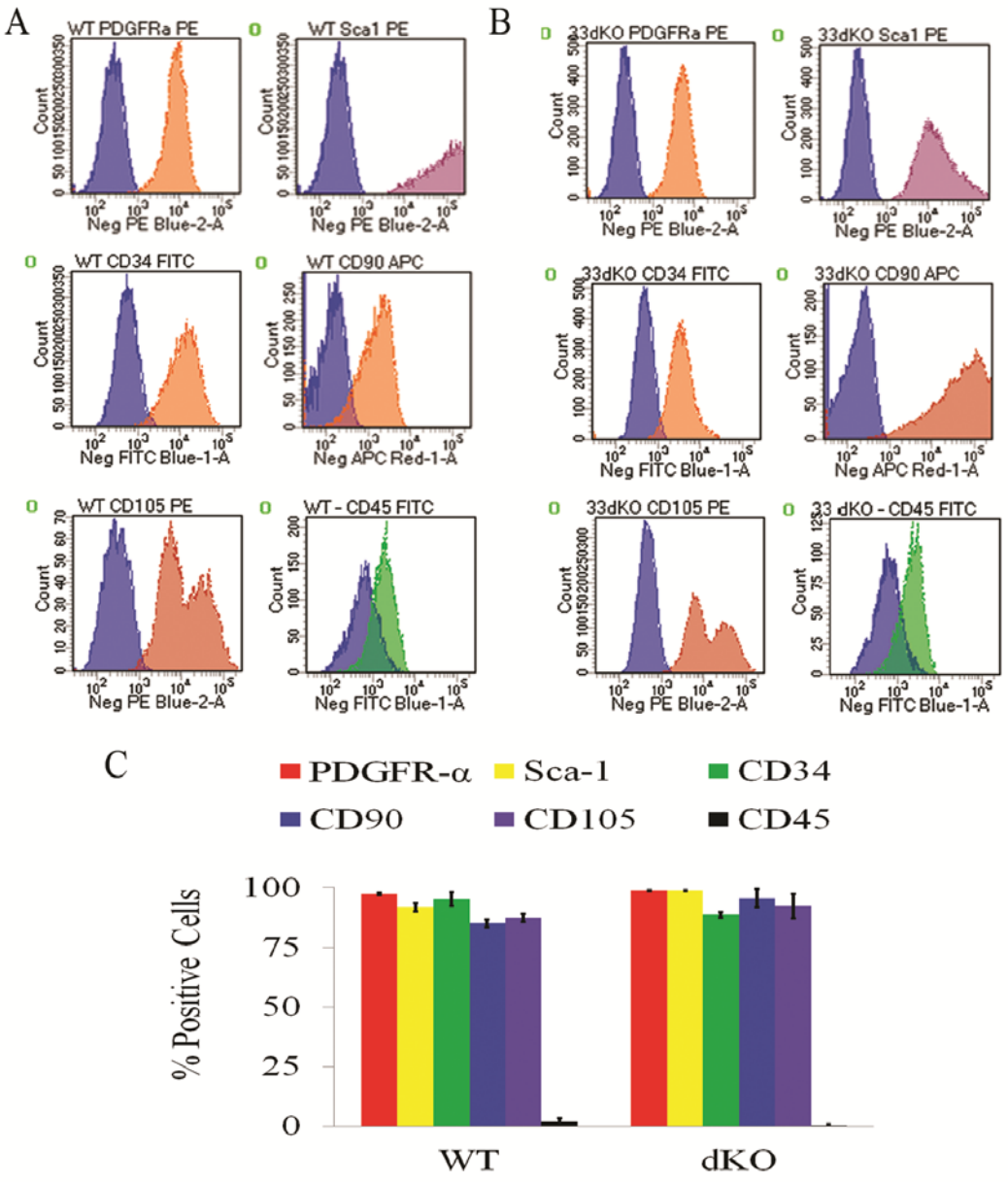

Figure 10. WT- and dKO-nmMSCs expressed multiple mesenchymal stem cell markers.

Freshly isolated (A) WT- and (B) dKO-nmMSCs were analyzed for multiple mesenchymal stem cell markers: PDGFRα, CD90, and CD105, a hematopoietic stem cell marker, CD45, and FAP markers, Sca-1 and CD34. (C) No statistically significant differences were observed in the percentage of marker expression between the WT and dKO cells (n=4). Error bars indicate 'mean ± SD'.

Proliferation and differentiation potentials of the nmMSCs are influenced by the disease progression in dKO mice.

To test whether the disease progression in dKO mice was associated with changes in nmMSCs function, nmMSCs isolated from 1, 4, and 6-8 week old dKO skeletal muscle were compared for their proliferation and differentiation potentials. Using Live Cell Imaging (LCI), we observed that nmMSCs isolated from 1 week old dKO mice displayed significantly decreased proliferation rates compared to nmMSCs isolated from 4 and 6-8 week old dKO mice **(Fig. 11A)**. The population doubling time for 1 week old dKO-nmMSCs was approximately 44 hours, and 36 and 30 hours, respectively, for the 4 and 6-8 week old dKO-nmMSCs. More importantly, our results revealed that the 4 and 6-8 week old dKO-nmMSCs displayed significantly increased adipogenic/osteogenic potentials when compared to 1 week old dKO-nmMSCs **(Fig. 11B-D)**. In addition, immunohistochemistry for PDGFRα (red) expression showed that the number of PDGFRα expressing cells was significantly higher in the 4 and 6-8 week old dKO-GAS when compared to the 1 week old dKO-GAS **(Fig. 11E&F)**. There were no significant differences in the number of endogenous PDGFRα^{+} cells, *in vitro* proliferation rates, and differentiation potentials between the 4 and 6-8 week dKO-nmMSCs. Our results suggest that the nmMSCs are gradually activated with age in terms of their proliferation and adipogenic/osteogenic differentiation potentials as the disease progresses in the dKO mice. Earlier, we showed that the accumulation of lipids, calcium deposits, and fibrotic tissue in the GAS of dKO mice started mildly at 1 week and became more severe as the mice grew older **(Fig. 9A-C)**. Taking these all these results in to account, we propose that nmMSCs become activated as the histopathology of the dKO mice progresses, suggesting that they are involved in the deposition of the non-muscle tissues observed in the 6-8 week old dKO mice.

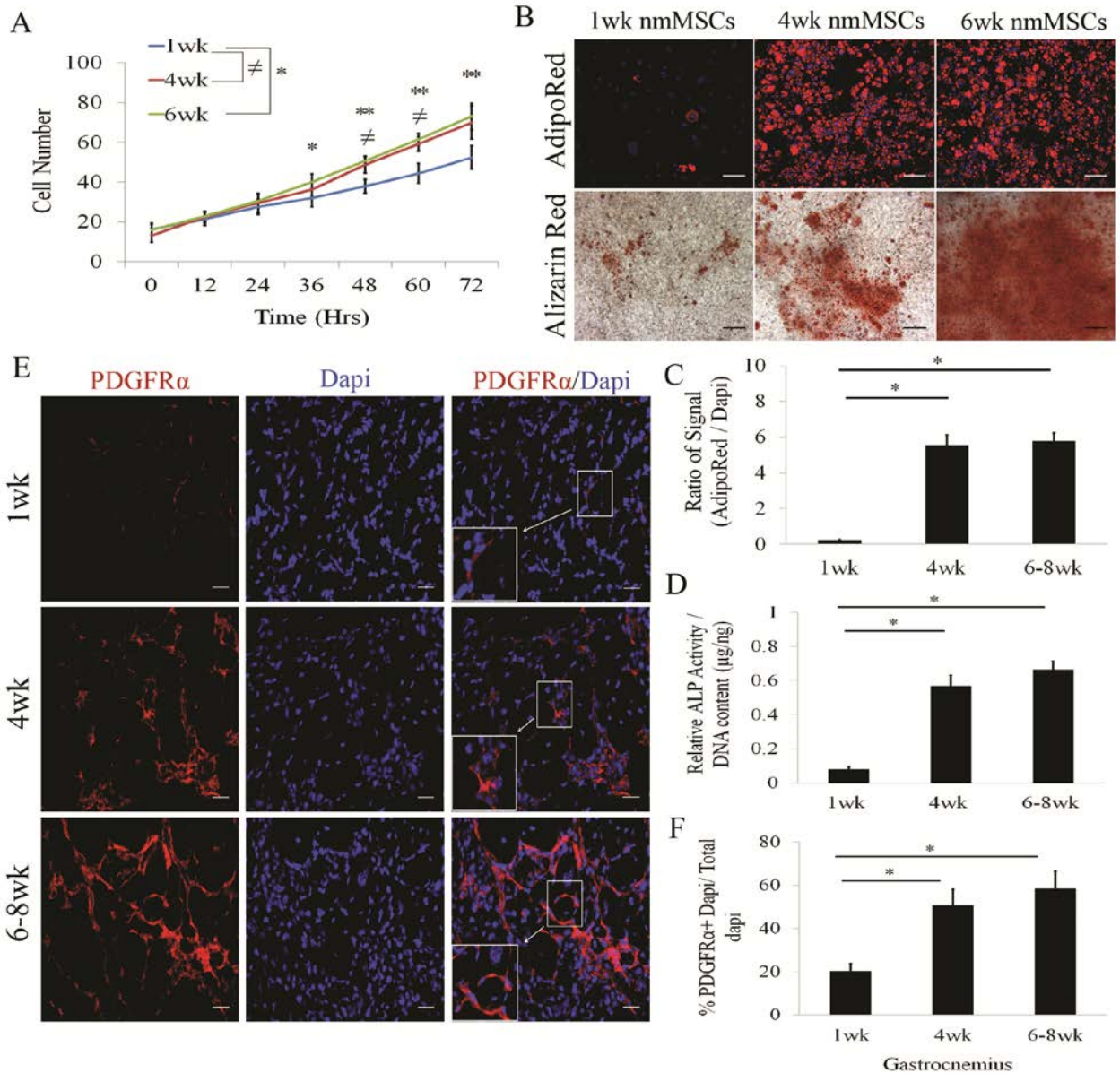

Figure 11. dKO-nmMSCs are progressively activated during the progression of the disease.

(A) Comparison of proliferation rates of nmMSCs isolated from 1, 4, and 6 week old dKO mice (n=4). Error bars indicate 'mean ± SD'. * $p < 0.05$, ** $p < 0.001$, ≠ $p < 0.05$. (B) Adipogenic (top) and osteogenic (bottom) differentiation potentials of dKO-nmMSCs from different aged mice were compared. All scale bars = 50µm. (C) AdipoRed staining was performed for the detection of lipid accumulation in the cells (n>3). Error bars indicate 'mean ± SD'. * $p < 0.05$. (D) Alkaline phosphatase activity was measured for the detection of calcium deposits (n>3). Error bars indicate 'mean ± SD'. * $p < 0.05$. (E) Immunohistochemistry for PDGFRα expression (red) and dapi (blue) in the skeletal muscle of 1, 4, and 6-8 week old dKO mice (n=4). Scale bar =25µm. (F) Quantification indicating the percentage of cells that expressed PDGFRα. Error bars indicate 'mean ± SD'. * $p < 0.05$.

dKO-nmMSCs show enhanced proliferation and adipogenic, osteogenic, and fibrogenic potentials compared to age-matched WT-nmMSCs.

Next, we compared the proliferation and differentiation potentials of nmMSCs isolated from 6-8 week old WT and dKO mice **(Fig. 12)**. Surprisingly, LCI analysis of the *in vitro* proliferation rates of 6 week old WT- and dKO-nmMSCs showed that the dKO-nmMSCs displayed significantly greater proliferation rates than the WT-nmMSCs **(Fig. 12A)**. We next examined the *in vivo* proliferation rates of the nmMSCs by performing immunohistochemistry for PDGFRα and Ki67, a proliferation marker, in the GAS of 6 week old WT and dKO mice. PDGFRα$^+$ nmMSCs were localized in the interstitial spaces between the muscle fibers **(Fig. 12B)**. Our results indicated that the number of actively proliferating Ki67$^+$PDGFRα$^+$ nmMSCs was ~15-fold higher in the dKO skeletal muscle when compared to the age-matched WT muscles **(Fig. 12C)**. We next investigated if the actively proliferating dKO-nmMSCs demonstrated an increase in their multilineage differentiation capacities. Our results indicated significant increases in the adipogenic **(Fig. 12D)**, osteogenic **(Fig. 12E)**, and fibrogenic differentiation **(Fig. 12F)** capacities of the nmMSCs isolated from 6 week old dKO mice compared to those isolated from age-matched WT mice. Upon quantification, dKO-nmMSCs exhibited a 4-fold higher adipogenic differentiation potential and 3.5-fold higher osteogenic potential when compared to the age-matched WT-nmMSCs. In addition, WT- and dKO-nmMSCs readily differentiated into Collagen I (Col I) - and Collagen III (Col III) –expressing cells under fibrogenic culture conditions. Adipogenic and fibrogenic differentiation were further evaluated by immunostaining of Col I and Col III for fibrogenic cells, and PPARγ and C/EBPα for adipocytes **(Fig. 12F)**. We found that there were more Col I- and Col III-positive cells in the dKO-nmMSC cultures compared to the WT-nmMSC cultures after fibrogenic induction. We also observed a significant

increase in the number of PPARγ- and C/EBPα-positive cells in the dKO-nmMSC cultures compared to the WT-nmMSC cultures, after 6 days of adipogenic induction **(Fig. 12F&G)**. Our results demonstrated that the function of the nmMSCs isolated from dKO mice were enhanced (increased proliferation and adipogenic, osteogenic, and fibrogenic differentiation potentials) when compared to their WT counterparts.

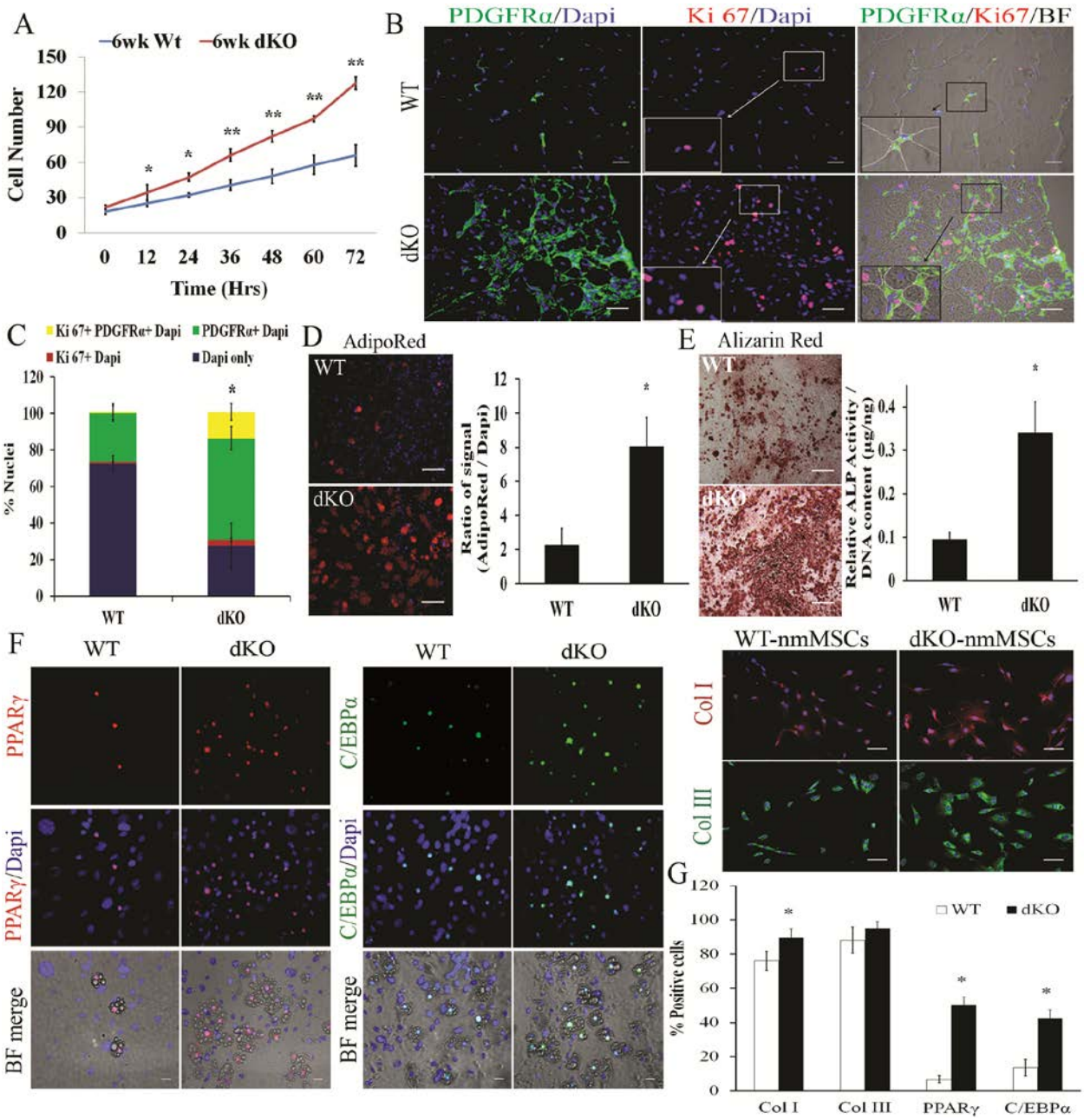

Figure 12. Proliferation and differentiation potentials of dKO-nmMSCs were significantly enhanced compared to that of age-matched WT-nmMSCs.

(A) Comparison of cell proliferation of WT- and dKO-nmMSCs from the skeletal muscle of 6-8 week old mice were investigated (n=4). (B) Immunostaining for PDGFRα (green) and Ki67 (red) in the skeletal muscle of 6 week old WT and dKO mice. Immunofluorescent images were merged with bright field images (n=4). Scale bar = 25μm. (C) Quantification indicating the percentage of cells expressing PDGFRα only, PDGFRα and Ki67, and Ki67 only. (D) Comparison of adipogenic and (E) osteogenic potentials of WT- and dKO-nmMSCs from 6 week old mice (n=4). Scale bar =50μm. (F) WT- and dKO-nmMSCs were treated with TGFβ1

for 3-5 days or adipogenic induction medium for 6 days and the number of Col I (red) and Col III (green) or PPARγ (red) and C/EBPα (green) expressing cells were examined. Scale bars = 50μm for Col I and Col III. Scale bars = 25μm for or PPARγ and C/EBPα. Immunostaining images were merged with bright field images. (G) Fibrogenic and adipogenic differentiation were evaluated by quantifying the percentages of Col I -, Col III-, and PPARγ-, C/EBPα - positive cells. For all graphs, error bars indicate 'mean ± SD'. * $p < 0.05$, ** $p < 0.001$.

Activated dKO-nmMSCs inhibit myotube formation of age-matched dKO-MDSCs.

Since the numbers of endogenous proliferating nmMSCs in the interstitial spaces of the GAS of 6-8 week old dKO mice were significantly increased compared to age-matched WT-GAS **(Fig. 5B)**, we examined the possibility that these cells might play a role in the development of the dystrophic phenotype by influencing the MDSCs. Cross-talk between MDSCs and nmMSC was tested to see if the nmMSCs could influence the myogenic differentiation potential of the MDSCs through a paracrine mechanism. MDSCs isolated from 6-8 week old dKO mice were co-cultured with age-matched WT- and dKO-nmMSCs using a transwell system, and the fusion index of the dKO-MDSCs was monitored. WT-nmMSCs were used as the control. To quantify the reduction in myogenic differentiation potential after co-cultivation, dKO-MDSCs were collected and immunostained for the terminal myogenic differentiation marker fMyHC. When dKO-MDSCs were co-cultured with WT-nmMSCs, the myogenic potential of the dKO-MDSCs was significantly enhanced **(Fig. 13A),** as previously described (73, 92, 93, 107). Surprisingly, the limited myogenic potential of the dKO-MDSCs was further exacerbated after co-culturing with the dKO-nmMSCs **(Fig. 13A)**. fMyHC expressing cells were dramatically decreased when dKO-MDSCs were cultured in the presence of dKO-nmMSCs compared to the dKO-MDSCs alone **(Fig. 13B)**. To rule out the possibility that the decrease in the dKO-MDSCs differentiation capacity was caused by the nmMSCs and not a secondary effect to a reduction in

dKO-MDSC proliferation, we measured the effect of co-cultivation of the dKO-MDSCs with dKO-nmMSCs on cell proliferation of the dKO-MDSCs using an MTS assay. No significant difference in proliferation was observed between the dKO-MDSCs alone and dKO-MDSCs co-cultured with dKO-nmMSCs during the first 2 days of co-culture **(Fig. 13C)**. Next, we further analyzed changes in the expression of myogenic markers expressed by the dKO-MDSCs after 3-4 days of culturing in differentiation induction media with/without dKO-nmMSC co-cultivation, using real time RT-PCR. We observed a significant reduction in the expression of the myogenic markers, MyoD, Myogenin, eMyHC and fMyHC in the dKO-MDSCs in the presence of dKO-nmMSCs **(Fig. 13D)**. These results suggest that nmMSCs isolated from 6-8 week old dKO mice further inhibited the differentiation potential of age-matched dKO-MDSCs via an unknown secreted factor(s).

One interesting observation from our *in vivo* studies was that the number of endogenous PDGFRα^+ nmMSCs was almost 3 fold higher in 6-8 week old dKO skeletal muscle compared to that of the age-matched WT skeletal muscle **(Fig. 12C)**. To mimic the *in vivo* dKO muscle micro-environment in our co-culture assay, we repeated the co-cultivation experiments above using 3:1, 1:1 and 1:6 ratios of dKO-nmMSCs to dKO-MDSCs. With a 3:1 ratio, we observed a larger effect of nmMSCs myogenic inhibition of the dKO-MDSCs compared to the 1:6 ratio. In fact, there was no significant difference in the formation of fMyHC expressing myotubes between the dKO-MDSCs only and dKO-MDSCs in the 1:6 ratio co-cultures **(Fig. 13 E&F)**. Taken together, these results suggest that signals originating from nmMSCs contribute to the microenvironment's ability to limit the myogenic differentiation capacity of the MDSCs in the dKO muscle.

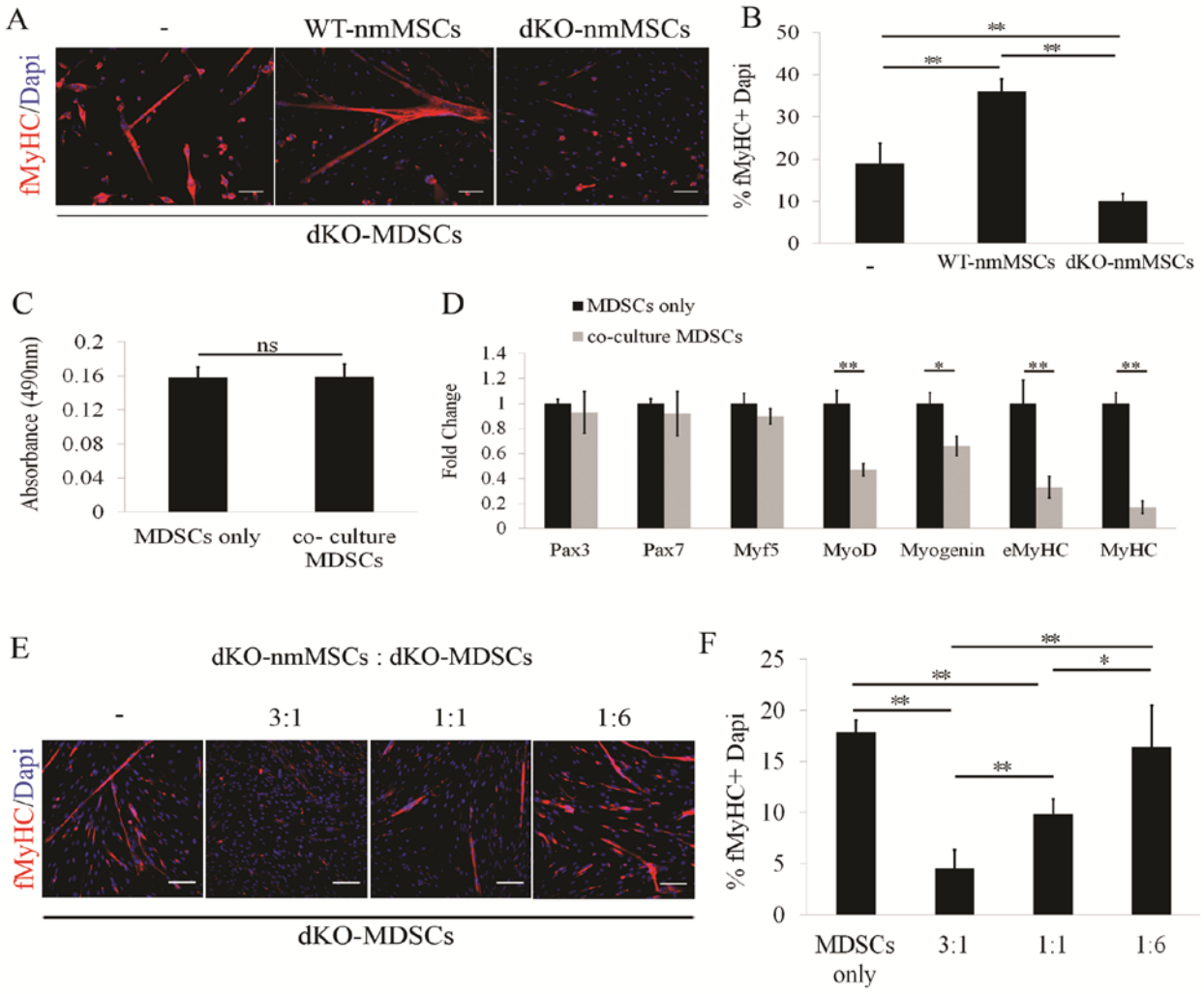

Figure 13. Limited myogenic potential of 6 week old dKO-MDSCs was further exacerbated by co-culturing the cells with 6 week old dKO-nmMSCs.

(A) Myogenic differentiation capacities were tested by co-cultivating WT- or dKO-nmMSCs with dKO-MDSCs using collagen type I coated transwell inserts. Immunohistochemistry for fMyHC was then performed for the detection of myotube formation. Dapi was used for counterstaining. Scale bar =50µm. (B) Quantification of the percentage of myotubes formed by the dKO-MDSCs after 3 days of myogenic differentiation with/without WT/dKO- nmMSCs co-cultivation (n>4). Error bars indicate 'mean ± SD'. ** $p < 0.001$. (C) MTS-based cell proliferation assay of dKO-MDSCs during first 48 hours of co-cultivation with/without dKO-nmMSCs. (D) Real time RT-PCR analysis was performed and myogenic gene expression was compared between the dKO-MDSCs co-cultivated with/without dKO-nmMSCs (n>4). Error bars indicate 'mean ± SD'. * $p < 0.05$, ** $p < 0.001$. (E) Co-culture myogenic differentiation experiments were done using 3:1, 1:1 and 1:6 ratios of dKO-nmMSCs to dKO-MDSCs. Scale bar =50µm. (F) Quantification of the percentage of myotubes formed by the dKO-MDSCs after 3 days of myogenic differentiation with 3:1, 1:1 and 1:6 ratios of dKO-nmMSCs to dKO-MDSCs co-cultivation (n=3). Error bars indicate 'mean ± SD'. * $p < 0.05$, ** $p < 0.001$.

3.4 DISCUSSION

Despite the fact that the underlying pathogenesis of DMD has been well studied, treatment options remain limited for that disease. Traditionally available treatments for DMD patients include cell, gene, and protein-mediated therapies to restore dystrophin; however, these technologies have major limitations (20, 25, 186). For instance, accumulation of intramuscular fat, calcium deposits, and fibrotic tissue significantly limits the success of these regenerative approaches for DMD patients (6, 44, 94, 187). In the current study, we showed that the accumulation of lipid, calcium deposits, and fibrotic tissue coincide with the progressive reduction in muscle regeneration in the skeletal muscle of dKO mice. The histopathology and skeletal muscle abnormalities remain mild by the age of 1 week, but progressively worsen by 4 and 6-8 weeks of age and consequently leads to death by 8-10 weeks of age. The development of intramuscular non-muscle tissue reduces muscle homeostasis and limits the potential for muscle regeneration (23). Therefore, the use of dystrophin replacement alone to treat the primary defect in DMD patients may not be successful for rescuing muscle from progressive degeneration and wasting, especially when performed at later stages of the disease (20, 25).

When searching for potential cell sources responsible for the accumulation of ectopic non-muscle tissues in dystrophic muscle, we considered resident skeletal muscle non-myogenic mesenchymal stem cells (nmMSCs), which can be isolated from the tissue via the preplate technique. We have previously reported that MPCs isolated from aged dKO mice progressively become defective in their proliferation and differentiation capacities, including myogenic, osteogenic, adipogenic and chondrogenic capacities (56). In the current study, we demonstrated that the function of the nmMSCs in 6-8 week old dKO mice appeared to be enhanced during disease progression. Six week old dKO mice displayed a significant increase in nmMSCs in their

GAS compared to age matched WT mice. Moreover, nmMSCs isolated from 6 week old dKO mice displayed increases in their *in vitro* proliferation and adipogenic, osteogenic, and fibrogenic differentiation potentials compared to age-matched WT-nmMSCs. More importantly, the proliferation and differentiation potentials of dKO-nmMSCs isolated from 1 week old dKO mice appeared to not be affected, but gradually became activated by 4 weeks and started to extensively proliferate and demonstrated an increase in adipogenic/osteogenic differentiation capacities by 6-8 weeks of age. These results taken together suggest that, the activation of the nmMSCs in the dKO mice might be involved with the occurrence of lipid and calcium deposition, and the formation of fibrotic tissue in the dKO muscle. Although it is not clear which event occurs initially, we posit that the activation of the nmMSCs is responsible for the accumulation of non-muscle tissues during the disease progression in dKO mice, and this in turn, influences the muscle micro milieu, which further alters the myogenic potential of the MDSCs.

Furthermore, the difference in proliferation and differentiation potentials among the 1, 4, and 6-8 week old dKO-nmMSCs suggests that the activation of nmMSCs in the aged dKO mice may not be caused by intrinsic differences, but by the changes in their microenvironment. This result is supported by a recently published study which reported that, the expression of transforming growth factor-β2 (TGFβ2) was induced in *mdx* muscle and this in turn further affected the behavior of muscle stem cells to become more pro-fibrogenic (95). This suggests that the local changes in the micro-milieu are responsible for stem cell dysfunction in dystrophic muscle. Therefore, we believe that the muscle environmental cues in the dKO mice influence the nmMSCs and likely play a role in determining stem cell fate.

Recently, using a FACS-based cell isolation method, two research groups identified 2 populations of resident skeletal muscle progenitor cells; 1) fibro/adipogenic progenitors (FAPs)

which express Sca-1 and CD34, and 2) PDGFRα^{+} mesenchymal stem/progenitor cells (MSCs). Both the FAPs and PDGFRα^{+} cells displayed high adipogenic and fibrogenic potentials in a glycerol-injected fatty degeneration model and in *mdx* mice (44, 73, 94). However, since *mdx* mice have a relatively normal life span and mild clinical features of the disease until very late in their life (51), our group utilized the dKO mouse model, which exhibits numerous clinically-relevant manifestations and life-threatening features similar to DMD patients. The current study results utilizing the dKO mouse model support the contention that PDGFRα and Sca-1 expressing nmMSCs are highly proliferative and have highly enhanced adipogenic /osteogenic potentials, which are likely associated with the deposition of lipid, calcification, and fibrosis in the dystrophic muscle of the mice during the progression of the disease.

Wosczyna et al. also reported that functionally and phenotypically similar muscle resident mesenchymal progenitor cells expressing the angiopoietin receptor (Tie2), PDGFRα, and Sca-1 cell surface markers, exhibit robust BMP-dependent osteogenic activity and mediate heterotopic ossification in mice that have experienced a traumatic injury (106). Knowing that Tie2^{+} cells (106), FAPs (73), PDGFRα^{+} MSCs (44) and nmMSCs share the same surface markers, anatomical location in the muscle, and trilineage differentiation potentials, we postulate that they may represent the same population of cells.

According to recent studies, these nmMSCs appear to possess dual roles, in addition to their involvement in muscle pathogenesis, and influence the myogenic potential of MPCs (44, 73, 92, 93, 107). Previously, we observed that the MPCs, including MDSCs, isolated from dKO mice displayed a significantly reduced myogenic potentials compared to age-matched WT cells (56). Therefore, we further investigated if the interaction between activated nmMSCs and the MDSCs contributed to the loss of function of the dKO-MDSCs. Co-culture experiments revealed

that proliferating dKO-nmMSCs significantly limited the myogenic differentiation potential, but not the proliferation rate, of the dKO-MDSCs. In addition, our results suggest that effect is mediated by down-regulation of genes that are critical for myoblast maturation and terminal myogenic differentiation, including MyoD, myogenin, eMyHC and MyHC. Interestingly, by decreasing the number of nmMSCs co-cultured with the dKO-MDSCs, the MDSCs could be rescued from the inhibitory effects of the nmMSCs. Therefore, knowing that dKO mice suffer from constant muscle wasting and degeneration, we posit that the extensive proliferation of the nmMSCs in the dKO mice may be a source of trophic signals for hindering muscle regeneration during the chronic disease progression of DMD.

FAPs' involvement in inhibiting the MPCs myogenic potential had also been described in a study by Mozzetta et al. where they reported that FAPs isolated from old *mdx* mice repressed satellite cell-mediated myofiber regeneration (93). Of note, although young *mdx* mice exhibited successful muscle regeneration and very mild symptoms of DMD, old *mdx* mice (18 months and older) exhibit severe muscle fibrosis (188), which is similar to what is seen more rapidly in the dKO mice and is more similar to what is seen in DMD patients. Our results suggest that nmMSCs isolated from 6 week old dKO mice are functionally equivalent to that of 18 month old *mdx* mice, which supports our previous findings that propose the dKO mouse as a severe model of muscular dystrophy with accelerated disease progression compared to *mdx* mice (55).

Recent studies suggest that skeletal muscle fibroblasts maybe the main source of intramuscular adipocytes in pathological conditions, including obesity, sarcopenia, and muscular dystrophies (189) and that their interactions with satellite cells are important for muscle regeneration (107). Murphy et al. showed that during muscle regeneration after injury, cells expressing transcription factor 4 (Tcf4) - a marker for fibroblasts - extensively proliferate in

close proximity to satellite cells and regenerating myofibers, and that the ablation of $Tcf4^+$ cells leads to premature satellite cell differentiation and depletion of the early satellite cell pool (107). In turn, ablation of $Pax7^+$ cells results in a complete loss of muscle regeneration capacity and a significant increase in connective tissue (107), suggesting that interactions between satellite cells and fibroblasts are critical for maintaining normal muscle homeostasis during regeneration. Agley et al., showed that TE-7^+ human skeletal muscle fibroblasts, but not myogenic cells, readily undergo adipogenic differentiation (189). Interestingly, both Tcf4 and TE-7 expressing fibroblasts are rapidly adhering cells (adhering to the culture dish in 2-72 hours) and are also positive for the PDGFRα antigen. When we compare the morphology, early adhering characteristics, marker profile, anatomical locations, differentiation potentials, and the role that the TE-7^+/$Tcf4^+$ fibroblasts and nmMSCs/FAPs play in muscle regeneration, it appears that fibroblasts and mesenchymal stem cells have more in common than previously reported. Taking this into account, these populations of cells may actually represent the same cell population; however, further studies need to be performed to compare the relationship between fibroblasts and nmMSCs.

Overall, our data suggests that compared to age matched WT-nmMSCs, nmMSCs isolated from 6-8 week old dKO mice are highly proliferative and their propensity for adipogenic, osteogenic, and fibrogenic differentiation is greatly increased. We therefore believe that the activation of nmMSCs coincides with the occurrence of fatty infiltration, ectopic calcification, and fibrotic tissue accumulation in the skeletal muscle of dKO mice. More importantly, we demonstrated that the nmMSCs represent a major contributor to the formation of ectopic fat, calcification, and fibrosis in the skeletal muscle of dKO mice, and that the activation of the nmMSCs may exacerbate the regeneration of the dystrophic muscle by inhibiting the myogenic

potential of MDSCs. Results from this study could provide insights into new approaches to alleviate muscle weakness and wasting in DMD patients by targeting nmMSCs during the disease process.

4.0 ADIPOGENIC DYSTROPHIC MUSCLE MICROENVIRONMENT INDUCES A CHANGE IN THE NON-MYOGENIC MESENCHYMAL STEM CELL ACTIVITY

4.1 INTRODUCTION

Figures 18&20 of Chapter 4 are adapted from a published article in *Human Molecular Genetics:*

Jihee Sohn[1], Aiping Lu[1], Ying Tang[1], Bing Wang[1], and Johnny Huard[1,2*]. (2015) Activation of non-myogenic mesenchymal stem cells during the disease progression in dystrophic dystrophin/utrophin knockout mice. *Hum Mol Gen* In press.

[1]Stem Cell Research Center, Department of Orthopaedic Surgery, University of Pittsburgh, School of Medicine

[2]Department of Microbiology and Molecular Genetics, University of Pittsburgh School of Medicine

Muscle wasting is a serious clinical problem associated with various types of diseases and health conditions, affecting individuals of all ages (56, 95). Muscular dystrophy (MD) encompasses a heterogeneous group of about 40 different forms of muscle wasting disease resulting from genetic mutations. Duchenne muscular dystrophy (DMD) is the most common and severe form of MD and it is invariably fatal. (10). In the case of DMD, a structural muscle protein, dystrophin, is missing, and its absence leads to progressive wasting and degeneration of skeletal muscle.

Currently, there is no effective treatment to end or reverse DMD (11). However, recent research studies suggest that cell/stem cell therapy might now offer some hope. Skeletal muscle is especially favorable to cell transplantation therapy since the mode of muscle repair and fiber formation is via the fusion of mononuclear cells, and transplanted donor cells can participate in this process (65). In addition, the stem cell secretome can simultaneously aid in reducing inflammation, which may slow the progress of the disease and increase the survival of transplanted donor cells. Indeed, myoblasts, mesoangioblasts, muscle-derived stem cells (MDSCs), bone-marrow derived mesenchymal stem cells (BM-MSCs), embryonic stem cells (ESCs), and induced pluripotent stem cells (iPSCs) have been reported to exhibit therapeutic potentials ameliorate dystrophic muscle pathology in DMD animal models (20, 65, 71).

Stem cells are undifferentiated cells that can differentiate into specialized, mature cell types and self-renew (190). Therefore, understanding the mechanisms that underlie stem cell maintenance and differentiation is essential to increase the efficacy of stem cell use for various therapeutic applications. The phenotypic characterization and function of stem cells are largely governed by the physical properties of the microenvironment of each tissue, which direct key cellular decisions including cell division, migration, and differentiation of cells (112, 116). For a stem cell, this information represents important cue that instructs the cells to select a given cell fate that matches the physical surroundings. In DMD, skeletal muscle is often replaced by ectopic adipocytes, calcium deposits, and fibrotic tissues and with chronic inflammation these non-muscle tissues impair the function of the muscle fibers, leading to increasing weakness and stiffness (10, 24, 56, 191). Therefore, understanding the effects of dystrophic muscle milieu on stem cells survival and function are important considerations for treating DMD.

Numerous investigations including ours, have reported that changes in muscle milieu due to disease or injury may alter the behavior or fate of muscle progenitor cells (MPCs), including satellite cells (SCs), myoblasts, and muscle derived stem cells (MDSCs), and compromise their myogenic potentials (95, 102, 121, 122). In addition to MPCs, proliferation, survival, and differentiation abilities of resident mesenchymal stem/progenitor cells can also be affected by changes in muscle microenvironment. For example, mesenchymal stem/progenitor cells readily undergo adipo-/fibrogenesis and contribute to deposition of skeletal muscle adipose tissue and fibrosis in glycerol induced fatty degenerating or *mdx* skeletal muscles. Also shown is that these cells are quiescent and unable to survive or engraft post-transplantation in healthy, wild type (WT) muscles (73). A recent study from our lab also demonstrated that surrounding muscle microenvironment governs the proliferation and differentiation potentials of skeletal muscle resident non-myogenic mesenchymal stem cells (nmMSCs) (191).

Utilizing dystrophin/utrophin double knockout, (dKO) mice, we demonstrated that muscle histopathology and muscular dystrophy in dKO mice started mildly at 1 week, but gradually became more severe as the mice grew older, at 6-8 week. Interestingly, we observed that the nmMSCs isolated from 6-8 week old dKO mice were activated in terms of their *in vitro* and *in vivo* proliferation and adipogenic/osteogenic potentials compared to age-matched WT cells. More importantly, when we compared the nmMSCs from 1-, 4-, and 6-8 week old dKO mice, the nmMSCs from 4 and 6-8 week old dKO mice displayed significantly increased proliferation and adipogenic/osteogenic potentials compared to 1 week old dKO-nmMSCs (191). Taken together, the difference in proliferation and differentiation potentials among the 1-, 4-, and 6-8 week old dKO-nmMSCs indicates that the aberrant activation of the nmMSCs in the aged

dKO mice may not be caused by intrinsic differences, but rather by the changes in microenvironment due to the severity of the disease.

In this investigation, we further examined the effects of muscle milieu on the nmMSCs function by comparing cellular activities of the nmMSCs isolated from two different muscle environments: 1) regenerating WT muscle injured with intramuscular injection of cardiotoxin (WT-CTX) (192), and 2) fibro-adipogenic degenerating dystrophic muscle. We found that the nmMSCs isolated from 6-8 week old WT-CTX and dKO mice exhibited similar proliferation and adipogenic/osteogenic differentiation potentials. We performed a co-culture assay to investigate how nmMSCs from WT-CTX and dKO mice would influence the myogenic potential of MDSCs through a paracrine mechanism. Interestingly, WT-CTX-nmMSCs significantly enhanced myogenic potential of the MDSCs while the dKO-nmMSCs strongly inhibited myotube formation of MDSCs. The inhibitory effect of the dKO-nmMSCs on dKO-MDSC myogenic potential was found to be mediated, at least in part, by the secretion of secreted frizzled-related protein 1 (sFRP1), a known inducer of adipogenesis as well as an inhibitor of myogenesis. Taken together, our data suggests that the activity of the nmMSCs in influencing MDSC myogenic potential may depend on the microenvironment which they reside in. We also provide new mechanistic insight into how the fibro-adipogenic degenerating dystrophic muscle milieu alters the stem cell function and demonstrated that increased expression of sFRP1 may contribute to dysfunction of the nmMSCs in chronic, degenerating muscle disease condition.

4.2 MATERIALS AND METHODS

Animals: C57BL/10J (wild type; WT) mice were purchased from the Jackson Laboratory (Bar Harbor, ME). Dystrophin/utrophin knockout (dKO) mice, originally characterized by Deconinck and colleagues (51), were generated by crossing heterozygous dystrophin-/-; utrophin+/- mice (55, 184). Genotyping was performed by polymerase chain reaction (PCR) analysis of tail samples. Mice ranged in age from 3 to 8 weeks. Specific ages for each experiment are described below. All animal protocols used for these experiments were approved by the University of Pittsburgh's Institutional Animal Care and Use Committee.

Cardiotoxin muscle injury model: WT (6-8 weeks old) mice were injured by the injection of 120μL of cardiotoxin (4μM, CTX, sigma, St. Louis, MO), as previously described (192). The animals were sacrificed 3 days after CTX injection.

Cell isolation and culture: Primary WT, WT-CTX, and dKO non-myogenic mesenchymal stem cells (nmMSCs) and muscle derived stem cells (MDSCs) were isolated from 6-8 week old WT, WT-CTX, and dKO mice using a modified preplate method previously described (56, 74, 166). Briefly, after enzymatic digestion of skeletal muscle tissue, muscle derived cells were re-plated on collagen type I (C9791, Sigma-Aldrich) coated flasks over a period of days. Two hours after isolation, a rapidly adhering cell population was collected and characterized as nmMSCs. 6 days after preplating, a slowly adhering cell population was obtained, which has been described to contain the MDSC fraction of cells (75). nmMSCs and MDSCs were cultured in proliferation medium (PM) containing 10% fetal bovine serum, 10% horse serum, 0.5% chick embryo extract and 1% Penicillin-Streptomycin in Dulbecco's modified Eagle's medium (DMEM, 11995-073, Invitrogen).

Fluorescence activated cell sorting (FACS): Flow cytometry was performed on WT-CTX-nmMSCs at the end of their third expansion passage. One-hundred thousand nmMSCs were collected, washed with PBS containing 2% FBS, centrifuged, and then placed on ice. The cells were then re-suspended in a 1:10 dilution of mouse serum (M5905, Sigma-Aldrich) in PBS and incubated for 10 minutes. PE-conjugated rat anti-PDGFRα (12140181, eBioscience), PE-conjugated rat anti-Sca-1 (553108, BD), and FITC-conjugated rat anti-CD45 (553080, BD) were added to each tube (1µl/100,000 cells) and incubated for 30 minutes on ice. Only one antibody was used in each tube. The cells were then rinsed in 300µl of cold washing buffer (2% FBS in PBS, 4 degrees). A single color antibody was used to optimize fluorescence compensation settings for multicolor analyses.

Immunofluorescence and histology: 5000 WT-CTX- or dKO-nmMSCs were cultured on 48 well plates. Cells were fixed with 4% paraformaldehyde for 8 minutes and blocked with 10% donkey serum for 1 hour. Slides were then incubated with goat anti-PDGFRα (1:100, R&D) in 5% donkey serum. Next, sections were incubated with secondary antibody, Alexa488-conjugated anti-goat IgG (1:300, Invitrogen) in PBS for 45 minutes. Muscle cryosections were fixed with 4% paraformaldehyde for 8 minutes and blocked with 10% donkey serum for 1 hour. Slides were then incubated with rabbit anti-beta catenin (1:200, Abcam), goat anti-PDGFRα (1:100, R&D) and rabbit anti-mouse Ki67 (1:200, Abcam) in 5% donkey serum. Next, sections were incubated with secondary antibodies including Alexa594-conjugated anti-rabbit IgG (1:300, Invitrogen) or Alexa488-conjugated anti-goat IgG (1:300, Invitrogen) in PBS for 45 minutes.

Proliferation assay: Cells were plated in 24-well plates at an initial density of 1000 cells/cm^2. Cell number at the prescribed time points was determined on the basis of dsDNA

concentration using the PicoGreen assay (Life technologies, Grand Island, NY, USA), and the doubling time was estimated using an exponential fit.

Myogenic differentiation and co-culture experiments: WT-CTX- and dKO-nmMSCs were co-cultured using transwell insert as described in Chapter 3. Cells were exposed to a neutralizing antibody against sFRP1 (Abcam) at the final concentration of 1- or 10µM.

MTS assay for MDSCs proliferation: The CellTiter 96 Aqueous One Solution Assay (Promega, Madison, WI), which is a colorimetric method for determining the number of viable cells in proliferation was used. 30,000 cells were plated in triplet on 24-well plate and 48 hour after CellTiter 96 AQueous One Solution was added (20µl/100µl PM). Plate was incubated for 4 hours and the absorbance at 490nm was read using plate reader.

Detection of sFRP1 secretion in nmMSCs: The amount of secreted frizzled-related protein 1 (sFRP1) from WT-CTX- and dKO-nmMSC cultures was measured with a mouse sFRP1 ELISA kit (MBS756370, MyBioSource) according to the manufacturer's instructions. Briefly, nmMSCs from 6 week old WT-CTX or dKO mice were plated on 6 well plates, in triplicate, and incubated in PM. 24 hours after initial plating, the cells were washed three times with PBS and PM was switched with serum free DMEM. 24 hours after switching to the serum free medium, the cell culture supernatants were collected and used to perform the ELISA for the sFRP1 protein. The results were immediately determined by comparing the Optical Density (O.D.) at 450 nm using a microplate reader (Infinite M200, TECAM, Inc.).

mRNA analysis was performed via reverse transcriptase polymerase chain reaction (RT-PCR): Total RNA was obtained from nmMSCs and gastrocnemius muscle tissues isolated from 6-8 week old WT-CTX and dKO animals using TRizol reagent (Invitrogen) and a RNeasy Mini Kit (Qiagen, Valencia, CA) according to the manufacturer's instructions. Reverse

transcription was performed using a Maxima first strand cDNA synthesis kit (Fermentas) according to the manufacturer's protocol. PCR reactions were performed using an iCycler Thermal Cycler (Bio-Rad) as previously described (24). Realtime RT-PCR was carried out using a Maxima Syber Green Assay kit (Thermo Scientific) in an iQ5 thermocycler (Bio Rad). Primers used in the study can be found in Table 3.

Axin2	CAGAGGGACAGGAACCACTC	TGCCAGTTTCTTTGGCTCTT	101
LGR5	TCGCCTTCCCCAGGTCCCTTC	GCCGTGGTCCACACCCCGAT	79

Table 4. Primer sequences used in Chapter 4.

Western Blot: Tissue lysates were prepared in RIPA buffer (Sigma) supplemented with protease and phosphatase inhibitors (1:100, Sigma) and quantified using the Bio Rad Protein Assay (500-0001, Bio Rad, Hercules, CA, USA). Immunoblotting was performed as previously described (12). Membranes were incubated with mouse monoclonal antibody to active-β-catenin (0.5µg/ml, Millipore, Temecula, CA) or rabbit polyclonal antibody to alpha tubulin (Abcam) at 4°C overnight in 5% milk in TBST. Alpha tubulin was used to evaluate equal loading.

Statistical analysis: Data from ≥4 samples from each subject were pooled for statistical analysis. Results are given as means ± SD. Statistical significance of any difference was calculated using Student's *t* test. Values of $p < 0.05$ were considered statistically significant.

4.3 RESULTS

Morphological characteristics of skeletal muscle regeneration.

Recently, we reported that the non-myogenic mesenchymal stem cells (nmMSCs) isolated from 6-8 week old dystrophic dKO mice were abnormally activated in their proliferation and differentiation potentials in comparison to their WT counterparts (191). Next, we examined whether changes in microenvironment would affect the function of nmMSCs by comparing cellular behaviors of the nmMSCs isolated from well-established cardiotoxin (WT-CTX) muscle injury mice (192) and dKO mice. First, we collected gastrocnemius muscles (GAS) of 6-8 weeks old WT mice 3 days post cardiotoxin injection and the age-matched dystrophic dKO mice. Hematoxylin and eosin (H&E) staining of tissue cross sections revealed that the WT-CTX muscle exhibited substantial histological evidence of the early events following muscle injury, when compared to age-matched WT muscle **(Fig. 14A&B)**. CTX injections resulted in the rapid muscle fiber necrosis and increased number of non-muscle mononucleate cells within the damaged site, leading to the loss of muscle architecture **(Fig. 14B)**. As we expected, dKO-GAS exhibited severe dystrophic muscle histopathology, including muscle damage, areas of myofiber necrosis, adipocyte infiltration, connective tissue deposition, and extensive mono-nuclei cell infiltration **(Fig. 14C)**. Accumulation of adipose cells or increase in fibrosis was not observed in tissue sections of WT-CTX mice. These results suggest that there are differences in morphological characteristics of skeletal muscle and micro-milieu between regenerating injured muscles with direct trauma and diseased muscles with innate genetic defects.

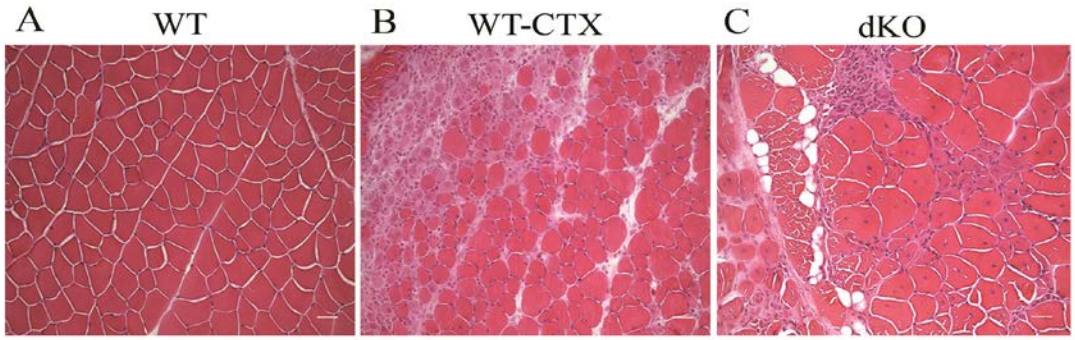

Figure 14. Morphological characteristics of skeletal muscles from WT, WT-cardiotoxin injured mice, and dystrophic mice.

Representative muscle sections of the 6-8 week old (A) WT, (B) WT-cardiotoxin injured mice (WT-CTX), and (C) dystrophic dKO mice. (B) Intra-muscular injection of cardiotoxin (CTX) in gastrocnemius muscle (GAS) resulted in rapid necrosis of myofibers and mono-nucleated cell infiltration. H&E staining of WT-CTX muscle section demonstrated the extent of tissue damage compared to age-matched WT muscles. (C) H&E staining of 6-8 week old dKO mice muscle sections showed severe dystrophic muscle histopathology.

Isolation and phenotypic characterization of the non-myogenic mesenchymal stem cells from cardiotoxin injured skeletal muscle.

Next, to examine the effect of microenvironment on nmMSC function, we isolated nmMSCs from WT-CTX and dKO skeletal muscles utilizing the modified preplate technique (74) and first compared their phenotypes. 2 hours after isolation, adherent WT-CTX-nmMSCs exhibited similar morphology as dKO-nmMSCs **(Fig. 15B)**. 3-4 passages after, cells were labeled with antibodies against, PDGFRα, Sca-1, and CD45, and subsequently analyzed by flow cytometry. Our results demonstrated that isolated WT-CTX-nmMSCs were highly positive for PDGFRα and Sca-1, but were negative for CD45 **(Fig. 15C&D)**. The immunophenotyping of WT-CTX-nmMSCs were very similar to that of dKO-nmMSCs **(Chapter 3)**. We next examined

the expression of PDGFRα protein by immunostaining, and found no significant differences in the number of cells expressing PDGFRα protein between WT-CTX- and dKO-nmMSCs **(Fig. 15E&F)**. These results suggest that we successfully isolated the nmMSCs from WT-CTX regenerating muscle, and there was no difference in phenotypic characteristics between WT-CTX and dKO cells.

WT-CTX-nmMSCs and dKO-nmMSCs exhibited similar proliferation and differentiation capacities.

Previously, we showed that the nmMSCs isolated from dKO mice were progressively activated during the disease progression. In addition, we reported that the proliferation and adipogenic, osteogenic, and fibrogenic differentiation potentials of dKO-nmMSCs were significantly enhanced compared to that of age-matched WT-nmMSCs (191), suggesting that disease muscle microenvironment may cause the aberrant proliferation and differentiation capacities of the nmMSCs. Therefore, we next examined proliferation and differentiation potentials of the nmMSCs isolated from 6-8 week old WT-CTX. After isolation, cells were expanded in growth medium for 3-4 passages, and then transferred to 24 well plates, and proliferation was determined on the basis of dsDNA concentration at different time points measured with the PicoGreen assay. There was no significant difference in the proliferation rate of the WT-CTX-nmMSCs compared to dKO-nmMSCs, except at one time point. At day 7, proliferation rate of dKO-nmMSCs was slightly greater **(Fig. 16A)** than WT-CTX-nmMSCs. We also examined *in vivo* proliferation of the nmMSCs from GAS of WT-CTX and dKO mice by performing immunostaining for PDGFRα and Ki67, a proliferation maker. Dapi-labeled cells that were positive for both PDGFRα and Ki67 were quantified. Upon quantification, we

observed no significant difference in the number of PDGFRα^{+}Ki67^{+} nmMSCs in GAS of WT-CTX and dKO mice **(Fig. 16B&C)**. Lastly, we compared adipogenic and osteogenic differentiation potentials of nmMSCs isolated from 6-8 week old WT-CTX and dKO muscles **(Fig. 16D&E)**. 21 days after adipogenic induction, both WT-CTX- and dKO-nmMSCs showed extensive accumulation of lipids. 10 days after osteogenic induction, both cell types were positive for Alizarin Red, which indicated presence of calcium deposits. Upon quantification, we did not observe any differences in adipogenic or osteogenic potentials of WT-CTX- and dKO-nmMSCs. These assays demonstrated similar proliferation and differentiation potentials between WT-CTX-nmMSCs and dKO-nmMSCs.

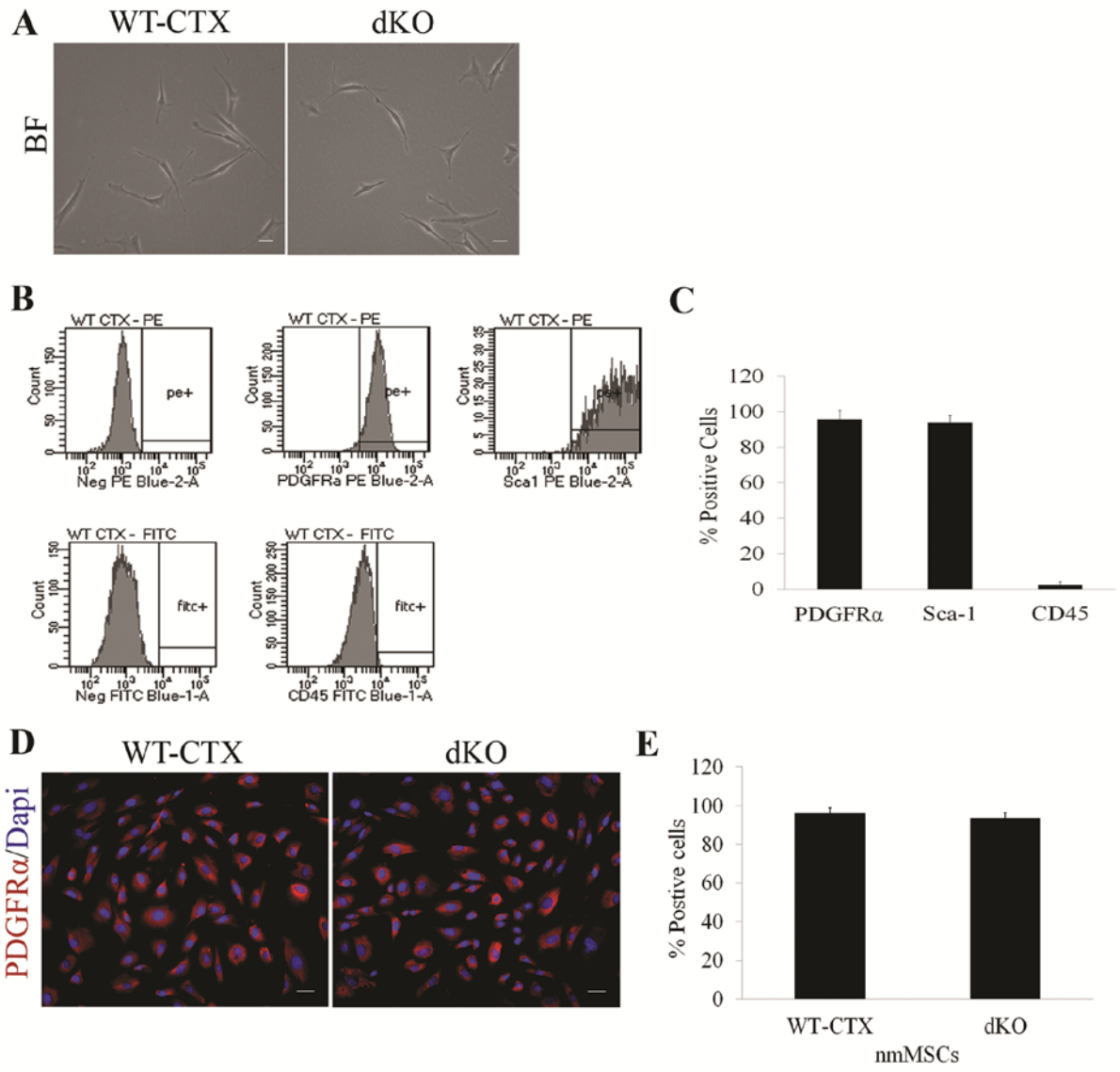

Figure 15. Phenotypic characterization of the nmMSCs isolated from WT-CTX skeletal muscle.

(A) WT-CTX-nmMSCs morphology was similar to that of dKO-nmMSCs under phase contrast microscopy. (C) Fluorescence activated cell sorting (FACS) plots show that WT-CTX-nmMSCs were positive for PDGFRα and Sca-1, but were negative for CD45. (D) Quantification of FACS results. Error bars indicated 'mean ± SD', n=4. (E) Immunostaining for the mesenchymal stem cell marker PDGFRα was also performed. (F) Quantification of immunostaining of PDGFRα. All Scale bars =50µm.

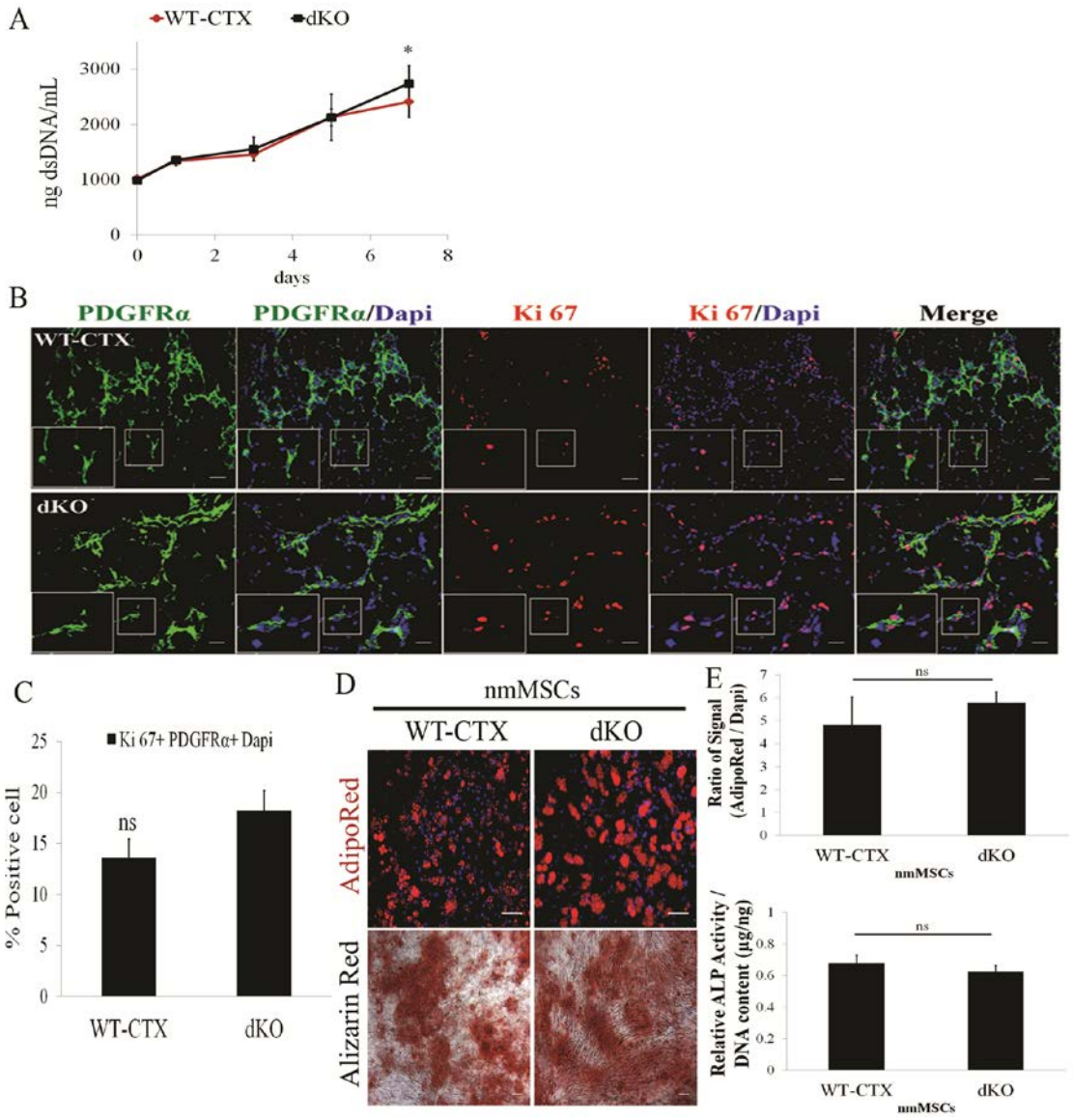

Figure 16. WT-CTX-nmMSCs and dKO-nmMSCs displayed similar proliferation and differentiation potentials.

(A) Proliferation rates of the nmMSCs isolated from WT-CTX- and dKO mice were assayed on the basis of dsDNA content for each time point, and no significant differences were detected, except for day 7. (n=4). Error bars indicate 'mean ± SD'. (B) Immunohistochemistry for PDGFRα (green) and Ki67 (Red) expression in the skeletal muscle of 6-8 week old WT-CTX and dKO mice. (n=4). Scale bar = 25μm. (C) Quantification indicating the percentage of cells expressing PDGFRα and Ki67. Error bars indicate 'mean ± SD'. (D) AdipoRed (adipogenesis) or Alizarin Red (osteogenesis) staining was performed after differentiation assays. Scale bar=50μm. (E) Quantification of adipogenesis (AdipoRed signal intensity was normalized to total Dapi signal intensity) and osteogenesis (relative ALP activity was normalized to total dsDNA content) indicated that there was no significant differences in adipogenic or osteogenic potentials between WT-CTX- and dKO-nmMSCs. (n=4). Error bars indicate 'mean ± SD'.

Myogenic potential of muscle progenitor cells (MPCs) is increased by nmMSCs from regenerating muscle, but inhibited by nmMSCs from dystrophic muscle.

In previous study, we showed that activated nmMSCs from dKO mice may contribute to continuous muscle wasting and degeneration by limiting myogenic potential of MPCs, especially muscle derived stem cells (MDSCs) (191). Since our results above indicated that WT-CTX-nmMSCs were also highly proliferative 3 days after injury, we further tested whether the nmMSCs isolated from WT-CTX regenerating muscles could positively or negatively influence fusion potential of MDSCs. In contrast to fibro-adipogenic degenerating dKO muscle, WT-CTX regenerating muscle rarely induces fatty infiltration or fibrosis formation in the skeletal muscle. Therefore, it is expected that the behavior of the nmMSCs in WT-CTX-GAS is regulated in a manner distinct than dKO-nmMSCs. 6 week old dKO-MDSCs were co-cultured with age-matched WT-CTX- or dKO-nmMSCs, using a transwell system, and the fusion index of the dKO-MDSCs was monitored **(Fig. 17A)**. Consistently, dKO-nmMSCs impaired the differentiation ability of dKO-MDSCs **(Fig. 17B)**. fMyHC expressing cells were dramatically decreased when dKO-MDSCs were cultured in the presence of the dKO-nmMSCs compared to the dKO-MDSCs alone **(Fig. 17C)**. By contrast, the nmMSCs isolated from WT-CTX muscles, significantly enhanced the myotube formation of dKO-MDSCs after co-cultivation compared to dKO-MDSCs only **(Fig. 17B&C)**. Proliferation rates of dKO-MDSCs without co-cultivation, co-cultivation with WT-CTX-nmMSCs, or co-cultivation with the dKO-nmMSCs were compared using a MTS assay during first two days in growth medium. We observed no significant differences in proliferation rates among three groups, suggesting that reduction or enhancement of dKO-MDSCs' myogenic potentials was not a secondary effect to the proliferation **(Fig. 17D)**. Taken together, our data suggest that after CTX injury the nmMSCs are activated and undergo

extensive proliferation to promote repair/regeneration process by facilitating MPC myogenic differentiation. Furthermore, these results indicated that the nmMSCs derived from distinct muscle environments modulate the regenerative capacity of MDSCs in a different manner.

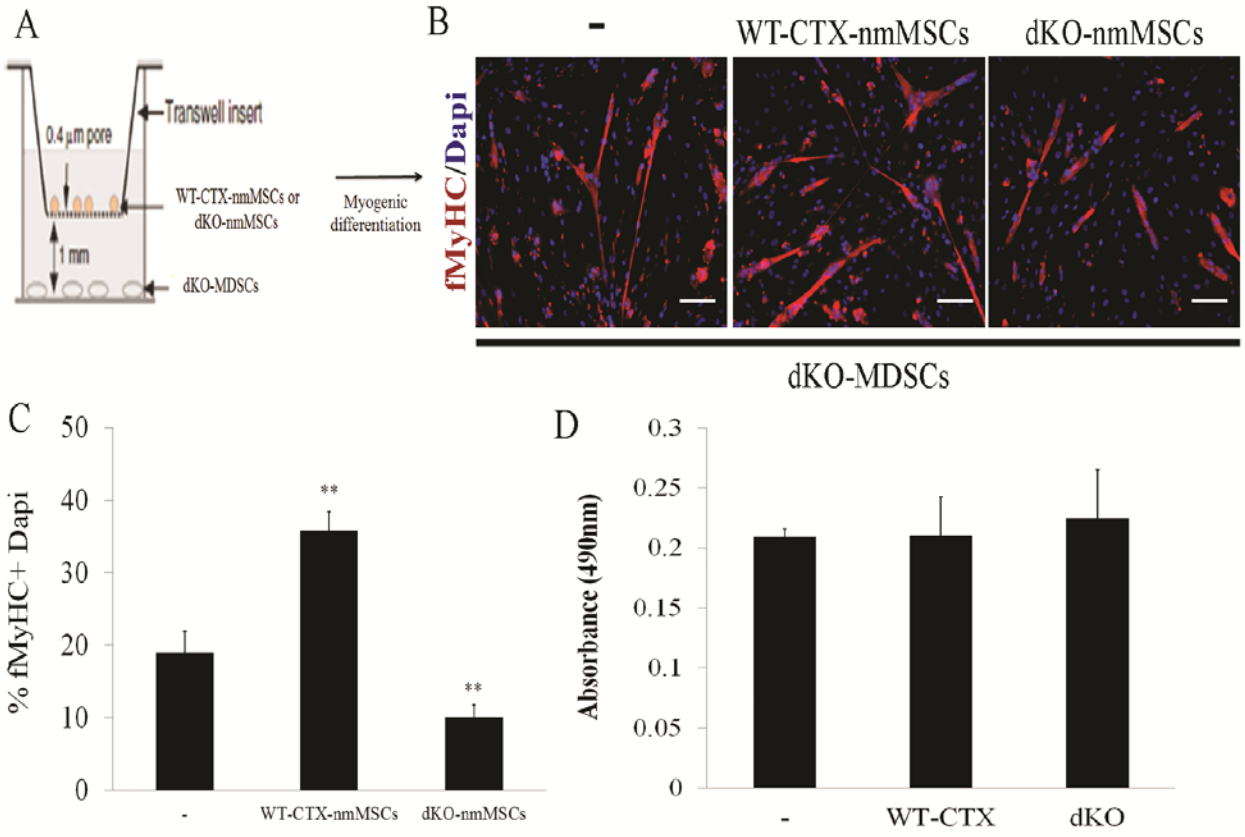

Figure 17. The nmMSCs from WT-CTX mice enhance the *in vitro* differentiation potential of MDSCs.

(A) Myogenic differentiation capacities were tested by co-cultivating WT-CTX- or dKO-nmMSCs with dKO-MDSCs using collagen type I coated transwell inserts. (B) Immunohistochemistry for fMyHC was then performed for the detection of myotube formation. Dapi was used for counterstaining. Scale bar =50µm. (C) Quantification of the percentage of myotubes formed by the dKO-MDSCs after 3 days of myogenic differentiation with/without WT-CTX-/dKO- nmMSCs co-cultivation (n>4). Error bars indicate 'mean ± SD'. ** $p < 0.001$. (D) MTS-based cell proliferation assay of dKO-MDSCs during first 48 hours of co-cultivation with/without dKO-nmMSCs. (n>4). Error bars indicate 'mean ± SD'.

Myotube formation of dKO-MDSCs is inhibited by the secreted frizzled-related protein 1 (sFRP1) released by the dKO-nmMSCs.

It has been known that PDGFRα^{+} cells secrete follistatin to promote myogenic activity of muscle stem cells (satellite cells) in injured muscles (93); however, the soluble factor that is released from the nmMSCs to inhibit myogenic potential of MPCs in dKO muscles is unknown. In search of a soluble factor responsible for functional interactions between the nmMSCs and MDSCs from dKO mice, we considered secreted frizzled-related protein 1 (sFRP1) as a potential candidate. In fact, it has been previously shown that sFRP1 inhibits myotube formation of C2C12 and satellite cells, with no significant effect on the cell cycle or apoptosis (193). We performed real time RT-PCR to examine the sFRP1 mRNA expression from total GAS of 6-8 week old WT-CTX- and dKO mice and values were normalized to sFRP1 mRNA expression of age-matched WT-GAS. We observed a significant increase in sFRP1 gene expression in the dKO-GAS compared to that of the WT-CTX-GAS **(Fig. 18A)**. Next, we examined if the dKO-nmMSCs expressed higher sFRP1 mRNA levels compared to that of WT-CTX-nmMSCs, which was confirmed by real time RT-PCR. sFRP1 gene expression was shown to be increased approximately 4.5 fold in the dKO-nmMSCs when compared with age-matched WT-CTX-nmMSCs **(Fig. 18B)**. sFRP1 is a secreted protein, therefore we next investigated if higher amounts of sFRP1 were secreted by the dKO-nmMSCs compared to the WT-CTX-nmMSCs. We collected cell culture supernatants from WT-CTX- and dKO-nmMSCs cultures and the levels of sFRP1 protein secreted from all cell types was assayed using a mouse specific sFRP1 ELISA kit. As expected, there was a significantly higher sFRP1 concentration in the cell culture supernatants isolated from the dKO-nmMSCs when compared to that of WT-CTX-nmMSCs (**Fig. 18C)**. These results suggest that the secretion of sFRP1 from dKO-nmMSCs might be

responsible for inhibiting the myogenic differentiation of dKO-MDSCs as previously described **(Fig. 17B&C).**

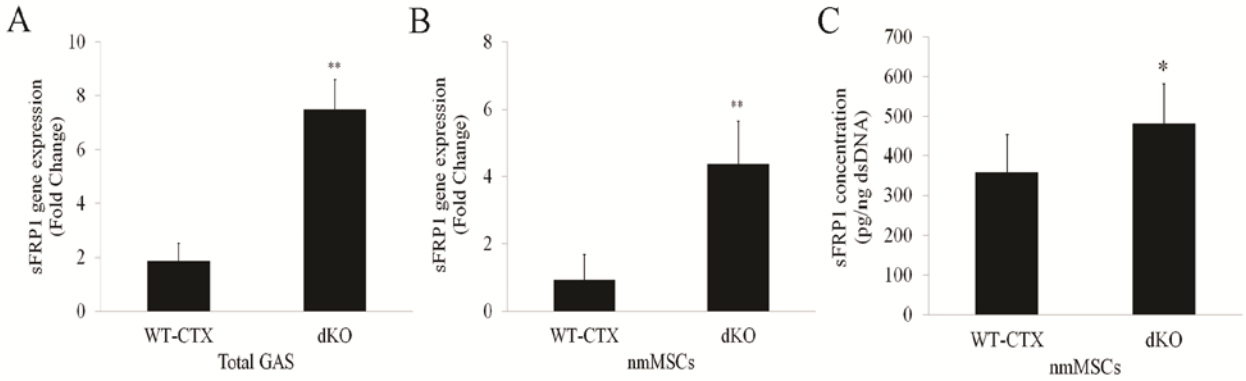

Figure 18. Higher sFRP1 expression was detected in dKO skeletal muscle when compared to WT-CTX muscle. dKO-nmMSCs secreted a higher level of sFRP1 than WT-CTX-nmMSCs.

RNA was extracted from frozen muscle tissue and real time RT-PCR was performed. Higher sFRP1 gene expression was observed from (A) dKO-GAS compared to age-matched WT-CTX-GAS (n>4) and (B) 6 week old dKO-nmMSCs compared to age-matched WT-CTX-nmMSCs (n>4). All values were normalized to sFRP1 gene expression of WT-GAS or WT-nmMSCs. Error bars indicate 'mean ± SD'. $^{**}p < 0.0001$. (C) Concentration of secreted sFRP1 from WT- or dKO-nmMSCs was measured with a mouse sFRP1 ELISA kit. The graph represents sFRP1 concentration per every 100,000 WT- or dKO-nmMSCs (n=6). Error bars indicate 'mean ± SD'. $^{**}p < 0.005$, $^{**}p < 0.0001$.

Blockade of secreted sFRP1 from the nmMSCs increases myogenic differentiation of dKO-MDSCs co-cultured with dKO-nmMSCs.

To confirm the above finding, we tested whether blocking secreted sFRP1 in culture medium could enhance the myogenic potential of dKO-MDSCs co-cultivated with dKO-nmMSCs. dKO-MDSCs were co-cultivated with dKO-nmMSCs and were exposed to differentiation medium containing neutralizing antibodies against sFRP1. In transwell co-culture

experiments, incubation of the dKO-nmMSCs with neutralizing antibodies against sFRP1 negate the inhibiting effect of the dKO-nmMSCs and significantly increased the formation of multinucleated myotubes from dKO-MDSCs **(Fig. 19A&B)**. This effect was dose-dependent as we observed greater myotube formation when we treated dKO-nmMSCs with 10μM concentration of antibody compared to that of 1μM. This result supports the conclusion that nmMSCs-derived sFRP1 inhibits the regeneration potential of MPCs in dystrophic muscles.

Wnt signaling is elevated in dKO muscle

The results above suggest that the upregulation of sFRP1 in skeletal muscle may contribute to the dystrophic phenotype observed in dKO mice. In order to better understand the molecular events behind the upregulation of sFRP1, we further investigated if the Wnt signaling pathway was involved, since sFRP1 is the modulator of Wnt signaling pathway and elevated Wnt signaling in *mdx* mice has been reported by other research groups (95, 194). In Figure 18, we observed that sFRP1 mRNA expression of dKO-GAS was significantly higher compared to, not only WT-CTX-GAS, but also WT-GAS and WT-nmMSCs. Therefore, here, we compared the activation of Wnt signaling in WT- and dKO-GAS. Western blot demonstrated that the amount of dephosphorylated β-catenin (active form) was increased in 6-8 week old dKO-GAS compared to age-matched WT-GAS **(Fig. 20A)**. Furthermore, we observed elevated β-catenin expression by immunofluorescence **(Fig. 20B&C)** and the increased mRNA expressions of Axin2 **(Fig. 20D)** and LGR5 **(Fig. 20E)**, the downstream targets of the Wnt signaling pathway (4, 195), by real time RT-PCR in 6-8 week old dKO-GAS compared to age-matched WT-GAS. Our results suggest that Wnt signaling is increased in dystrophic dKO muscle.

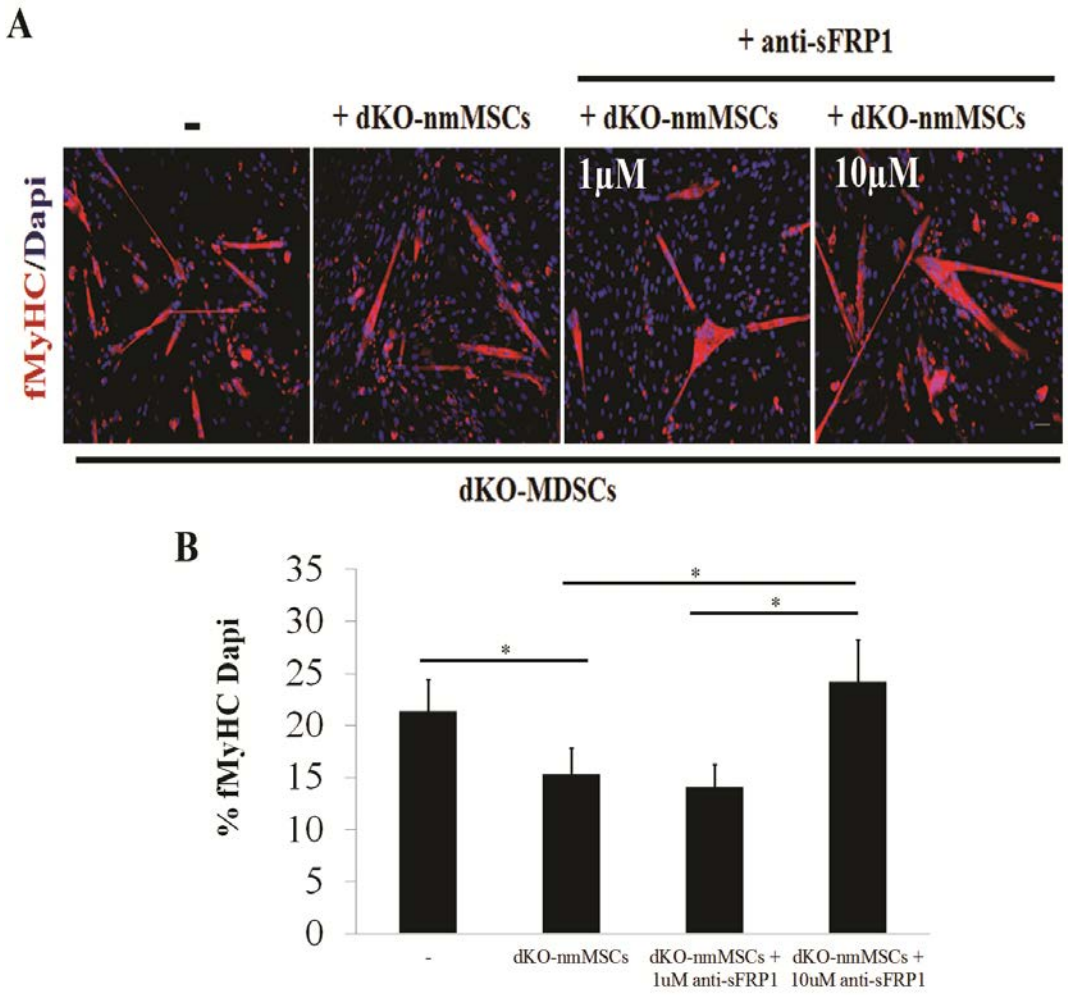

Figure 19. dKO-nmMSCs treated with neutralizing antibodies against sFRP1 increase dKO-MDSC myogenic potential.

(A) MDSCs and nmMSCs isolated from 6-8 week old dKO mice were co-cultured in transwell chambers. dKO-nmMSCs were plated on the transwell insert and dKO-MDSCs were plated on the bottom compartment. After 3-5 days of co-cultures in the presence or absence of neutralizing antibodies against sFRP1, dKO-MDSCs were immunostained for fMyHC (Red) and nuclei counterstained by Dapi (Blue). Scale bar =50µm. (B) Quantification of the percentage of myotubes formed by the dKO-MDSCs of the experiment represented in (A). (n=3). Error bars indicate 'mean ± SD'. *$p < 0.005$.

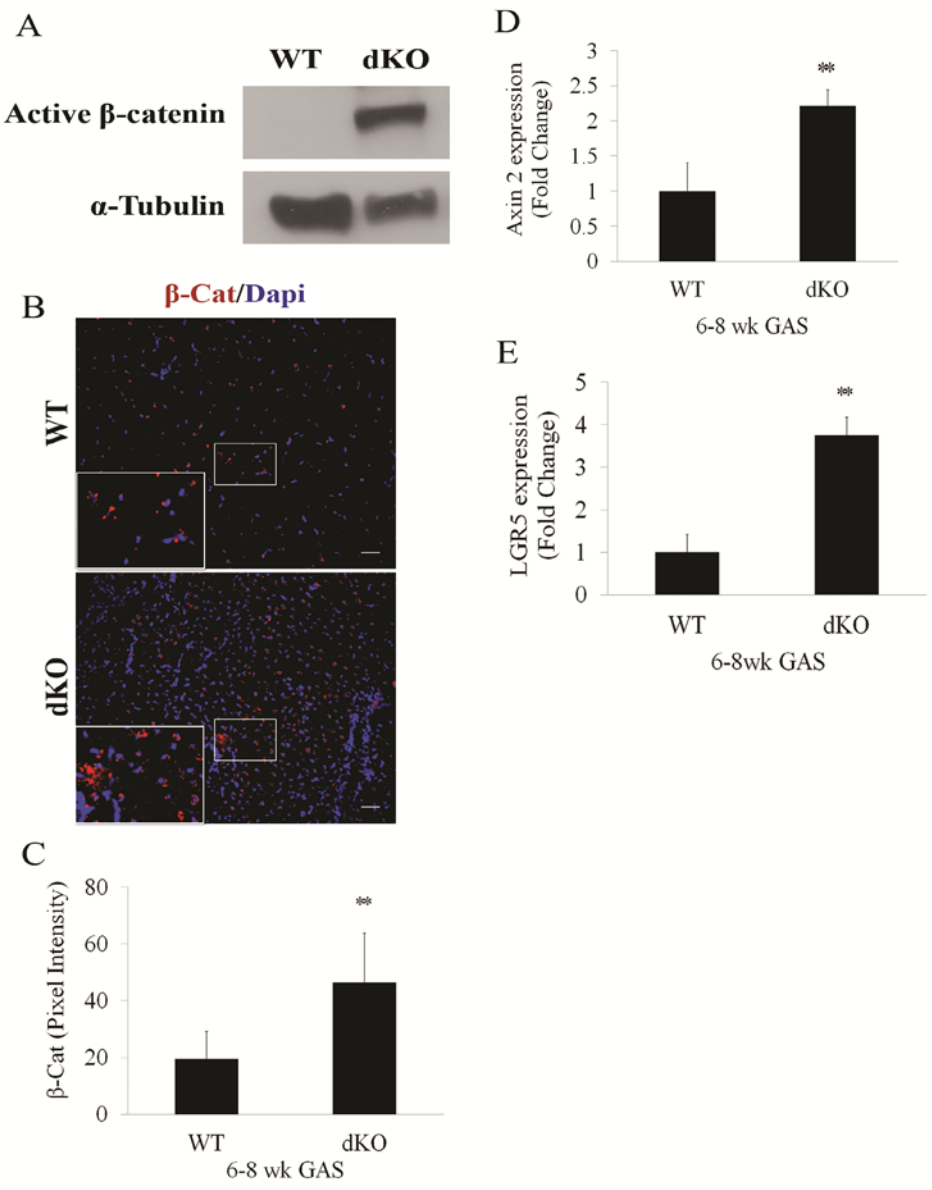

Figure 20. Enhance Wnt signaling in dKO muscles.

(A) Representative Western blots of active β-catenin (92kDa) and α-Tubulin (55kDa) in GAS of 6-8 week old dKO and WT mice. α-Tubulin was used as a loading control. (n=4) (B) β-catenin (β-Cat) staining of muscles from 6-8 week old dKO and WT mice (n>4). Scale bar =50μm. (C) The average pixel intensity corresponding to β-catenin staining was evaluated with Image J. Error bars indicate 'mean ± SD'. $^{**}p < 0.0001$. RNA was extracted from frozen muscle tissue and real time RT-PCR was performed. Higher (D) Axin2 and (E) LGR5 gene expressions were observed from dKO-GAS compared to age-matched WT-GAS (n>4). Error bars indicate 'mean ± SD'. $^{**}p < 0.0001$.

4.4 DISCUSSION

Skeletal muscle possesses the remarkable ability to grow and regenerate itself from both acute and chronic damages (10, 61). Despite this, in several pathological conditions, such as Duchenne muscular dystrophy (DMD), the skeletal muscle integrity is exacerbated by the infiltration of ectopic fat, calcium deposits, and fibrotic tissues (10, 191). In general, declined regeneration and accumulation of fat and fibrotic tissue are also associated with the aging process (121). These changes in muscle microenvironment could impact stem cell function to delay repair and regeneration, and enhance inflammation, which exacerbates the disease condition. Therefore, pathological phenotypes of DMD may involve a complex interactions of muscle resident stem/progenitor cells with the surrounding microenvironment (93, 125).

To better understand effects of muscle milieu on determining stem cell activities, we evaluated proliferation and differentiation potentials of non-myogenic mesenchymal stem cells (nmMSCs) from skeletal muscles of dystrophic mice (dKO) and cardiotoxin (CTX) injured regenerating mice (WT-CTX). Histologic analysis of gastrocnemius muscle (GAS) cryosections of dKO mice revealed the expected variations in muscle fiber size, infiltration of mononucleated cells, and the presence of adipocytes and fibrotic tissue. CTX injections for 3 days in WT mice resulted in the rapid muscle fiber necrosis and increased number of mononucleated cells within the damaged site, leading to the loss of muscle architecture; however, there was no evidence of accumulation of lipids or fibrosis as expected.

Interestingly, the nmMSCs isolated from 6-8 week old dKO and WT-CTX mice exhibited similar *in vitro* and *in vivo* proliferation and adipogenic/osteogenic potentials. Previously, we showed that the nmMSCs isolated from 6-8 week old dKO mice are abnormally activated in their proliferation and differentiation capacities compared to that of the WT-

nmMSCs. Taken these results together, we concluded that the nmMSCs from WT-CTX mice were also activated after injury. Further co-cultivation experiments indicated that the nmMSCs from regenerating WT-CTX muscles have ability to promote the myogenic potential of MDSCs, whereas the nmMSCs from dystrophic dKO mice significantly inhibit the myogenic potential of MDSCs in dKO muscle, which further exacerbates muscular dystrophy.

Our results are supported by other studies that have reported the presence of muscle resident cells/stem cells, which play an important role in supporting SCs to ensure efficient muscle repair. Among those cell types is a mesenchymal lineage cell known as fibro/adipogenic progenitors (FAPs) whose role in muscle regeneration has been mostly discovered (73, 92). Although FAPs do not arise from the myogenic lineage, nor directly participate in forming myotubes/myofibers, they have been shown to facilitate muscle regeneration after injury (92). In the context of acute muscle injury, muscle damage induces rapid recruitment of pro-inflammatory immune cells, including eosinophils, which secret IL-4/IL-13 immune signals. The activation of IL-4/IL-13 signaling results in activation of FAPs. Activated FAPs can then differentiate into the fibroblast lineage while inhibiting their differentiation into adipocytes, to create a fibrotic scaffold that supports muscle regeneration (92). In addition, FAPs also generate a transient pro-myogenic differentiation niche that facilitates myoblast differentiation (73). A more recent study suggests that follistatin is the soluble mediator of functional interactions between FAPs and SCs (93). In the context of chronic muscle degenerative disease, such as DMD, FAPs undergo extensive proliferation due to unknown factors, and differentiate into fibrogenic cells or adipocytes, contributing to accumulation of fatty and fibrotic tissues in skeletal muscle (73). In previous study, we also showed that the nmMSCs, which are believed to be the similar cell populations to FAPs, in dKO mice showed significantly enhanced adipogenic,

osteogenic, and fibrogenic differentiation potentials, suggesting that they may contribute to accumulation of non-muscle tissues observed in dKO muscles (191). These studies, including ours, provide evidence that FAP/nmMSC phenotype and function are highly influenced by the micro-environmental changes occurring in dystrophic muscle.

In order to decipher the mechanisms behind the inhibitory effects that the nmMSCs impart on the myogenic potential of MDSCs, we postulated that the secreted frizzled-related protein 1 (sFRP1) might be involved in the process. sFRP1 is known to be an antagonist of Wnt signaling and the constitutive ectopic expression of sFRP1 in preadipocytes disrupts Wnt/β-catenin signaling, which results in the promotion of adipogenesis *in vitro* and adipose tissue expansion *in vivo* (140, 193, 194, 196). Moreover, sFRP1 has also been reported to inhibit the myogenesis of satellite cells by down-regulating the expression of myogenin and Mrf4, both of which play roles in myoblast fusion and myofiber maturation (193). We observed higher sFRP1 mRNA levels in the dKO-nmMSCs compared to age-matched WT-CTX-nmMSCs. ELISA results further confirmed that the dKO-nmMSCs were secreting more sFRP1 protein than the WT-CTX-nmMSCs, further validating our hypothesis that sFRP1 secreted by the dKO-nmMSCs contributes, at least in part, to the micro-environment that inhibits the myogenic differentiation of the MDSCs in dKO muscle. Only weak expression of sFRP1 has been reported in WT skeletal muscle (194); yet we observed an approximate 8 fold increase in sFRP1 mRNA expression from the GAS of 6-8 week old dKO mice compared to age-matched WT-GAS and 4.5 fold increase compared to WT-CTX-GAS. These results suggest that sFRP1 may be associated with increased proliferation and the adipogenic potential of the nmMSCs isolated from dKO mice. Furthermore, it also appears that sFRP1 may play a role in the elevation of adipogenic gene expression and the accumulation of lipids observed in the dKO skeletal muscle; however, further studies are

required to confirm whether the sFRP1 released by the nmMSCs could contribute to the pro-adipogenic muscle microenvironment, which promotes fatty infiltration in the skeletal muscle of the dKO mice.

It has been reported that the Wnt signaling is up-regulated in both aged and dystrophic *mdx* skeletal muscle, which consequently leads to an alteration of muscle stem cell differentiation from myogenesis to fibrogenesis (7, 95). Indeed, the up-regulation of dephosphorylated β-catenin and increased mRNA expressions of Axin2 and LGR5, well-known canonical Wnt signaling target genes (4, 195) suggests that Wnt is also elevated in 6-8 week old dKO muscle compared to age-matched WT muscle. This finding was unexpected since sFRP1 is a known inhibitor of Wnt signaling pathways. Secreted protein sFRP1 is known to directly bind to Wnt molecules to block activation of Wnt/β-catenin signaling pathway (196). Ironically, our results indicated that both sFRP1 and Wnt signaling are elevated in dKO skeletal muscles. It may be possible that sFRP1 is activated in dKO muscle to antagonize the over-expression of Wnt signaling; however, the severe dystrophic muscle micro-milieu in dKO mice may cause the dysregulation of sFRP1. As a result, elevated sFRP1 in dKO muscles may involve in promoting adipogenesis and fatty degeneration instead of blocking Wnt singling. Further studies required to increase our understanding of how sFRP1 interacts with Wnt signaling that promotes the differentiation of nmMSCs toward an adipogenic lineage, which may contribute to the severe dystrophic phenotype observed in the dKO mice.

Overall, our data indicated that changes in muscle micro-milieu may affect the stem cell activities and behavior of the nmMSCs. We showed that the nmMSCs isolated from WT-CTX regenerating muscle produce pro-myogenic signals to MPCs and facilitate myogenic differentiation of MPCs, suggesting that they play a crucial role in muscle repair after acute

injury. On the other hand, the nmMSCs isolated from fibro-adipogenic dKO skeletal muscle significantly impaired the myogenic potential of MPCs, suggesting that the activity of the nmMSCs is altered in the chronic disease muscle. We proposed that sFRP1 protein secreted from the nmMSCs might be responsible for the inhibitory effect of dKO-nmMSCs on the myogenic potential of MPCs. We believe that dysregulation of Wnt signaling in dKO mice is potentially involved in the increased sFRP1 protein expression. This may represent one possible mechanism behind the up-regulation of sFRP1 in dKO skeletal muscle. However, further studies validating our finding and investigating other potential mechanisms are needed. Finally, based on our findings, blockade of sFRP1 might be a new therapeutic approach to reduce muscle wasting and degeneration in dystrophic muscle.

5.0 SUMMARY AND FUTURE DIRECTIONS

Adult skeletal muscle possesses a remarkable regenerative ability which largely depends on muscle progenitor cells such as satellite cells (57). However, in severe muscular dystrophies, such as Duchenne muscular dystrophy (DMD), skeletal muscle integrity is debilitated and it is often replaced by a mixture of fibrous tissue and white adipocytes in a process termed fibro-adipogenic degeneration (10, 24, 56, 191). Heterotopic ossification and accumulation of ectopic fat and fibrotic tissues in skeletal muscle may alter muscle microenvironment, induce stem/progenitor cell dysregulation, and interrupt muscle homeostasis which ultimately lead to skeletal muscle weakness. However, current therapies have not found a solution to block or replace formation of non-muscle tissues in the DMD skeletal muscle, and the precise origin of ectopic adipocytes or fibrotic tissue in dystrophic muscle is also not clearly understood.

In Chapter 2, based on a previously published preplate technique, we isolated two distinct populations of muscle derived cells from skeletal muscles; 1) a rapidly adhering cell population (RACs), which is non-myogenic, $Pax7^-$ and express the mesenchymal stem cell (MSCs) marker PDGFRα, hence we termed this population of cells, non-myogenic MSCs (nmMSCs); and 2) a slowly adhering cell population (SACs) which is $Pax7^+$ and highly myogenic, termed muscle progenitor cells (MPCs). Although previously considered as fibroblast-like cells, in this thesis, RACs were characterized as mesenchymal lineage stem cells, displaying strong adipogenic,

osteogenic, and chondrogenic differentiation potentials and likely involved in the fibrotic and fatty infiltration in dystrophic skeletal muscle.

Previously, we demonstrated that the rapid progression of skeletal muscle wasting and degeneration observed in dystrophin/utrophin double knockout (dys-/- utro-/-, dKO) mice is closely associated with a rapid depletion of the MPC population pool. (56). In Chapters 3, we focused our study on investigating the role of the nmMSCs in skeletal muscle histopathogenesis of dKO mice. Accumulation of lipids, calcium deposits, and fibrosis occurred in the skeletal muscle of dKO mice as early as 5-7 days of age and histopathologies progressively worsened with age. Since MPCs become impaired during the progression of the disease, we hypothesized that the nmMSCs may be the primary cells responsible for fibrosis and ectopic adipocytes and calcium deposits in DMD. We observed that the nmMSCs isolated from dKO muscle favor adipogenesis, osteogenesis, and fibrogenesis more strongly than age-matched wild type (WT) counterparts. Moreover, our results indicated that the proliferation and adipogenic/osteogenic potentials of the nmMSCs isolated from 1, 4, and 6-8 week old dKO mice were progressively activated during the course of the disease, suggesting that the activation of the nmMSCs is closely associated with the deposition of non-muscle tissues in the skeletal muscle of dKO mice.

Fat accumulation/infiltration is also a commonly recognized consequence of massive rotator cuff tears (RCTs), which is a tear of one or more of the tendons of the four rotator cuff muscles of the shoulder (197, 198). RCTs are among the most common injuries seen by orthopaedic surgeons and massive RCTs have been found to be associated with atrophy, fibrosis, and fat accumulation/infiltration (197). Clinically, these pathologic changes have been shown to be irreversible and have been correlated with poor prognosis and functional outcomes; however, the pathophysiology behind fat accumulation is still not clear (199). It has been suggested that

loss of mechanical stretch in muscles could trigger adipogenic lineage differentiation in MSCs or precursor cells within the muscle, possibly leading to the fatty degeneration observed in massive RCTs (197). Interestingly, one previous study proposed that mechanical stretch of muscles, which occurs during normal activity, activates the classical NF-κB pathways in *mdx* mice and this pathway could be predominately active in DMD since dystrophin deficiency in *ndx* mice causes skeletal muscles to be more susceptible to mechanical stretch or injury (200). These studies suggest that persistent stimulation of skeletal muscle fibers by mechanical forces or stress may regulate adipogenic potential of nmMSCs or other muscle resident progenitors and result in the development of muscular dystrophy. Future studies investigating effects of mechanical stretch on proliferation or differentiation potentials of nmMSCs will facilitate development of a novel therapy to prevent the progression of fat accumulation and enhance muscle regeneration in patients with DMD and massive RCTs.

Aside from contributing to formation of ectopic non-muscles tissues in dystrophic muscle, the nmMSCs may be a potential source of inhibitory muscle regeneration signaling that occurs during the chronic disease progression of DMD. As discussed in Chapter 3, the nmMSCs isolated from 6-8 week old dKO mice severely inhibit the myogenic differentiation of dKO-MPCs through the down-regulating genes that are important for myoblast maturation and terminal myogenic differentiation. Taken all together, our data indicated that the activation of the nmMSCs in dKO muscles may escalate the disease process by depositing fat, calcium aggregates, and fibrotic tissues in skeletal muscle as well as impair muscle regeneration through inhibition of the myogenic potential of MPCs. We further investigated soluble factor(s) secreted from the dKO-nmMSCs that limit the myogenic potentials of MPCs in the later chapter.

Experiments done in Chapter 4 suggest that the inhibitory effect of the nmMSCs on the myogenic potential of MPC was mediated by the secretion of secreted frizzled-related protein 1 (sFRP1). In fact, blockade of soluble sFRP1 secreted from dKO-nmMSCs using neutralized antibodies significantly improved myotube formation by MPCs co-cultivated with dKO-nmMSCs, supporting our hypothesis that sFRP1 is likely the secreting factor that inhibit the myogenic potential of MPCs.

Finally, we also examined the role of the nmMSCs in skeletal muscle regeneration. The purpose of this study was to determine how muscle microenvironment affects the activities and function of the nmMSC. In contrast to fibro-adipogenic environment in dKO skeletal muscle, WT-CTX muscle rarely induces adipocyte or fibrosis accumulation in the skeletal muscle. Therefore, we hypothesized that the behavior of the nmMSCs in WT-CTX-GAS is regulated in a manner distinct to those in dKO skeletal muscle. Interestingly, our results indicated that the nmMSCs were activated after acute muscle injury to facilitate MPC myogenesis via paracrine mechanism. We observed significantly higher level of myotube formation from MPCs co-cultured with the nmMSCs isolated from cardiotoxin injured regenerating muscle compared to MPCs alone. Our finding is supported by other investigations suggesting that the nmMSCs are in fact a crucial cellular compartment necessary for successful muscle repair and tissue homeostasis in WT muscle (44, 73, 92). The precise pro-myogenic signals/factors released from the nmMSCs during muscle repair process remain unidentified although interleukin-6 and follistatin are under investigation as candidates (73, 93). Our results suggest that the supporting effect of the nmMSCs in WT skeletal muscle regeneration through activation of MPCs is completely altered in the dKO skeletal muscle, an effect likely related to the fibro-adipogenic micro milieu in the

dKO skeletal muscle. This finding confirms our hypothesis that changes in muscle microenvironment induce abnormal alterations in stem cell activities.

In conclusion, based on our results and summarized in **Figure 21**, we propose that the nmMSCs represent a major contributor to the formation of ectopic fat, calcification, and fibrosis in the skeletal muscle of dKO mice, and that the activation of the nmMSCs may exacerbate the regeneration of the dystrophic muscle by inhibiting the myogenic potential of MPCs. More interestingly, in regenerating skeletal muscle of WT mice, the nmMSCs potentially support muscle regeneration of MPCs and are required for successful muscle repair, suggesting that in disease setting, these cells adopt a different fate leading to the development of fibrosis and fatty infiltration. It has been reported that MPCs from dKO mice are rapidly depleted, contributing to continuous muscle wasting and degeneration (201). Studies done in this dissertation reveal that while MPCs are depleted, the nmMSCs are activated and worsen the disease progression by forming ectopic non-muscle tissues and impairing muscle regeneration. Overall, data from this dissertation propose that a therapeutic strategy targeting activated nmMSCs could be a potential treatment for DMD.

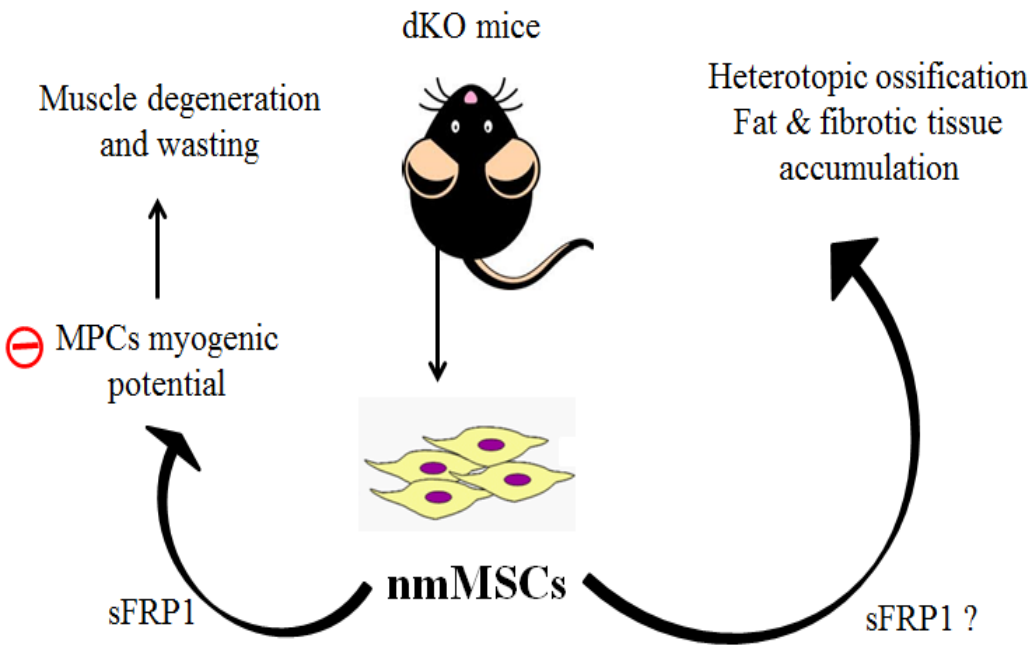

Figure 21. A schematic represents the role of the nmMSCs in skeletal muscle of dKO mice.

Our results agree with several other studies reporting presence of mesenchymal lineage progenitor cells, named PDGFRα^{+} cells, FAPs, and Tie2^{+} cells, in the skeletal muscle, whose activation in disease model or chemically induced fatty degenerating mouse resulted in formation of ectopic bone or adipose/fibrotic tissues (73, 94, 106). PDGFRα is the common cell surface maker shared by all of the above cell types and therefore, preventing the activation of PDGFRα expressing cells in skeletal muscle may be a promising therapy to improve muscle wasting and fibro-adipogenic degeneration in DMD. Most recently, Ito et al. reported that imatinib mesylate, which inhibits signaling of tyrosine kinase receptors, including PDGFRα, attenuates muscle necrosis, calcium accumulation, and fibrosis in *mdx* mice. Their study showed imatinib treatment in *mdx* mice inhibited proliferation and fibrosis-gene expression in muscle PDGFRα^{+} cells, without affecting myoblasts. However, they observed several unexpected side effects of imatinib,

including heart problem, no effect on fibrosis of diaphragm, and impaired muscle regeneration. In addition, the role of imatinib on other type of cells, such as infiltrating mononuclear cells, in the skeletal muscle is unclear (202). DMD is a genetic disorder that requires a long-term treatment to prevent any pathological changes. A study done by Ito et al. suggests that more-specific PDGFRα inhibitors are required.

Our data demonstrated that targeting sFRP1 might be a better therapeutic approach for treating DMD. sFRP1 has reported to inhibit C2C12 cell myogenic differentiation (193), but it is also a well-known inhibitor of Wnt signaling pathway whose action leads to activation of adipogenic genes and adipogenesis (143, 194). Results from Chapter 4 indicated that sFRP1 gene expression was elevated in dKO skeletal muscle and the dKO-nmMSCs secreted higher sFRP1 protein compared to WT controls. Therefore, we proposed that not only does the sFRP1 released by the nmMSCs hinder muscle regeneration, but it also contributes to establishing a pro-adipogenic muscle microenvironment, which promotes fibro-adipogenic degeneration in the skeletal muscles of the dKO mice. This finding strongly urged us to investigate whether the blockade of sFRP1 in dKO muscle would reduce fat/fibrotic tissue accumulation and delay muscle degeneration, ultimately improving muscle function and extending life and health span. Furthermore, for more general applications of sFRP1 in other types of muscle disease, better understanding of how and why sFRP1 expression was upregulated in dKO muscles is needed.

BIBLIOGRAPHY

1 Engel, A. and Banker, B.Q. (1986) *Myology : basic and clinical*. McGraw-Hill, New York.

2 Hoffman, E.P., Monaco, A.P., Feener, C.C. and Kunkel, L.M. (1987) Conservation of the Duchenne muscular dystrophy gene in mice and humans. *Science*, **238**, 347-350.

3 Zubrzycka-Gaarn, E.E., Bulman, D.E., Karpati, G., Burghes, A.H., Belfall, B., Klamut, H.J., Talbot, J., Hodges, R.S., Ray, P.N. and Worton, R.G. (1988) The Duchenne muscular dystrophy gene product is localized in sarcolemma of human skeletal muscle. *Nature*, **333**, 466-469.

4 Koenig, M., Beggs, A.H., Moyer, M., Scherpf, S., Heindrich, K., Bettecken, T., Meng, G., Muller, C.R., Lindlof, M., Kaariainen, H. *et al.* (1989) The molecular basis for Duchenne versus Becker muscular dystrophy: correlation of severity with type of deletion. *Am. J. Hum. Genet.*, **45**, 498-506.

5 Grady, R.M., Teng, H., Nichol, M.C., Cunningham, J.C., Wilkinson, R.S. and Sanes, J.R. (1997) Skeletal and cardiac myopathies in mice lacking utrophin and dystrophin: a model for Duchenne muscular dystrophy. *Cell*, **90**, 729-738.

6 Sussman, M. (2002) Duchenne muscular dystrophy. *J. Am. Acad. Orthop. Surg.*, **10**, 138-151.

7 Lapidos, K.A., Kakkar, R. and McNally, E.M. (2004) The dystrophin glycoprotein complex: signaling strength and integrity for the sarcolemma. *Circ. Res.*, **94**, 1023-1031.

8 Mendell, J.R., Campbell, K., Rodino-Klapac, L., Sahenk, Z., Shilling, C., Lewis, S., Bowles, D., Gray, S., Li, C., Galloway, G. *et al.* (2010) Dystrophin immunity in Duchenne's muscular dystrophy. *N. Engl. J. Med.*, **363**, 1429-1437.

9 Webster, C. and Blau, H.M. (1990) Accelerated age-related decline in replicative life-span of Duchenne muscular dystrophy myoblasts: implications for cell and gene therapy. *Somat. Cell Mol. Genet.*, **16**, 557-565.

10 Tiidus, P.M. (2008) *Skeletal muscle damage and repair*. Human Kinetics, Champaign, IL.

11 Hoffman, E.P., Brown, R.H., Jr. and Kunkel, L.M. (1987) Dystrophin: the protein product of the Duchenne muscular dystrophy locus. *Cell*, **51**, 919-928.

12 Wong, B.L. and Christopher, C. (2002) Corticosteroids in Duchenne muscular dystrophy: a reappraisal. *J. Child Neurol.*, **17**, 183-190.

13 Manzur, A.Y., Kuntzer, T., Pike, M. and Swan, A. (2008) Glucocorticoid corticosteroids for Duchenne muscular dystrophy. *Cochrane Database Syst Rev*, in press., CD003725.

14 Baltgalvis, K.A., Call, J.A., Nikas, J.B. and Lowe, D.A. (2009) Effects of prednisolone on skeletal muscle contractility in mdx mice. *Muscle Nerve*, **40**, 443-454.

15 Passaquin, A.C., Metzinger, L., Leger, J.J., Warter, J.M. and Poindron, P. (1993) Prednisolone enhances myogenesis and dystrophin-related protein in skeletal muscle cell cultures from mdx mouse. *J. Neurosci. Res.*, **35**, 363-372.

16 Manzur, A.Y., Kinali, M. and Muntoni, F. (2008) Update on the management of Duchenne muscular dystrophy. *Arch. Dis. Child.*, **93**, 986-990.

17 Evans, N.P., Misyak, S.A., Robertson, J.L., Bassaganya-Riera, J. and Grange, R.W. (2009) Immune-mediated mechanisms potentially regulate the disease time-course of duchenne muscular dystrophy and provide targets for therapeutic intervention. *PM R*, **1**, 755-768.

18 Biggar, W.D., Harris, V.A., Eliasoph, L. and Alman, B. (2006) Long-term benefits of deflazacort treatment for boys with Duchenne muscular dystrophy in their second decade. *Neuromuscul. Disord.*, **16**, 249-255.

19 Duan, D. (2011) Duchenne muscular dystrophy gene therapy: Lost in translation? *Res. Rep. Biol.*, **2011**, 31-42.

20 Cossu, G. and Sampaolesi, M. (2007) New therapies for Duchenne muscular dystrophy: challenges, prospects and clinical trials. *Trends Mol. Med.*, **13**, 520-526.

21 Kinali, M., Arechavala-Gomeza, V., Cirak, S., Glover, A., Guglieri, M., Feng, L., Hollingsworth, K.G., Hunt, D., Jungbluth, H., Roper, H.P. *et al.* (2011) Muscle histology vs MRI in Duchenne muscular dystrophy. *Neurology*, **76**, 346-353.

22 Engel, A. and Franzini-Armstrong, C. (2004) *Myology : basic and clinical*. McGraw-Hill, Medical Pub. Division, New York.

23 Tuttle, L.J., Sinacore, D.R. and Mueller, M.J. (2012) Intermuscular adipose tissue is muscle specific and associated with poor functional performance. *J. Aging Res.*, **2012**, 172957.

24 Mu, X., Usas, A., Tang, Y., Lu, A., Wang, B., Weiss, K. and Huard, J. (2013) RhoA mediates defective stem cell function and heterotopic ossification in dystrophic muscle of mice. *FASEB J.*, **27**, 3619-3631.

25 Bonilla, E., Samitt, C.E., Miranda, A.F., Hays, A.P., Salviati, G., DiMauro, S., Kunkel, L.M., Hoffman, E.P. and Rowland, L.P. (1988) Duchenne muscular dystrophy: deficiency of dystrophin at the muscle cell surface. *Cell*, **54**, 447-452.

26 Chan, W.P. and Liu, G.C. (2002) MR imaging of primary skeletal muscle diseases in children. *AJR Am. J. Roentgenol.*, **179**, 989-997.

27 Triplett, W.T., Baligand, C., Forbes, S.C., Willcocks, R.J., Lott, D.J., DeVos, S., Pollaro, J., Rooney, W.D., Sweeney, H.L., Bonnemann, C.G. *et al.* (2014) Chemical shift-based MRI to measure fat fractions in dystrophic skeletal muscle. *Magn. Reson. Med.*, **72**, 8-19.

28 Reimers, C.D. and Finkenstaedt, M. (1997) Muscle imaging in inflammatory myopathies. *Curr. Opin. Rheumatol.*, **9**, 475-485.

29 Delmonico, M.J., Harris, T.B., Visser, M., Park, S.W., Conroy, M.B., Velasquez-Mieyer, P., Boudreau, R., Manini, T.M., Nevitt, M., Newman, A.B. *et al.* (2009) Longitudinal study of muscle strength, quality, and adipose tissue infiltration. *Am. J. Clin. Nutr.*, **90**, 1579-1585.

30 Pahor, M. and Kritchevsky, S. (1998) Research hypotheses on muscle wasting, aging, loss of function and disability. *J. Nutr. Health Aging*, **2**, 97-100.

31 Visser, M., Goodpaster, B.H., Kritchevsky, S.B., Newman, A.B., Nevitt, M., Rubin, S.M., Simonsick, E.M. and Harris, T.B. (2005) Muscle mass, muscle strength, and muscle fat infiltration as predictors of incident mobility limitations in well-functioning older persons. *J. Gerontol. A Biol. Sci. Med. Sci.*, **60**, 324-333.

32 Goodpaster, B.H. and Wolf, D. (2004) Skeletal muscle lipid accumulation in obesity, insulin resistance, and type 2 diabetes. *Pediatr. Diabetes*, **5**, 219-226.

33 Barany, M., Venkatasubramanian, P.N., Mok, E., Siegel, I.M., Abraham, E., Wycliffe, N.D. and Mafee, M.F. (1989) Quantitative and qualitative fat analysis in human leg muscle of neuromuscular diseases by 1H MR spectroscopy in vivo. *Magn. Reson. Med.*, **10**, 210-226.

34 Vettor, R., Milan, G., Franzin, C., Sanna, M., De Coppi, P., Rizzuto, R. and Federspil, G. (2009) The origin of intermuscular adipose tissue and its pathophysiological implications. *Am. J. Physiol. Endocrinol. Metab.*, **297**, E987-998.

35 Schulz, T.J., Huang, T.L., Tran, T.T., Zhang, H., Townsend, K.L., Shadrach, J.L., Cerletti, M., McDougall, L.E., Giorgadze, N., Tchkonia, T. *et al.* (2011) Identification of inducible brown adipocyte progenitors residing in skeletal muscle and white fat. *Proc. Natl. Acad. Sci. U. S. A.*, **108**, 143-148.

36 Kim, H.K., Merrow, A.C., Shiraj, S., Wong, B.L., Horn, P.S. and Laor, T. (2013) Analysis of fatty infiltration and inflammation of the pelvic and thigh muscles in boys with Duchenne muscular dystrophy (DMD): grading of disease involvement on MR imaging and correlation with clinical assessments. *Pediatr. Radiol.*, **43**, 1327-1335.

37 Gaeta, M., Messina, S., Mileto, A., Vita, G.L., Ascenti, G., Vinci, S., Bottari, A., Vita, G., Settineri, N., Bruschetta, D. *et al.* (2012) Muscle fat-fraction and mapping in Duchenne muscular dystrophy: evaluation of disease distribution and correlation with clinical assessments. Preliminary experience. *Skeletal Radiol.*, **41**, 955-961.

38 Yao, L. and Gai, N. (2012) Fat-corrected T2 measurement as a marker of active muscle disease in inflammatory myopathy. *AJR Am. J. Roentgenol.*, **198**, W475-481.

39 Marden, F.A., Connolly, A.M., Siegel, M.J. and Rubin, D.A. (2005) Compositional analysis of muscle in boys with Duchenne muscular dystrophy using MR imaging. *Skeletal Radiol.*, **34**, 140-148.

40 Wren, T.A., Bluml, S., Tseng-Ong, L. and Gilsanz, V. (2008) Three-point technique of fat quantification of muscle tissue as a marker of disease progression in Duchenne muscular dystrophy: preliminary study. *AJR Am. J. Roentgenol.*, **190**, W8-12.

41 Clavel, S., Siffroi-Fernandez, S., Coldefy, A.S., Boulukos, K., Pisani, D.F. and Derijard, B. (2010) Regulation of the intracellular localization of Foxo3a by stress-activated protein kinase signaling pathways in skeletal muscle cells. *Mol. Cell. Biol.*, **30**, 470-480.

42 Fukada, S., Morikawa, D., Yamamoto, Y., Yoshida, T., Sumie, N., Yamaguchi, M., Ito, T., Miyagoe-Suzuki, Y., Takeda, S., Tsujikawa, K. *et al.* (2010) Genetic background affects properties of satellite cells and mdx phenotypes. *Am. J. Pathol.*, **176**, 2414-2424.

43 Hu, E., Tontonoz, P. and Spiegelman, B.M. (1995) Transdifferentiation of myoblasts by the adipogenic transcription factors PPAR gamma and C/EBP alpha. *Proc. Natl. Acad. Sci. U. S. A.*, **92**, 9856-9860.

44 Uezumi, A., Fukada, S., Yamamoto, N., Takeda, S. and Tsuchida, K. (2010) Mesenchymal progenitors distinct from satellite cells contribute to ectopic fat cell formation in skeletal muscle. *Nat. Cell Biol.*, **12**, 143-152.

45 Birbrair, A., Zhang, T., Wang, Z.M., Messi, M.L., Enikolopov, G.N., Mintz, A. and Delbono, O. (2013) Role of pericytes in skeletal muscle regeneration and fat accumulation. *Stem Cells Dev*, **22**, 2298-2314.

46 Agley, C.C., Rowlerson, A.M., Velloso, C.P., Lazarus, N.R. and Harridge, S.D. (2013) Human skeletal muscle fibroblasts, but not myogenic cells, readily undergo adipogenic differentiation. *J. Cell Sci.*, **126**, 5610-5625.

47 Willmann, R., Possekel, S., Dubach-Powell, J., Meier, T. and Ruegg, M.A. (2009) Mammalian animal models for Duchenne muscular dystrophy. *Neuromuscul. Disord.*, **19**, 241-249.

48 Wang, Z., Chamberlain, J.S., Tapscott, S.J. and Storb, R. (2009) Gene therapy in large animal models of muscular dystrophy. *ILAR journal / National Research Council, Institute of Laboratory Animal Resources*, **50**, 187-198.

49 Nguyen, F., Cherel, Y., Guigand, L., Goubault-Leroux, I. and Wyers, M. (2002) Muscle lesions associated with dystrophin deficiency in neonatal golden retriever puppies. *J. Comp. Pathol.*, **126**, 100-108.

50 Collins, C.A. and Morgan, J.E. (2003) Duchenne's muscular dystrophy: animal models used to investigate pathogenesis and develop therapeutic strategies. *Int. J. Exp. Pathol.*, **84**, 165-172.

51 Deconinck, A.E., Rafael, J.A., Skinner, J.A., Brown, S.C., Potter, A.C., Metzinger, L., Watt, D.J., Dickson, J.G., Tinsley, J.M. and Davies, K.E. (1997) Utrophin-dystrophin-deficient mice as a model for Duchenne muscular dystrophy. *Cell*, **90**, 717-727.

52 McLoon, L.K. (2008) Focusing on fibrosis: halofuginone-induced functional improvement in the mdx mouse model of Duchenne muscular dystrophy. *Am. J. Physiol. Heart Circ. Physiol.*, **294**, H1505-1507.

53 Nagaraju, K. (2001) Immunological capabilities of skeletal muscle cells. *Acta Physiol. Scand.*, **171**, 215-223.

54 Wagatsuma, A. (2007) Adipogenic potential can be activated during muscle regeneration. *Mol. Cell. Biochem.*, **304**, 25-33.

55 Isaac, C., Wright, A., Usas, A., Li, H., Tang, Y., Mu, X., Greco, N., Dong, Q., Vo, N., Kang, J. *et al.* (2013) Dystrophin and utrophin "double knockout" dystrophic mice exhibit a spectrum of degenerative musculoskeletal abnormalities. *J. Orthop. Res.*, **31**, 343-349.

56 Lu, A., Poddar, M., Tang, Y., Proto, J.D., Sohn, J., Mu, X., Oyster, N., Wang, B. and Huard, J. (2014) Rapid depletion of muscle progenitor cells in dystrophic mdx/utrophin-/- mice. *Hum. Mol. Genet.*, in press.

57 Mauro, A. (1961) Satellite cell of skeletal muscle fibers. *J Biophys Biochem Cytol*, **9**, 493-495.

58 Beauchamp, J.R., Heslop, L., Yu, D.S., Tajbakhsh, S., Kelly, R.G., Wernig, A., Buckingham, M.E., Partridge, T.A. and Zammit, P.S. (2000) Expression of CD34 and Myf5 defines the majority of quiescent adult skeletal muscle satellite cells. *J. Cell Biol.*, **151**, 1221-1234.

59 Peault, B., Rudnicki, M., Torrente, Y., Cossu, G., Tremblay, J.P., Partridge, T., Gussoni, E., Kunkel, L.M. and Huard, J. (2007) Stem and progenitor cells in skeletal muscle development, maintenance, and therapy. *Mol. Ther.*, **15**, 867-877.

60 Yoshida, N., Yoshida, S., Koishi, K., Masuda, K. and Nabeshima, Y. (1998) Cell heterogeneity upon myogenic differentiation: down-regulation of MyoD and Myf-5 generates 'reserve cells'. *J. Cell Sci.*, **111 (Pt 6)**, 769-779.

61 Bischoff, R. (1986) Proliferation of muscle satellite cells on intact myofibers in culture. *Dev. Biol.*, **115**, 129-139.

62 Asakura, A., Komaki, M. and Rudnicki, M. (2001) Muscle satellite cells are multipotential stem cells that exhibit myogenic, osteogenic, and adipogenic differentiation. *Differentiation*, **68**, 245-253.

63 Halevy, O., Piestun, Y., Allouh, M.Z., Rosser, B.W., Rinkevich, Y., Reshef, R., Rozenboim, I., Wleklinski-Lee, M. and Yablonka-Reuveni, Z. (2004) Pattern of Pax7 expression during myogenesis in the posthatch chicken establishes a model for satellite cell differentiation and renewal. *Dev. Dyn.*, **231**, 489-502.

64 Cusella-De Angelis, M.G., Lyons, G., Sonnino, C., De Angelis, L., Vivarelli, E., Farmer, K., Wright, W.E., Molinaro, M., Bouche, M., Buckingham, M. *et al.* (1992) MyoD, myogenin independent differentiation of primordial myoblasts in mouse somites. *J. Cell Biol.*, **116**, 1243-1255.

65 Partridge, T.A., Morgan, J.E., Coulton, G.R., Hoffman, E.P. and Kunkel, L.M. (1989) Conversion of mdx myofibres from dystrophin-negative to -positive by injection of normal myoblasts. *Nature*, **337**, 176-179.

66 Huard, J., Acsadi, G., Jani, A., Massie, B. and Karpati, G. (1994) Gene transfer into skeletal muscles by isogenic myoblasts. *Hum. Gene Ther.*, **5**, 949-958.

67 Zhang, J.Y., Wang, F., Zhang, H., Lu, J.Q. and Qiao, Y.J. (2014) Rapid Identification of Polymethoxylated Flavonoids in Traditional Chinese Medicines with a Practical Strategy of Stepwise Mass Defect Filtering Coupled to Diagnostic Product Ions Analysis based on a Hybrid LTQ-Orbitrap Mass Spectrometer. *Phytochem Anal*, in press.

68 Kinoshita, I., Vilquin, J.T., Guerette, B., Asselin, I., Roy, R. and Tremblay, J.P. (1994) Very efficient myoblast allotransplantation in mice under FK506 immunosuppression. *Muscle Nerve*, **17**, 1407-1415.

69 Song, F., Zhou, Y., Li, Y.S., Meng, X.M., Meng, X.Y., Liu, J.Q., Lu, S.Y., Ren, H.L., Hu, P., Liu, Z.S. *et al.* (2014) A rapid immunomagnetic beads-based immunoassay for the detection of beta-casein in bovine milk. *Food Chem*, **158**, 445-448.

70 Mitchell, K.J., Pannerec, A., Cadot, B., Parlakian, A., Besson, V., Gomes, E.R., Marazzi, G. and Sassoon, D.A. (2010) Identification and characterization of a non-satellite cell muscle resident progenitor during postnatal development. *Nat. Cell Biol.*, **12**, 257-266.

71 Deasy, B.M. and University of Pittsburgh. School of Engineering. (2004). University of Pittsburgh, Pittsburgh, PA, in press.

72 Zhang, D., Meng, S., Xu, P., Lu, H., Zhuang, M., Wu, G., Liu, Y., Pan, X., Yan, H., Chen, X. *et al.* (2014) Experience of offering HIV rapid testing to at-risk patients in community health centers in eight Chinese cities. *PLoS One*, **9**, e86609.

73 Joe, A.W., Yi, L., Natarajan, A., Le Grand, F., So, L., Wang, J., Rudnicki, M.A. and Rossi, F.M. (2010) Muscle injury activates resident fibro/adipogenic progenitors that facilitate myogenesis. *Nat. Cell Biol.*, **12**, 153-163.

74 Gharaibeh, B., Lu, A., Tebbets, J., Zheng, B., Feduska, J., Crisan, M., Peault, B., Cummins, J. and Huard, J. (2008) Isolation of a slowly adhering cell fraction containing stem cells from murine skeletal muscle by the preplate technique. *Nat. Protoc.*, **3**, 1501-1509.

75 Qu-Petersen, Z., Deasy, B., Jankowski, R., Ikezawa, M., Cummins, J., Pruchnic, R., Mytinger, J., Cao, B., Gates, C., Wernig, A. *et al.* (2002) Identification of a novel population of muscle stem cells in mice: potential for muscle regeneration. *J. Cell Biol.*, **157**, 851-864.

76 Wu, X., Wang, S., Chen, B. and An, X. (2010) Muscle-derived stem cells: isolation, characterization, differentiation, and application in cell and gene therapy. *Cell Tissue Res.*, **340**, 549-567.

77 Jankowski, R.J., Haluszczak, C., Trucco, M. and Huard, J. (2001) Flow cytometric characterization of myogenic cell populations obtained via the preplate technique: potential for rapid isolation of muscle-derived stem cells. *Hum. Gene Ther.*, **12**, 619-628.

78 Chirieleison, S.M., Feduska, J.M., Schugar, R.C., Askew, Y. and Deasy, B.M. (2012) Human muscle-derived cell populations isolated by differential adhesion rates: phenotype and contribution to skeletal muscle regeneration in Mdx/SCID mice. *Tissue Eng Part A*, **18**, 232-241.

79 Deasy, B.M., Gharaibeh, B.M., Pollett, J.B., Jones, M.M., Lucas, M.A., Kanda, Y. and Huard, J. (2005) Long-term self-renewal of postnatal muscle-derived stem cells. *Mol. biol. of the cell*, **16**, 3323-3333.

80 Jankowski, R.J., Deasy, B.M., Cao, B., Gates, C. and Huard, J. (2002) The role of CD34 expression and cellular fusion in the regeneration capacity of myogenic progenitor cells. *J. Cell Sci.*, **115**, 4361-4374.

81 Rose, T., Peng, H., Shen, H.C., Usas, A., Kuroda, R., Lill, H., Fu, F.H. and Huard, J. (2003) The role of cell type in bone healing mediated by ex vivo gene therapy. *Langenbecks Arch. Surg.*, **388**, 347-355.

82 Deasy, B.M., Li, Y. and Huard, J. (2004) Tissue engineering with muscle-derived stem cells. *Curr. Opin. Biotechnol.*, **15**, 419-423.

83 Payne, T.R., Oshima, H., Okada, M., Momoi, N., Tobita, K., Keller, B.B., Peng, H. and Huard, J. (2007) A relationship between vascular endothelial growth factor, angiogenesis, and cardiac repair after muscle stem cell transplantation into ischemic hearts. *J. Am. Coll. Cardiol.*, **50**, 1677-1684.

84 Urish, K.L., Vella, J.B., Okada, M., Deasy, B.M., Tobita, K., Keller, B.B., Cao, B., Piganelli, J.D. and Huard, J. (2009) Antioxidant levels represent a major determinant in the regenerative capacity of muscle stem cells. *Mol. Biol. Cell*, **20**, 509-520.

85 Drowley, L., Okada, M., Beckman, S., Vella, J., Keller, B., Tobita, K. and Huard, J. (2010) Cellular antioxidant levels influence muscle stem cell therapy. *Mol. Ther.*, **18**, 1865-1873.

86 Vella, J.B., Thompson, S.D., Bucsek, M.J., Song, M. and Huard, J. (2011) Murine and human myogenic cells identified by elevated aldehyde dehydrogenase activity: implications for muscle regeneration and repair. *PLoS One*, **6**, e29226.

87 Beckman, S.A., Chen, W.C., Tang, Y., Proto, J.D., Mlakar, L., Wang, B. and Huard, J. (2013) Beneficial effect of mechanical stimulation on the regenerative potential of muscle-derived stem cells is lost by inhibiting vascular endothelial growth factor. *Arterioscler. Thromb. Vasc. Biol.*, **33**, 2004-2012.

88 Rouger, K., Larcher, T., Dubreil, L., Deschamps, J.Y., Le Guiner, C., Jouvion, G., Delorme, B., Lieubeau, B., Carlus, M., Fornasari, B. *et al.* (2011) Systemic delivery of allogenic muscle stem cells induces long-term muscle repair and clinical efficacy in duchenne muscular dystrophy dogs. *Am. J. Pathol.*, **179**, 2501-2518.

89 Okada, M., Payne, T.R., Drowley, L., Jankowski, R.J., Momoi, N., Beckman, S., Chen, W.C., Keller, B.B., Tobita, K. and Huard, J. (2012) Human skeletal muscle cells with a slow adhesion rate after isolation and an enhanced stress resistance improve function of ischemic hearts. *Mol. Ther.*, **20**, 138-145.

90 Carr, L.K., Steele, D., Steele, S., Wagner, D., Pruchnic, R., Jankowski, R., Erickson, J., Huard, J. and Chancellor, M.B. (2008) 1-year follow-up of autologous muscle-derived stem cell injection pilot study to treat stress urinary incontinence. *Int. Urogynecol. J. Pelvic Floor Dysfunct.*, **19**, 881-883.

91 Dominici, M., Le Blanc, K., Mueller, I., Slaper-Cortenbach, I., Marini, F., Krause, D., Deans, R., Keating, A., Prockop, D. and Horwitz, E. (2006) Minimal criteria for defining multipotent mesenchymal stromal cells. The International Society for Cellular Therapy position statement. *Cytotherapy*, **8**, 315-317.

92 Heredia, J.E., Mukundan, L., Chen, F.M., Mueller, A.A., Deo, R.C., Locksley, R.M., Rando, T.A. and Chawla, A. (2013) Type 2 innate signals stimulate fibro/adipogenic progenitors to facilitate muscle regeneration. *Cell*, **153**, 376-388.

93 Mozzetta, C., Consalvi, S., Saccone, V., Tierney, M., Diamantini, A., Mitchell, K.J., Marazzi, G., Borsellino, G., Battistini, L., Sassoon, D. *et al.* (2013) Fibroadipogenic progenitors mediate the ability of HDAC inhibitors to promote regeneration in dystrophic muscles of young, but not old Mdx mice. *EMBO Mol. Med.*, **5**, 626-639.

94 Uezumi, A., Ito, T., Morikawa, D., Shimizu, N., Yoneda, T., Segawa, M., Yamaguchi, M., Ogawa, R., Matev, M.M., Miyagoe-Suzuki, Y. *et al.* (2011) Fibrosis and adipogenesis originate from a common mesenchymal progenitor in skeletal muscle. *J. Cell Sci.*, **124**, 3654-3664.

95 Biressi, S., Miyabara, E.H., Gopinath, S.D., PM, M.C. and Rando, T.A. (2014) A Wnt-TGFbeta2 axis induces a fibrogenic program in muscle stem cells from dystrophic mice. *Sci. Transl. Med.*, **6**, 267ra176.

96 Birbrair, A., Zhang, T., Wang, Z.M., Messi, M.L., Mintz, A. and Delbono, O. (2013) Type-1 pericytes participate in fibrous tissue deposition in aged skeletal muscle. *Am. J. Physiol. Cell Physiol.*, **305**, C1098-1113.

97 Mao, H., Wang, H., Wang, B., Liu, X., Gao, H., Xu, M., Zhao, H., Deng, X. and Lin, D. (2009) Systemic metabolic changes of traumatic critically ill patients revealed by an NMR-based metabonomic approach. *J. Proteome Res.*, **8**, 5423-5430.

98 Lee, J.Y., Qu-Petersen, Z., Cao, B., Kimura, S., Jankowski, R., Cummins, J., Usas, A., Gates, C., Robbins, P., Wernig, A. *et al.* (2000) Clonal isolation of muscle-derived cells capable of enhancing muscle regeneration and bone healing. *J. Cell Biol.*, **150**, 1085-1100.

99 Cao, B., Zheng, B., Jankowski, R.J., Kimura, S., Ikezawa, M., Deasy, B., Cummins, J., Epperly, M., Qu-Petersen, Z. and Huard, J. (2003) Muscle stem cells differentiate into haematopoietic lineages but retain myogenic potential. *Nat. Cell Biol.*, **5**, 640-646.

100 Usas, A. and Huard, J. (2007) Muscle-derived stem cells for tissue engineering and regenerative therapy. *Biomaterials*, **28**, 5401-5406.

101 Gupta, M., Kamynina, E., Morley, S., Chung, S., Muakkassa, N., Wang, H., Brathwaite, S., Sharma, G. and Manor, D. (2013) Plekhg4 is a novel Dbl family guanine nucleotide exchange factor protein for rho family GTPases. *J. Biol. Chem.*, **288**, 14522-14530.

102 Li, Y. and Huard, J. (2002) Differentiation of muscle-derived cells into myofibroblasts in injured skeletal muscle. *Am. J. Pathol.*, **161**, 895-907.

103 Pannerec, A., Formicola, L., Besson, V., Marazzi, G. and Sassoon, D.A. (2013) Defining skeletal muscle resident progenitors and their cell fate potentials. *Development*, **140**, 2879-2891.

104 Zhang, J.Y., Wang, Z.J., Zhang, Q., Wang, F., Ma, Q., Lin, Z.Z., Lu, J.Q. and Qiao, Y.J. (2014) Rapid screening and identification of target constituents using full scan-parent ions list-dynamic exclusion acquisition coupled to diagnostic product ions analysis on a hybrid LTQ-Orbitrap mass spectrometer. *Talanta*, **124**, 111-122.

105 Chen, W., Zhang, J., Lu, G., Yuan, Z., Wu, Q., Li, J., Xu, G., He, A., Zheng, J. and Zhang, J. (2014) Development of an immunochromatographic lateral flow device for rapid diagnosis of Vibrio cholerae O1 serotype Ogawa. *Clin. Biochem.*, **47**, 448-454.

106 Wosczyna, M.N., Biswas, A.A., Cogswell, C.A. and Goldhamer, D.J. (2012) Multipotent progenitors resident in the skeletal muscle interstitium exhibit robust BMP-dependent osteogenic activity and mediate heterotopic ossification. *J. Bone Miner. Res.*, **27**, 1004-1017.

107 Murphy, M.M., Lawson, J.A., Mathew, S.J., Hutcheson, D.A. and Kardon, G. (2011) Satellite cells, connective tissue fibroblasts and their interactions are crucial for muscle regeneration. *Development*, **138**, 3625-3637.

108 Luaces, J.P., Rossi, L.F., Sciurano, R.B., Rebuzzini, P., Merico, V., Zuccotti, M., Merani, M.S. and Garagna, S. (2014) Loss of Sertoli-germ cell adhesion determines the rapid germ cell elimination during the seasonal regression of the seminiferous epithelium of the large hairy armadillo Chaetophractus villosus. *Biol. Reprod.*, **90**, 48.

109 Fan, X., Jin, W.Y., Lu, J., Wang, J. and Wang, Y.T. (2014) Rapid and reversible knockdown of endogenous proteins by peptide-directed lysosomal degradation. *Nat. Neurosci.*, **17**, 471-480.

110 Hao, Q.F., Yang, Y.X., Wang, Y., Chen, L.M., Sheng, G.Y. and Luan, Z. (2014) Rapid generation of Epstein-Barr virus-specific T cells for cellular therapy. *Transplant. Proc.*, **46**, 21-25.

111 Morrison, S.J., Shah, N.M. and Anderson, D.J. (1997) Regulatory mechanisms in stem cell biology. *Cell*, **88**, 287-298.

112 Moore, K.A. and Lemischka, I.R. (2006) Stem cells and their niches. *Science*, **311**, 1880-1885.

113 Fortunel, N.O., Otu, H.H., Ng, H.H., Chen, J., Mu, X., Chevassut, T., Li, X., Joseph, M., Bailey, C., Hatzfeld, J.A. *et al.* (2003) Comment on " 'Stemness': transcriptional profiling of embryonic and adult stem cells" and "a stem cell molecular signature". *Science*, **302**, 393; author reply 393.

114 Ivanova, N.B., Dimos, J.T., Schaniel, C., Hackney, J.A., Moore, K.A. and Lemischka, I.R. (2002) A stem cell molecular signature. *Science*, **298**, 601-604.

115 Ramalho-Santos, M., Yoon, S., Matsuzaki, Y., Mulligan, R.C. and Melton, D.A. (2002) "Stemness": transcriptional profiling of embryonic and adult stem cells. *Science*, **298**, 597-600.

116 Tenney, R.M. and Discher, D.E. (2009) Stem cells, microenvironment mechanics, and growth factor activation. *Curr. Opin. Cell Biol.*, **21**, 630-635.

117 Guilak, F., Cohen, D.M., Estes, B.T., Gimble, J.M., Liedtke, W. and Chen, C.S. (2009) Control of stem cell fate by physical interactions with the extracellular matrix. *Cell stem cell*, **5**, 17-26.

118 Blau, O., Hofmann, W.K., Baldus, C.D., Thiel, G., Serbent, V., Schumann, E., Thiel, E. and Blau, I.W. (2007) Chromosomal aberrations in bone marrow mesenchymal stroma cells from patients with myelodysplastic syndrome and acute myeloblastic leukemia. *Exp. Hematol.*, **35**, 221-229.

119 Hu, X., Shen, H., Tian, C., Yu, H., Zheng, G., XuFeng, R., Ju, Z., Xu, J., Wang, J. and Cheng, T. (2009) Kinetics of normal hematopoietic stem and progenitor cells in a Notch1-induced leukemia model. *Blood*, **114**, 3783-3792.

120 Tian, C., Zheng, G., Cao, Z., Li, Q., Ju, Z., Wang, J., Yuan, W. and Cheng, T. (2013) Hes1 mediates the different responses of hematopoietic stem and progenitor cells to T cell leukemic environment. *Cell cycle*, **12**, 322-331.

121 Brack, A.S., Conboy, M.J., Roy, S., Lee, M., Kuo, C.J., Keller, C. and Rando, T.A. (2007) Increased Wnt signaling during aging alters muscle stem cell fate and increases fibrosis. *Science*, **317**, 807-810.

122 Chakkalakal, J.V., Jones, K.M., Basson, M.A. and Brack, A.S. (2012) The aged niche disrupts muscle stem cell quiescence. *Nature*, **490**, 355-360.

123 Jackson, W.M., Lozito, T.P., Djouad, F., Kuhn, N.Z., Nesti, L.J. and Tuan, R.S. (2011) Differentiation and regeneration potential of mesenchymal progenitor cells derived from traumatized muscle tissue. *J. Cell. Mol. Med.*, **15**, 2377-2388.

124 Sacco, A., Mourkioti, F., Tran, R., Choi, J., Llewellyn, M., Kraft, P., Shkreli, M., Delp, S., Pomerantz, J.H., Artandi, S.E. *et al.* (2010) Short telomeres and stem cell exhaustion model Duchenne muscular dystrophy in mdx/mTR mice. *Cell*, **143**, 1059-1071.

125 Saccone, V., Consalvi, S., Giordani, L., Mozzetta, C., Barozzi, I., Sandona, M., Ryan, T., Rojas-Munoz, A., Madaro, L., Fasanaro, P. *et al.* (2014) HDAC-regulated myomiRs control BAF60 variant exchange and direct the functional phenotype of fibro-adipogenic progenitors in dystrophic muscles. *Genes Dev.*, **28**, 841-857.

126 von Maltzahn, J., Chang, N.C., Bentzinger, C.F. and Rudnicki, M.A. (2012) Wnt signaling in myogenesis. *Trends Cell Biol.*, **22**, 602-609.

127 Brack, A.S., Conboy, I.M., Conboy, M.J., Shen, J. and Rando, T.A. (2008) A temporal switch from notch to Wnt signaling in muscle stem cells is necessary for normal adult myogenesis. *Cell stem cell*, **2**, 50-59.

128 Han, X.H., Jin, Y.R., Seto, M. and Yoon, J.K. (2011) A WNT/beta-catenin signaling activator, R-spondin, plays positive regulatory roles during skeletal myogenesis. *J. Biol. Chem.*, **286**, 10649-10659.

129 Polesskaya, A., Seale, P. and Rudnicki, M.A. (2003) Wnt signaling induces the myogenic specification of resident CD45+ adult stem cells during muscle regeneration. *Cell*, **113**, 841-852.
130 Hogan, P.G., Chen, L., Nardone, J. and Rao, A. (2003) Transcriptional regulation by calcium, calcineurin, and NFAT. *Genes Dev.*, **17**, 2205-2232.

131 Munsterberg, A.E., Kitajewski, J., Bumcrot, D.A., McMahon, A.P. and Lassar, A.B. (1995) Combinatorial signaling by Sonic hedgehog and Wnt family members induces myogenic bHLH gene expression in the somite. *Genes Dev.*, **9**, 2911-2922.

132 Tajbakhsh, S., Borello, U., Vivarelli, E., Kelly, R., Papkoff, J., Duprez, D., Buckingham, M. and Cossu, G. (1998) Differential activation of Myf5 and MyoD by different Wnts in explants of mouse paraxial mesoderm and the later activation of myogenesis in the absence of Myf5. *Development*, **125**, 4155-4162.

133 Brunelli, S., Relaix, F., Baesso, S., Buckingham, M. and Cossu, G. (2007) Beta catenin-independent activation of MyoD in presomitic mesoderm requires PKC and depends on Pax3 transcriptional activity. *Dev. Biol.*, **304**, 604-614.

134 Otto, A., Schmidt, C., Luke, G., Allen, S., Valasek, P., Muntoni, F., Lawrence-Watt, D. and Patel, K. (2008) Canonical Wnt signalling induces satellite-cell proliferation during adult skeletal muscle regeneration. *J. Cell Sci.*, **121**, 2939-2950.

135 de Lau, W.B., Snel, B. and Clevers, H.C. (2012) The R-spondin protein family. *Genome Biol.*, **13**, 242.

136 Niehrs, C. (2006) Function and biological roles of the Dickkopf family of Wnt modulators. *Oncogene*, **25**, 7469-7481.

137 Itasaki, N., Jones, C.M., Mercurio, S., Rowe, A., Domingos, P.M., Smith, J.C. and Krumlauf, R. (2003) Wise, a context-dependent activator and inhibitor of Wnt signalling. *Development*, **130**, 4295-4305.

138 Le Grand, F., Jones, A.E., Seale, V., Scime, A. and Rudnicki, M.A. (2009) Wnt7a activates the planar cell polarity pathway to drive the symmetric expansion of satellite stem cells. *Cell stem cell*, **4**, 535-547.

139 Rochat, A., Fernandez, A., Vandromme, M., Moles, J.P., Bouschet, T., Carnac, G. and Lamb, N.J. (2004) Insulin and wnt1 pathways cooperate to induce reserve cell activation in differentiation and myotube hypertrophy. *Mol. Biol. Cell*, **15**, 4544-4555.

140 Lagathu, C., Christodoulides, C., Tan, C.Y., Virtue, S., Laudes, M., Campbell, M., Ishikawa, K., Ortega, F., Tinahones, F.J., Fernandez-Real, J.M. *et al.* (2010) Secreted frizzled-related protein 1 regulates adipose tissue expansion and is dysregulated in severe obesity. *Int. J. Obes. (Lond)*, **34**, 1695-1705.

141 Schaniel, C., Sirabella, D., Qiu, J., Niu, X., Lemischka, I.R. and Moore, K.A. (2011) Wnt-inhibitory factor 1 dysregulation of the bone marrow niche exhausts hematopoietic stem cells. *Blood*, **118**, 2420-2429.

142 Choi, H.J., Park, H., Lee, H.W. and Kwon, Y.G. (2012) The Wnt pathway and the roles for its antagonists, DKKS, in angiogenesis. *IUBMB life*, **64**, 724-731.

143 Christodoulides, C., Lagathu, C., Sethi, J.K. and Vidal-Puig, A. (2009) Adipogenesis and WNT signalling. *Trends Endocrinol. Metab.*, **20**, 16-24.

144 Vertino, A.M., Taylor-Jones, J.M., Longo, K.A., Bearden, E.D., Lane, T.F., McGehee, R.E., Jr., MacDougald, O.A. and Peterson, C.A. (2005) Wnt10b deficiency promotes coexpression of myogenic and adipogenic programs in myoblasts. *Mol. Biol. Cell*, **16**, 2039-2048.

145 Ross, S.E., Hemati, N., Longo, K.A., Bennett, C.N., Lucas, P.C., Erickson, R.L. and MacDougald, O.A. (2000) Inhibition of adipogenesis by Wnt signaling. *Science*, **289**, 950-953.

146 Itoigawa, Y., Kishimoto, K.N., Sano, H., Kaneko, K. and Itoi, E. (2011) Molecular mechanism of fatty degeneration in rotator cuff muscle with tendon rupture. *J. Orthop. Res.*, **29**, 861-866.

147 Wei, X., Yang, X., Han, Z.P., Qu, F.F., Shao, L. and Shi, Y.F. (2013) Mesenchymal stem cells: a new trend for cell therapy. *Acta Pharmacol. Sin.*, **34**, 747-754.

148 Pittenger, M.F. and Martin, B.J. (2004) Mesenchymal stem cells and their potential as cardiac therapeutics. *Circ. Res.*, **95**, 9-20.

149 Noth, U., Steinert, A.F. and Tuan, R.S. (2008) Technology insight: adult mesenchymal stem cells for osteoarthritis therapy. *Nat. Clin. Pract. Rheumatol.*, **4**, 371-380.

150 Erokhin, V.V., Vasil'eva, I.A., Konopliannikov, A.G., Chukanov, V.I., Tsyb, A.F., Bagdasarian, T.R., Danilenko, A.A., Lepekhina, L.A., Kal'sina, S., Semenkova, I.V. *et al.* (2008) [Systemic transplantation of autologous mesenchymal stem cells of the bone marrow in the treatment of patients with multidrug-resistant pulmonary tuberculosis]. *Problemy tuberkuleza i boleznei legkikh*, in press., 3-6.

151 Le Blanc, K., Rasmusson, I., Sundberg, B., Gotherstrom, C., Hassan, M., Uzunel, M. and Ringden, O. (2004) Treatment of severe acute graft-versus-host disease with third party haploidentical mesenchymal stem cells. *Lancet*, **363**, 1439-1441.

152 Garcia-Olmo, D., Garcia-Arranz, M., Herreros, D., Pascual, I., Peiro, C. and Rodriguez-Montes, J.A. (2005) A phase I clinical trial of the treatment of Crohn's fistula by adipose mesenchymal stem cell transplantation. *Dis. Colon Rectum*, **48**, 1416-1423.

153 Horwitz, E.M., Prockop, D.J., Fitzpatrick, L.A., Koo, W.W., Gordon, P.L., Neel, M., Sussman, M., Orchard, P., Marx, J.C., Pyeritz, R.E. *et al.* (1999) Transplantability and therapeutic effects of bone marrow-derived mesenchymal cells in children with osteogenesis imperfecta. *Nat. Med.*, **5**, 309-313.

154 Friedenstein, A.J., Chailakhyan, R.K., Latsinik, N.V., Panasyuk, A.F. and Keiliss-Borok, I.V. (1974) Stromal cells responsible for transferring the microenvironment of the hemopoietic tissues. Cloning in vitro and retransplantation in vivo. *Transplantation*, **17**, 331-340.

155 Prockop, D.J. (1997) Marrow stromal cells as stem cells for nonhematopoietic tissues. *Science*, **276**, 71-74.

156 Granero-Molto, F., Weis, J.A., Longobardi, L. and Spagnoli, A. (2008) Role of mesenchymal stem cells in regenerative medicine: application to bone and cartilage repair. *Expert Opin. Biol. Ther.*, **8**, 255-268.

157 Reyes, M., Lund, T., Lenvik, T., Aguiar, D., Koodie, L. and Verfaillie, C.M. (2001) Purification and ex vivo expansion of postnatal human marrow mesodermal progenitor cells. *Blood*, **98**, 2615-2625.

158 Pittenger, M.F., Mackay, A.M., Beck, S.C., Jaiswal, R.K., Douglas, R., Mosca, J.D., Moorman, M.A., Simonetti, D.W., Craig, S. and Marshak, D.R. (1999) Multilineage potential of adult human mesenchymal stem cells. *Science*, **284**, 143-147.

159 Tzaribachev, N., Vaegler, M., Schaefer, J., Reize, P., Rudert, M., Handgretinger, R. and Muller, I. (2008) Mesenchymal stromal cells: a novel treatment option for steroid-induced avascular osteonecrosis. *Isr. Med. Assoc. J.*, **10**, 232-234.

160 Richardson, S.M. and Hoyland, J.A. (2008) Stem cell regeneration of degenerated intervertebral discs: current status. *Curr Pain Headache Rep*, **12**, 83-88.

161 Han, Z., Jing, Y., Zhang, S., Liu, Y., Shi, Y. and Wei, L. (2012) The role of immunosuppression of mesenchymal stem cells in tissue repair and tumor growth. *Cell & bioscience*, **2**, 8.

162 Uccelli, A., Moretta, L. and Pistoia, V. (2008) Mesenchymal stem cells in health and disease. *Nat. Rev. Immunol.*, **8**, 726-736.

163 Uezumi, A., Fukada, S., Yamamoto, N., Ikemoto-Uezumi, M., Nakatani, M., Morita, M., Yamaguchi, A., Yamada, H., Nishino, I., Hamada, Y. *et al.* (2014) Identification and characterization of PDGFRalpha+ mesenchymal progenitors in human skeletal muscle. *Cell Death Dis.*, **5**, e1186.

164 Morikawa, S., Mabuchi, Y., Kubota, Y., Nagai, Y., Niibe, K., Hiratsu, E., Suzuki, S., Miyauchi-Hara, C., Nagoshi, N., Sunabori, T. *et al.* (2009) Prospective identification, isolation, and systemic transplantation of multipotent mesenchymal stem cells in murine bone marrow. *J. Exp. Med.*, **206**, 2483-2496.

165 Morikawa, S., Mabuchi, Y., Niibe, K., Suzuki, S., Nagoshi, N., Sunabori, T., Shimmura, S., Nagai, Y., Nakagawa, T., Okano, H. *et al.* (2009) Development of mesenchymal stem cells partially originate from the neural crest. *Biochem. Biophys. Res. Commun.*, **379**, 1114-1119.

166 Lavasani, M., Lu, A., Thompson, S.D., Robbins, P.D., Huard, J. and Niedernhofer, L.J. (2013) Isolation of muscle-derived stem/progenitor cells based on adhesion characteristics to collagen-coated surfaces. *Methods Mol. Biol.*, **976**, 53-65.

167 Kishimoto, K.N., Oxford, C.L. and Reddi, A.H. (2009) Stimulation of the side population fraction of ATDC5 chondroprogenitors by hypoxia. *Cell Biol. Int.*, **33**, 1222-1229.

168 Soleimani, M. and Nadri, S. (2009) A protocol for isolation and culture of mesenchymal stem cells from mouse bone marrow. *Nat. Protoc.*, **4**, 102-106.

169 Houlihan, D.D., Mabuchi, Y., Morikawa, S., Niibe, K., Araki, D., Suzuki, S., Okano, H. and Matsuzaki, Y. (2012) Isolation of mouse mesenchymal stem cells on the basis of expression of Sca-1 and PDGFR-alpha. *Nat. Protoc.*, **7**, 2103-2111.

170 Lin, C.S., Ning, H., Lin, G. and Lue, T.F. (2012) Is CD34 truly a negative marker for mesenchymal stromal cells? *Cytotherapy*, **14**, 1159-1163.

171 Lin, C.S., Xin, Z.C., Dai, J. and Lue, T.F. (2013) Commonly used mesenchymal stem cell markers and tracking labels: Limitations and challenges. *Histol. Histopathol.*, **28**, 1109-1116.

172 Zheng, B., Cao, B., Li, G. and Huard, J. (2006) Mouse adipose-derived stem cells undergo multilineage differentiation in vitro but primarily osteogenic and chondrogenic differentiation in vivo. *Tissue Eng.*, **12**, 1891-1901.

173 Appelbaum, F.R. (2007) Hematopoietic-cell transplantation at 50. *N. Engl. J. Med.*, **357**, 1472-1475.

174 Peister, A., Mellad, J.A., Larson, B.L., Hall, B.M., Gibson, L.F. and Prockop, D.J. (2004) Adult stem cells from bone marrow (MSCs) isolated from different strains of inbred mice vary in surface epitopes, rates of proliferation, and differentiation potential. *Blood*, **103**, 1662-1668.

175 Copland, I., Sharma, K., Lejeune, L., Eliopoulos, N., Stewart, D., Liu, P., Lachapelle, K. and Galipeau, J. (2008) CD34 expression on murine marrow-derived mesenchymal stromal cells: impact on neovascularization. *Exp. Hematol.*, **36**, 93-103.

176 Muller, A.M., Hermanns, M.I., Skrzynski, C., Nesslinger, M., Muller, K.M. and Kirkpatrick, C.J. (2002) Expression of the endothelial markers PECAM-1, vWf, and CD34 in vivo and in vitro. *Exp. Mol. Pathol.*, **72**, 221-229.

177 Unger, R.E., Krump-Konvalinkova, V., Peters, K. and Kirkpatrick, C.J. (2002) In vitro expression of the endothelial phenotype: comparative study of primary isolated cells and cell lines, including the novel cell line HPMEC-ST1.6R. *Microvasc. Res.*, **64**, 384-397.

178 Testa, J.E., Chrastina, A., Oh, P., Li, Y., Witkiewicz, H., Czarny, M., Buss, T. and Schnitzer, J.E. (2009) Immunotargeting and cloning of two CD34 variants exhibiting restricted expression in adult rat endothelia in vivo. *Am. J. Physiol. Lung Cell Mol. Physiol.*, **297**, L251-262.

179 Boxall, S.A. and Jones, E. (2012) Markers for characterization of bone marrow multipotential stromal cells. *Stem cells international*, **2012**, 975871.

180 Huard, J., Cao, B. and Qu-Petersen, Z. (2003) Muscle-derived stem cells: potential for muscle regeneration. *Birth Defects Res. C. Embryo Today*, **69**, 230-237.

181 Judson, R.N., Zhang, R.H. and Rossi, F.M. (2013) Tissue-resident mesenchymal stem/progenitor cells in skeletal muscle: collaborators or saboteurs? *FEBS J*, **280**, 4100-4108.
182 Emery, A.E. (2002) The muscular dystrophies. *Lancet*, **359**, 687-695.

183 Blau, H.M., Webster, C. and Pavlath, G.K. (1983) Defective myoblasts identified in Duchenne muscular dystrophy. *Proc. Natl. Acad. Sci. U. S. A.*, **80**, 4856-4860.

184 Wang, B., Li, J., Fu, F.H. and Xiao, X. (2009) Systemic human minidystrophin gene transfer improves functions and life span of dystrophin and dystrophin/utrophin-deficient mice. *J. Orthop. Res.*, **27**, 421-426.

185 Deasy, B.M., Jankowski, R.J., Payne, T.R., Cao, B., Goff, J.P., Greenberger, J.S. and Huard, J. (2003) Modeling stem cell population growth: incorporating terms for proliferative heterogeneity. *Stem Cells*, **21**, 536-545.

186 Hayes, J., Veyckemans, F. and Bissonnette, B. (2008) Duchenne muscular dystrophy: an old anesthesia problem revisited. *Paediatr. Anaesth.*, **18**, 100-106.

187 Uezumi, A., Ikemoto-Uezumi, M. and Tsuchida, K. (2014) Roles of nonmyogenic mesenchymal progenitors in pathogenesis and regeneration of skeletal muscle. *Front Physiol*, **5**, 68.

188 Lefaucheur, J.P., Pastoret, C. and Sebille, A. (1995) Phenotype of dystrophinopathy in old mdx mice. *Anat. Rec.*, **242**, 70-76.

189 Pisani, D.F., Dechesne, C.A., Sacconi, S., Delplace, S., Belmonte, N., Cochet, O., Clement, N., Wdziekonski, B., Villageois, A.P., Butori, C. *et al.* (2010) Isolation of a highly myogenic CD34-negative subset of human skeletal muscle cells free of adipogenic potential. *Stem Cells*, **28**, 753-764.

190 Chateauvieux, S., Ichante, J.L., Delorme, B., Frouin, V., Pietu, G., Langonne, A., Gallay, N., Sensebe, L., Martin, M.T., Moore, K.A. *et al.* (2007) Molecular profile of mouse stromal mesenchymal stem cells. *Physiol Genomics*, **29**, 128-138.

191 Sohn, J., Lu, A., Tang, Y., Wang, B. and Huard, J. (2015) Activation of non-myogenic mesenchymal stem cells during the disease progression in dystrophic dystrophin/utrophin knockout mice. *Hum. Mol. Genet.*, in press.

192 Charge, S.B. and Rudnicki, M.A. (2004) Cellular and molecular regulation of muscle regeneration. *Physiol. Rev.*, **84**, 209-238.

193 Descamps, S., Arzouk, H., Bacou, F., Bernardi, H., Fedon, Y., Gay, S., Reyne, Y., Rossano, B. and Levin, J. (2008) Inhibition of myoblast differentiation by Sfrp1 and Sfrp2. *Cell Tissue Res.*, **332**, 299-306.

194 Svensson, A., Norrby, M., Libelius, R. and Tagerud, S. (2008) Secreted frizzled related protein 1 (Sfrp1) and Wnt signaling in innervated and denervated skeletal muscle. *J. Mol. Histol.*, **39**, 329-337.

195 Liechti-Gallati, S., Koenig, M., Kunkel, L.M., Frey, D., Boltshauser, E., Schneider, V., Braga, S. and Moser, H. (1989) Molecular deletion patterns in Duchenne and Becker type muscular dystrophy. *Hum. Genet.*, **81**, 343-348.

196 Kawano, Y. and Kypta, R. (2003) Secreted antagonists of the Wnt signalling pathway. *J. Cell Sci.*, **116**, 2627-2634.

197 Kang, J.R. and Gupta, R. (2012) Mechanisms of fatty degeneration in massive rotator cuff tears. *J. Shoulder Elbow Surg.*, **21**, 175-180.

198 Samagh, S.P., Kramer, E.J., Melkus, G., Laron, D., Bodendorfer, B.M., Natsuhara, K., Kim, H.T., Liu, X. and Feeley, B.T. (2013) MRI quantification of fatty infiltration and muscle atrophy in a mouse model of rotator cuff tears. *J. Orthop. Res.*, **31**, 421-426.

199 Laron, D., Samagh, S.P., Liu, X., Kim, H.T. and Feeley, B.T. (2012) Muscle degeneration in rotator cuff tears. *J. Shoulder Elbow Surg.*, **21**, 164-174.

200 Kumar, A. and Boriek, A.M. (2003) Mechanical stress activates the nuclear factor-kappaB pathway in skeletal muscle fibers: a possible role in Duchenne muscular dystrophy. *FASEB J.*, **17**, 386-396.

201 Lu, S.Y., Tanaka, K.A., Abuelkasem, E., Planinsic, R.M. and Sakai, T. (2014) Clinical Applicability of Rapid Thrombelastography and Functional Fibrinogen Thrombelastography in Adult Liver Transplantation. *Liver Transpl.*, in press.

202 Ito, T., Ogawa, R., Uezumi, A., Ohtani, T., Watanabe, Y., Tsujikawa, K., Miyagoe-Suzuki, Y., Takeda, S., Yamamoto, H. and Fukada, S. (2013) Imatinib attenuates severe mouse dystrophy and inhibits proliferation and fibrosis-marker expression in muscle mesenchymal progenitors. *Neuromuscul. Disord.*, **23**, 349-356.